AD-A069 086 ARMY ARMAMENT RESEARCH AND DEVELOPMENT COMMAND ABERD--ETC F/G 19/4
BLAST LOADING ON MODEL MUNITION STORAGE MAGAZINES.(U)
FEB 79 C N KINGERY, G A COULTER, G T WATSON

UNCLASSIFIED ARBRL-TR-02140 SBIE-AD-E430 224 NL

1 OF 2
AD A069086

(12) LEVEL III

AD AF430 234

AD A069086

DDC FILE COPY

TECHNICAL REPORT ARBRL-TR-02140

BLAST LOADING ON MODEL MUNITION STORAGE MAGAZINES

Charles N. Kingery
George A. Coulter
George T. Watson

DDC
RECEIVED
MAY 29 1979
B

February 1979

US ARMY ARMAMENT RESEARCH AND DEVELOPMENT COMMAND
BALLISTIC RESEARCH LABORATORY
ABERDEEN PROVING GROUND, MARYLAND

Approved for public release; distribution unlimited.

Destroy this report when it is no longer needed.
Do not return it to the originator.

Secondary distribution of this report by originating or sponsoring activity is prohibited.

Additional copies of this report may be obtained from the National Technical Information Service, U.S. Department of Commerce, Springfield, Virginia 22161.

The findings in this report are not to be construed as an official Department of the Army position, unless so designated by other authorized documents.

The use of trade names or manufacturers' names in this report does not constitute indorsement of any commercial product.

UNCLASSIFIED

SECURITY CLASSIFICATION OF THIS PAGE (When Data Entered)

REPORT DOCUMENTATION PAGE	READ INSTRUCTIONS BEFORE COMPLETING FORM
1. REPORT NUMBER: TECHNICAL REPORT ARBRL-TR-02140	2. GOVT ACCESSION NO. / 3. RECIPIENT'S CATALOG NUMBER
4. TITLE (and Subtitle): BLAST LOADING ON MODEL MUNITION STORAGE MAGAZINES	5. TYPE OF REPORT & PERIOD COVERED: Final 6. PERFORMING ORG. REPORT NUMBER
7. AUTHOR(s): Charles N. Kingery, George A. Coulter, George T. Watson	8. CONTRACT OR GRANT NUMBER(s): CE-BRL-77-1
9. PERFORMING ORGANIZATION NAME AND ADDRESS: US Army Ballistic Research Laboratory (ATTN: DRDAR-BLT) Aberdeen Proving Ground, MD 21005	10. PROGRAM ELEMENT, PROJECT, TASK AREA & WORK UNIT NUMBERS
11. CONTROLLING OFFICE NAME AND ADDRESS: US Army Armament Research & Development Command, US Army Ballistic Research Laboratory (ATTN: DRDAR-BL) Aberdeen Proving Ground, MD 21005	12. REPORT DATE: FEBRUARY 1979 13. NUMBER OF PAGES: 116
14. MONITORING AGENCY NAME & ADDRESS (if different from Controlling Office): Department of Defense Explosive Safety Board, Forrestal Building GB-270, Washington, D.C. 20314	15. SECURITY CLASS. (of this report): UNCLASSIFIED 15a. DECLASSIFICATION/DOWNGRADING SCHEDULE

16. DISTRIBUTION STATEMENT (of this Report)

Approved for public release; distribution unlimited.

17. DISTRIBUTION STATEMENT (of the abstract entered in Block 20, if different from Report)

18. SUPPLEMENTARY NOTES

This work was performed for and funded by the Department of Defense Explosive Safety Board.

This report supersedes Interim Memorandum Report No. 590 dated January 1978.

19. KEY WORDS (Continue on reverse side if necessary and identify by block number)

Munition magazines
Scaled model tests
Explosive safety
Scaling techniques
Structure loading

20. ABSTRACT (Continue on reverse side if necessary and identify by block number) (mba)

This report contains the results obtained from a series of high explosive tests designed to determine the blast loading on scaled models of earth covered munition storage magazines from an accidental explosion. The donor model was a 1/50th scale of an earth covered munition storage magazine. The acceptor models were 1/50th scale non-responding models constructed of cast concrete. Charge weights of 0.357, 1.066, and 1.792 kg were used to simulate 44625, 133250, and 224000 kg in full size storage magazines. Blast loading trends are established

(continued)

DD FORM 1 JAN 73 1473 EDITION OF 1 NOV 65 IS OBSOLETE

UNCLASSIFIED

SECURITY CLASSIFICATION OF THIS PAGE (When Data Entered)

(Item 20 continued)

for structures located at established safe separation distances. Correlation with the United Kingdom 1/10 scaled model results and US full scale results are also presented.

ACCESSION for
NTIS White Section
DDC Buff Section
UNANNOUNCED
JUSTIFICATION
BY
DISTRIBUTION/AVAILABILITY CODES
Dist. AVAIL. and/or SPECIAL
A

TABLE OF CONTENTS

		Page
	LIST OF ILLUSTRATIONS	5
	LIST OF TABLES	9
I.	INTRODUCTION	11
	A. Background	11
	B. Objectives	11
II.	TEST PROCEDURE	11
	A. Model Magazine Design	11
	1. The Donor Model	11
	2. The Acceptor Models	13
	B. Test Charges	18
	C. Test Instrumentation	18
	1. Pressure Transducers	18
	2. Tape Recorder System	18
	D. Test Layout	19
	1. Acceptor Structure A	19
	2. Acceptor Structure B	19
	3. Acceptor Structure C	19
	E. Test Matrix	25
III.	RESULTS	25
	A. Blast Loading on Structure A	25
	1. Overpressure on Rear Slope of Structure A	25
	2. Overpressure and Impulses on the Top and Side of Structure A	28
	3. Overpressure and Impulse on Headwall of Structure A	28
	B. Blast Loading on Structure B	32
	1. Overpressure and Impulse on Front Slope - Station B-1	32
	2. Overpressure and Impulse on Headwall - Station B-2	32

79 04 27 014

TABLE OF CONTENTS

		Page
	3. Overpressure and Impulse on Top of Structure B	32
	a. Test Series I	35
	b. Test Series II	35
	c. Test Series III	35
	4. Overpressure and Impulse on End Slope - Station B-6	39
	5. Overpressure and Impulse on Back Slope - Station B-7	39
C.	Blast Loading on Structure C	39
	1. Overpressure and Impulse on Headwall of Structure C	39
	2. Overpressure and Impulse on the Top and Sides of Structure C	48
IV.	COMPARISON OF RESULTS	51
A.	Comparison of Blast Loading on Structure A	51
B.	Comparison of Blast Loading on Structure B	55
C.	Comparison of Blast Loading on Structure C	55
	1. Comparison of UK and US Model Results on Headwall of Structure to Rear of Donor	55
	2. Comparison of Predictions with Experimental Results	63
	3. Comparison of Results from Top of UK Structure 3 and US Structure C	69
V.	CONCLUSIONS AND RECOMMENDATIONS	69
	APPENDIXES	73
	A - Overpressure and Impulse versus Time From Gauge Stations A-1 Through A-8, Test Series II, Shot 4	75
	B - Overpressure and Impulse versus Time From Gauge Stations B-1 Through B-7, Test Series II, Shot 3	85
	C - Overpressure and Impulse versus Time From Gauge Stations C-1 Through C-8 and F-1, Test Series II, Shot 3	95
	DISTRIBUTION LIST	107

LIST OF ILLUSTRATIONS

Figure		Page
1.	Standard Munition Storage Magazine	12
2.	Internal Portion of Model Donor Magazine	14
3.	Wooden Form for Installing Sand Cover	15
4.	Donor Model with Form Removed	16
5.	Photograph of Acceptor Models	17
6.	Instrumentation System	20
7.	Test Layout	21
8.	Gauge Station Locations on Structure A	22
9.	Gauge Station Locations on Structure B	24
10.	Gauge Station Locations on Structure C	26
11.	Overpressure and Impulse versus Time, Station A-4 and A-5, Test Series III	29
12.	Overpressure and Impulse versus Time, Station A-6 and A-7, Test Series III	30
13.	Overpressure and Impulse versus Time, Station A-8, Test Series II	31
14.	Overpressure versus Time, Station B-2, Test Series I, II, and III	34
15.	Overpressure versus Time, Station B-3, B-4, and B-5, Shot 9, Test Series I	36
16.	Overpressure versus Time, Station B-3, B-4, and B-5, Shot 4, Test Series II	37
17.	Overpressure versus Time, Station B-3, B-4, and B-5, Shot 6, Test Series III	38
18.	Overpressure and Impulse versus Time, Station B-6, Shot 5, Test Series III	40
19.	Overpressure versus Time, Station B-7, Test Series I, II, and III	41

LIST OF ILLUSTRATIONS

Figure		Page
20.	Blast Wave Profiles to Rear of Donor Magazine	44
21.	Shock Interactions on Headwall of Structure C	45
22.	Shock Wave Profiles Recorded on the Front of Model Structure C - Shot 8	46
23.	Effect of Arrival Time on Magnitude of Second Reflected Shock	47
24.	Overpressure and Impulse versus Time, Station C-5, and C-6, Shot 6, Test Series III	49
25.	Overpressure and Impulse versus Time, Station C-7, and C-8, Shot 3, Test Series II	50
26.	UK and US Gauge Locations - Structure A	52
27.	UK, 1/10th Scale Donor Model	53
28.	Gauge Locations on ESKIMO III	56
29.	Peak Overpressure (kPa) Comparison, Model versus ESKIMO III	58
30.	Positive Impulse (kPa-ms) Comparison, Model versus ESKIMO III	59
31.	Gauge Locations on Front of US Model Structure C and UK Model Structure 3	60
32.	Incident Peak Overpressure versus Mach Overpressure for an Angle of 63.4 Degrees	64
33.	Incident Peak Overpressure versus Reflected Overpressure for an Angle of 26.6 Degrees	65
34.	Incident Peak Overpressure versus Head-on Reflected Peak Overpressure	68
35.	Gauge Locations on US Model Structure C and UK Model Structure 3	70
A-1.	Overpressure and Impulse versus Time, Station A-1	77
A-2.	Overpressure and Impulse versus Time, Station A-2	78

LIST OF ILLUSTRATIONS

Figure		Page
A-3.	Overpressure and Impulse versus Time, Station A-3	79
A-4.	Overpressure and Impulse versus Time, Station A-4	80
A-5.	Overpressure and Impulse versus Time, Station A-5	81
A-6.	Overpressure and Impulse versus Time, Station A-6	82
A-7.	Overpressure and Impulse versus Time, Station A-7	83
A-8.	Overpressure and Impulse versus Time, Station A-8	84
B-1.	Overpressure versus Time, Station B-1	87
B-2.	Overpressure and Impulse versus Time, Station B-2	88
B-3.	Overpressure and Impulse versus Time, Station B-3	89
B-4.	Overpressure and Impulse versus Time, Station B-4	90
B-5.	Overpressure and Impulse versus Time, Station B-5	91
B-6.	Overpressure and Impulse versus Time, Station B-6	92
B-7.	Overpressure and Impulse versus Time, Station B-7	93
C-1.	Overpressure and Impulse versus Time, Station C-1	97
C-2.	Overpressure and Impulse versus Time, Station C-2	98
C-3.	Overpressure and Impulse versus Time, Station C-3	99
C-4.	Overpressure and Impulse versus Time, Station C-4	100
C-5.	Overpressure and Impulse versus Time, Station C-5	101
C-6.	Overpressure and Impulse versus Time, Station C-6	102
C-7.	Overpressure and Impulse versus Time, Station C-7	103
C-8.	Overpressure and Impulse versus Time, Station C-8	104
C-9.	Overpressure and Impulse versus Time, Station F-1	105

LIST OF TABLES

Table		Page
I.	Dimensions of Structure and Model	13
II.	Gauge Distances from Ground Zero to Locations on Structures A, B, and C	23
III.	Blast Parameters Loading Structure A	27
IV.	Blast Parameters Loading Structure B	33
V.	Blast Parameters Loading Structure C	42
VI.	Comparison of Blast Loading on Acceptor Structure in Front of Donor	54
VII.	Comparison of Blast Loading on Acceptor Structure to Side of Donor	57
VIII.	Peak Overpressure on Headwall of Structure to Rear of Donor	61
IX.	Positive Impulse on Headwall of Structure to Rear of Donor	62
X.	Predicted Incident Peak Overpressure	66
XI.	Roof Loading on Acceptor to Rear of Donor	71

PRECEDING PAGE BLANK

I. INTRODUCTION

A. Background

The blast generated from accidental explosions in munition storage magazines is the primary mechanism for damage to other storage magazines. The free-field blast parameters from explosions in scaled model earth covered munition storage magazines were determined and reported in Reference 1, where a good correlation with full-scale test results was described.

This report will cover a general study sponsored by the Department of Defense Explosives Safety Board (DDESB) to determine the blast loading on model acceptor magazines from explosions in model donor magazines when located at the accepted safe-separation distances. The results will be compared to available full-scale data as well as other model studies.

B. Objectives

The primary objectives of the planned series of tests are as follows:

1. Determine the blast loading on model acceptor magazines placed at safe separation distances to the front, side, and rear of a model donor magazine.

2. Determine the validity of using results from model tests to predict loading on full size structures.

II. TEST PROCEDURE

The test procedures followed, to meet the stated objectives, were similar to those used in Reference 1, i.e., design the model donor and acceptor magazines, determine the instrumentation requirements, and develop the field layout.

A. Model Magazine Designs

The designs of the donor and acceptor models are described in following sections.

1. The Donor Model. The standard munition storage magazine being modeled for this test program is shown in Figure 1. The dimensions associated with the letters in Figure 1 are listed in Table I for both

[1] *C. Kingery, G. Coulter, G. Watson, "Blast Parameters from Explosions in Model Earth Covered Magazines," BRL Memorandum Report No. 2680, September 1976.*

PRECEDING PAGE BLANK

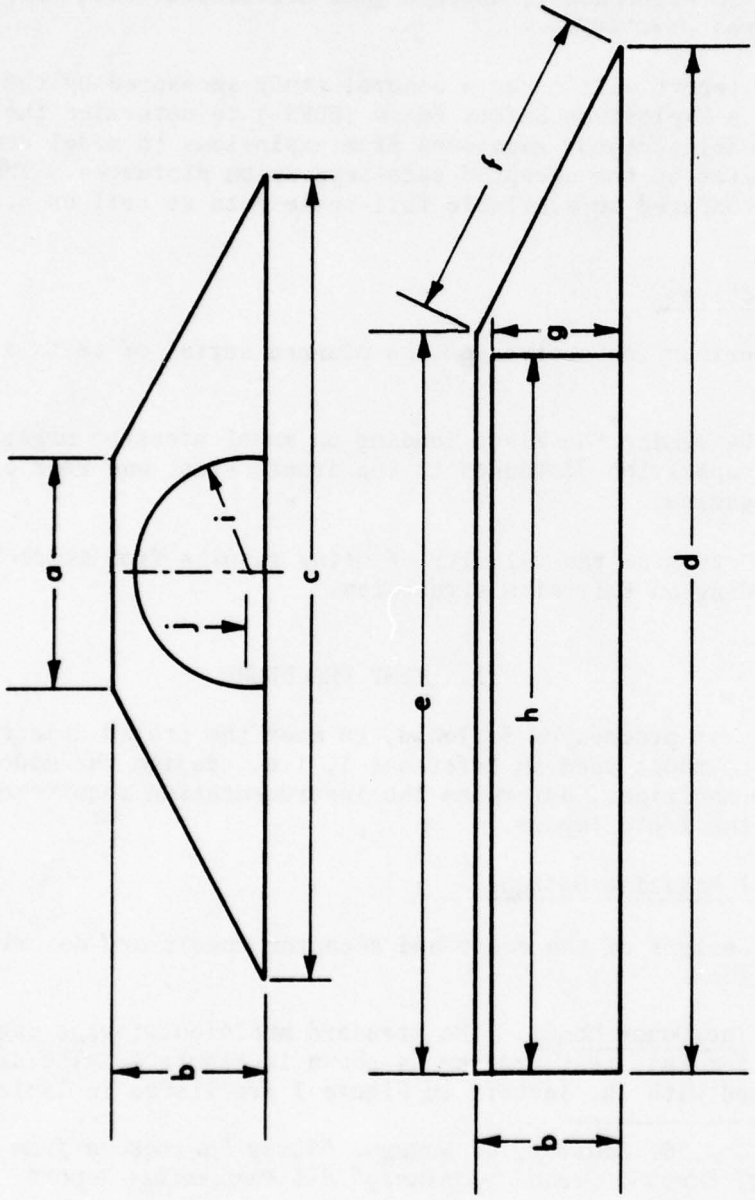

Figure 1. Standard Munition Storage Magazine

Table I. Dimensions of Structure and Model

	Full-Size Feet	Full-Size Metres	1/50 Scale Metres
a	26	7.92	.158
b	16	4.88	.098
c	90	27.43	.549
d	115	35.05	.701
e	83	25.30	.506
f	35.8	10.91	.218
g	14	4.27	.085
h	80	24.38	.488
i	13	3.96	.079
j	1	0.305	.006

the full-size structure and 1/50th scaled model. The volume of the interior of the full-size structure is 660 m^3.

For the 1/50th scale model all dimensions were reduced by a factor of 50. Therefore the volume of the interior of the model was 0.00528 m^3. A 1/50 scaled model of the interior arch and headwall of the donor magazine is shown in Figure 2. The arch is .020 aluminum, the rear wall .006 m (1/4-inch) plywood and the headwall .006 m (1/4-inch) masonite. When preparing the donor model for a test firing, a wooden form is placed over the interior portion as shown in Figure 3. A special modeling sand is packed into the wooden form giving a final configuration, when the form is removed, as shown in Figure 4. The sand used for the earth cover is 80 grit, and for each 45.4 kg of sand a mix of .908 kg of Actival (adhesive), .908 kg of Bentonite (clay), and .000946 m^3 20 wt motor oil (1 quart) are blended to form a special modeling sand.

2. The Acceptor Models. There were three acceptor models. They were also 1/50th scale but were non-responding cast concrete, and therefore only the exterior dimensions of the full size structure are scaled. A photograph of the models is shown in Figure 5. Gauge mounts and cable conduits were cast into the concrete. Note that a base was added to the model which was placed below the ground surface to add greater stability.

Special gauge mounts were fabricated to de-couple the gauge from the concrete model. This was done to overcome a problem encountered on previous tests, where the shock traversing the concrete reached the

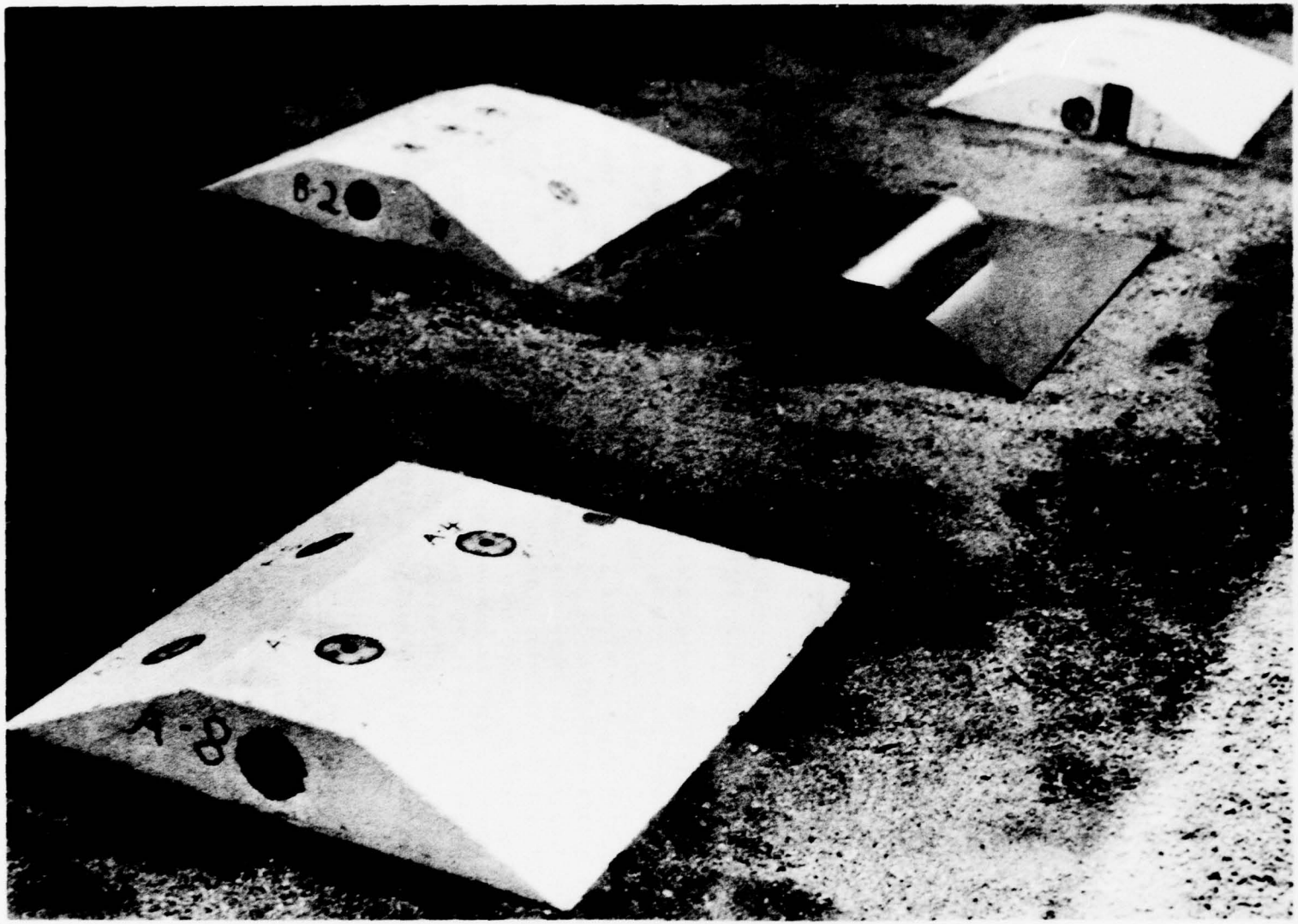

Figure 2. Internal Portion of Model Donor Magazine

Figure 3. Wooden Form for Installing Sand Cover

Figure 4. Donor Model with Form Removed

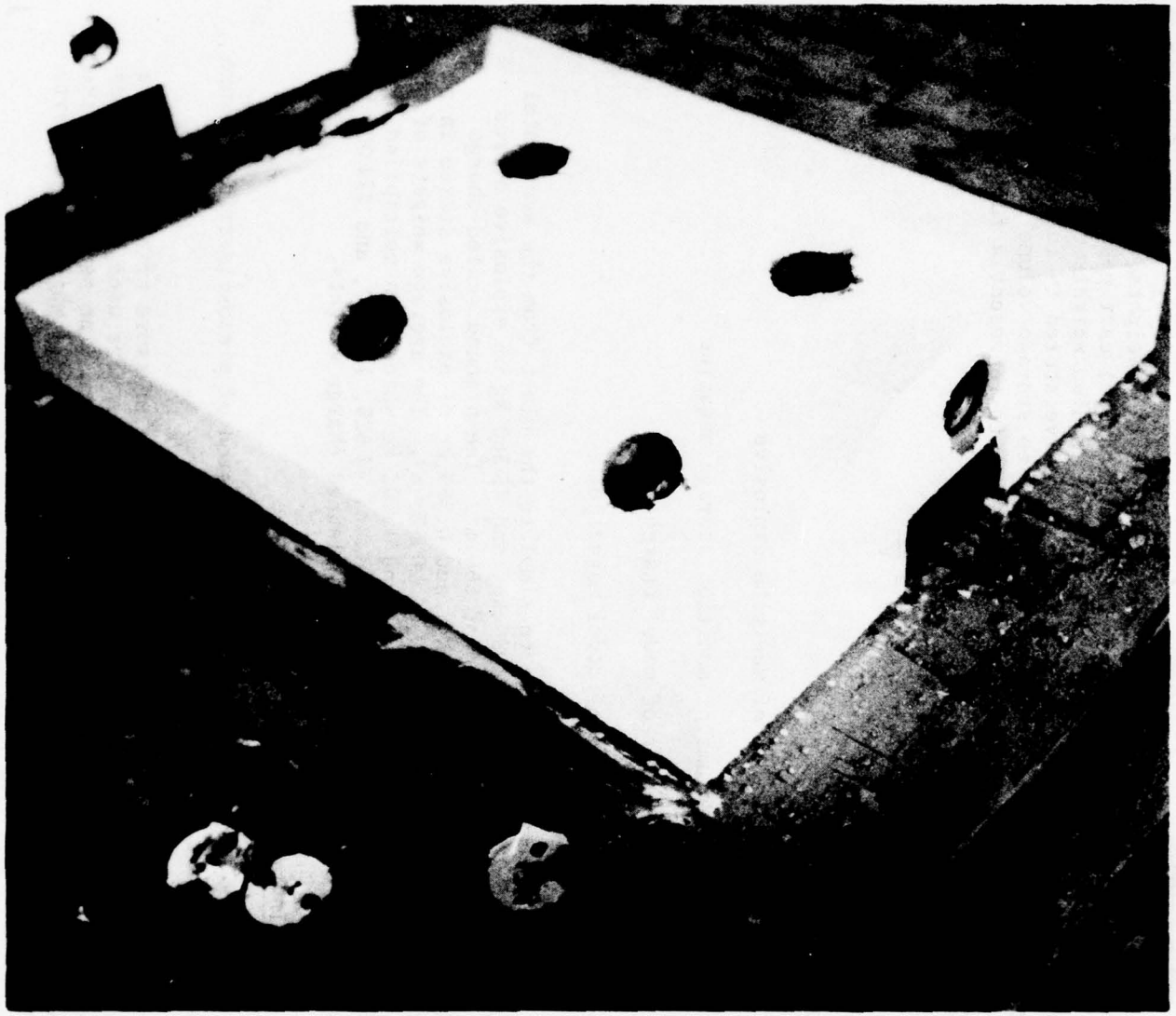

Figure 5. Photograph of Acceptor Models

gauge prior to the air shock, causing spurious signals to be recorded. A gauge mount made of a soft plastic material (Polylux) alleviated this problem.

B. Test Charges

The test charges were the same configuration, weights, and explosive as used in Reference 1. They were hemicylindrical cast pentolite weighing 0.363 kg, 1.088 kg and 1.814 kg. These scaled weights represented 45360 kg, 136080 kg, and 226800 kg of explosive stored in full-size magazines. The ratio of the charge weight to storage volume should be maintained when designing a model experiment to represent a full-size storage magazine.

$$\frac{W}{V} = \frac{W_m}{V_m} \tag{1}$$

where

W = Weight of munition explosive

V = Volume of munition storage magazine

W_m = Weight of model charge

V_m = Volume of model magazine.

The program was designed to simulate the blast from the accidental explosion of 226 800 kg, 136 080 kg, and 45 360 kg of explosive stored in a magazine having a volume of 660 m^3. The planned scaled charge weights were 1.814 kg, 1.088 kg, and 0.363 kg of explosive stored in a model magazine having a volume of .00528 m^3. The average weights of the charges fired were 0.357, 1.066, and 1.792 kg which when multiplied by 50^3 (125 000) gives full-scale weights of 44 625, 133 250, and 224 000 kg. All test layouts were based on the planned charge weights.

C. Test Instrumentation

The test instrumentation system consisted of piezo-electric pressure transducers and magnetic tape recorders.

1. Pressure Transducers. Piezo-electric pressure transducers were used throughout the series of tests. Two types were used, one type was the Susquehanna Instruments Model ST-4 with tourmaline sensors, and the second type was a PCB Electronics Inc., Model 113A24 which had a quartz sensing element and a built-in source follower.

2. Tape Recorder System. The tape recorders consisted of three basic units, the power supply and voltage calibrator, the amplifier,

and the FM recorder. The FM tape recorder used was a Honeywell 7600 having a frequency response of 80 kHz. Once the signal was recorded on the magnetic tape it was played back and recorded on a Honeywell Model 1858 Visicorder. This oscillograph has excellent frequency response and the overpressure versus time recorded at the individual positions were read directly from the oscillograph playback for preliminary data analysis. For final analysis and reporting the magnetic tapes were processed through an analog to digital converter and then through a computer and plotting routine where the data were tabulated and plotted as overpressure and impulse versus time. The data gathering instrumentation system is shown in Figure 6.

D. Test Layout

The primary objective of this test series was to determine the blast loading on acceptor magazines located at established safe-separation distances to the front, side, and rear of a donor magazine. The safe separation distance in metres is defined as $0.8Q^{1/3}$ for magazines located to the front or rear of the donor and $0.5Q^{1/3}$ for side to side separation, where Q is the weight of explosive (in kilograms) stored in the magazine. The safe separation distance is measured from interior wall of the donor to the interior wall of the acceptor. All gauge locations were measured from the geometric center of the donor magazine floor where the center of the explosive charge was placed. All charges were detonated at the end nearest the donor magazine entrance. The test layout showing donor and acceptor magazines is presented in Figure 7.

1. Acceptor Structure A. The 1/50 scale model of an earth covered munition storage magazine located to the front of the donor magazine was designated acceptor structure A. The safe separation distances for the 0.363, 1.088, and 1.814 kg charges were 0.571, 0.823, and 0.976 metres. Structure A was instrumented with eight pressure transducers as shown in Figure 8 with each gauge location preceded by the letter A. The gauge locations relative to ground zero are listed in Table II for the three charge weights. Distances are in-place measurements.

2. Acceptor Structure B. This magazine was placed to the side of the donor as shown in Figure 7. The side to side safe separation distance is $0.5Q^{1/3}$. The safe separation distances for the planned 0.363, 1.088, and 1.814 kg charges were 0.357, 0.514, and 0.610 metres. Structure B was instrumented with seven pressure gauges. The locations are shown in Figure 9. Each gauge location is preceded by the letter B. The in-place gauge distances from ground zero are listed in Table II.

3. Acceptor Structure C. Structure C was placed to the rear of the donor as shown in Figure 7. The safe separation distances are the same for Structure C and Structure A; i.e., $0.8Q^{1/3}$. For planned charge weights of 0.363, 1.088, and 1.814 kg the safe separation

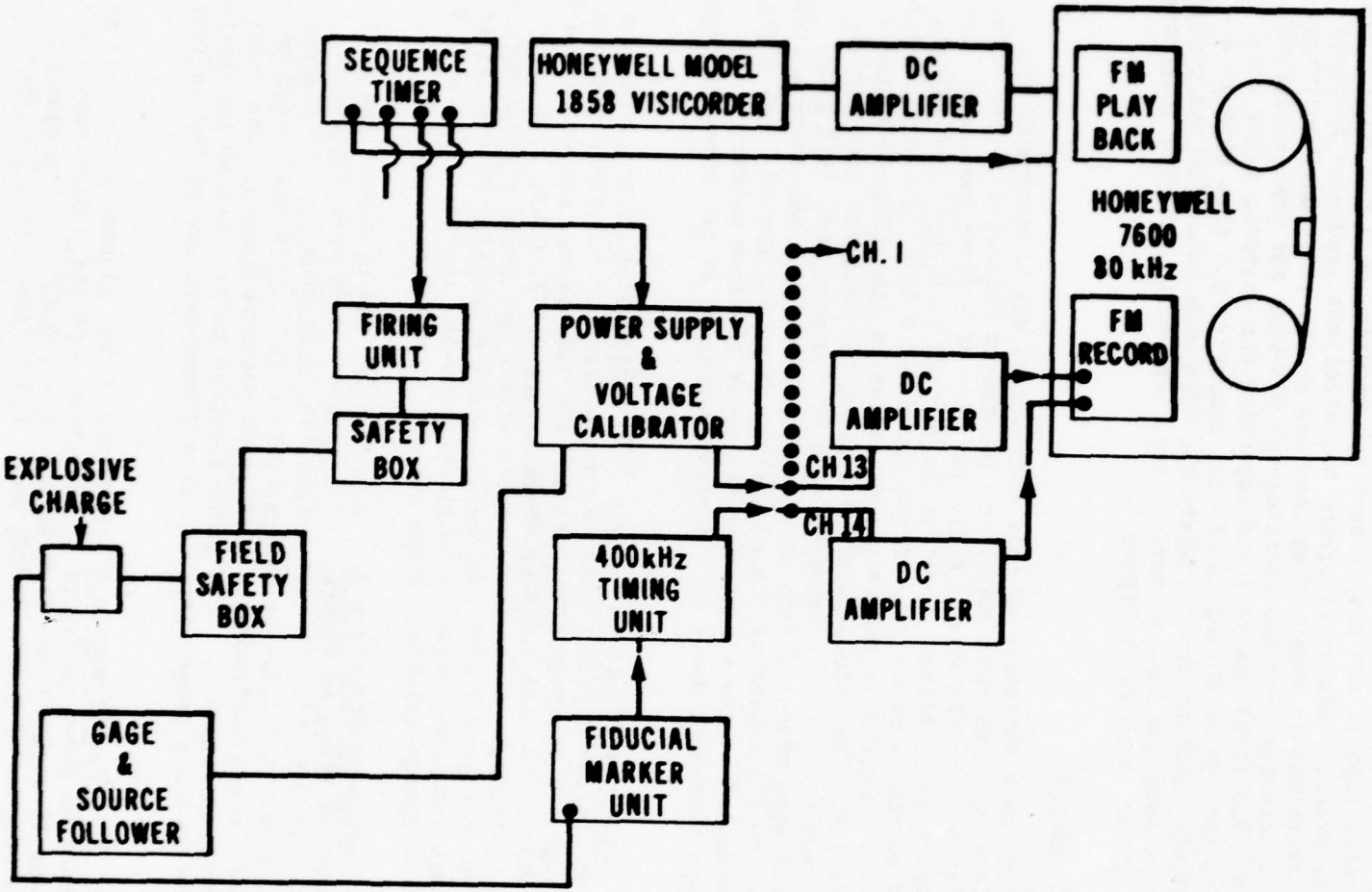

Figure 6. Instrumentation System

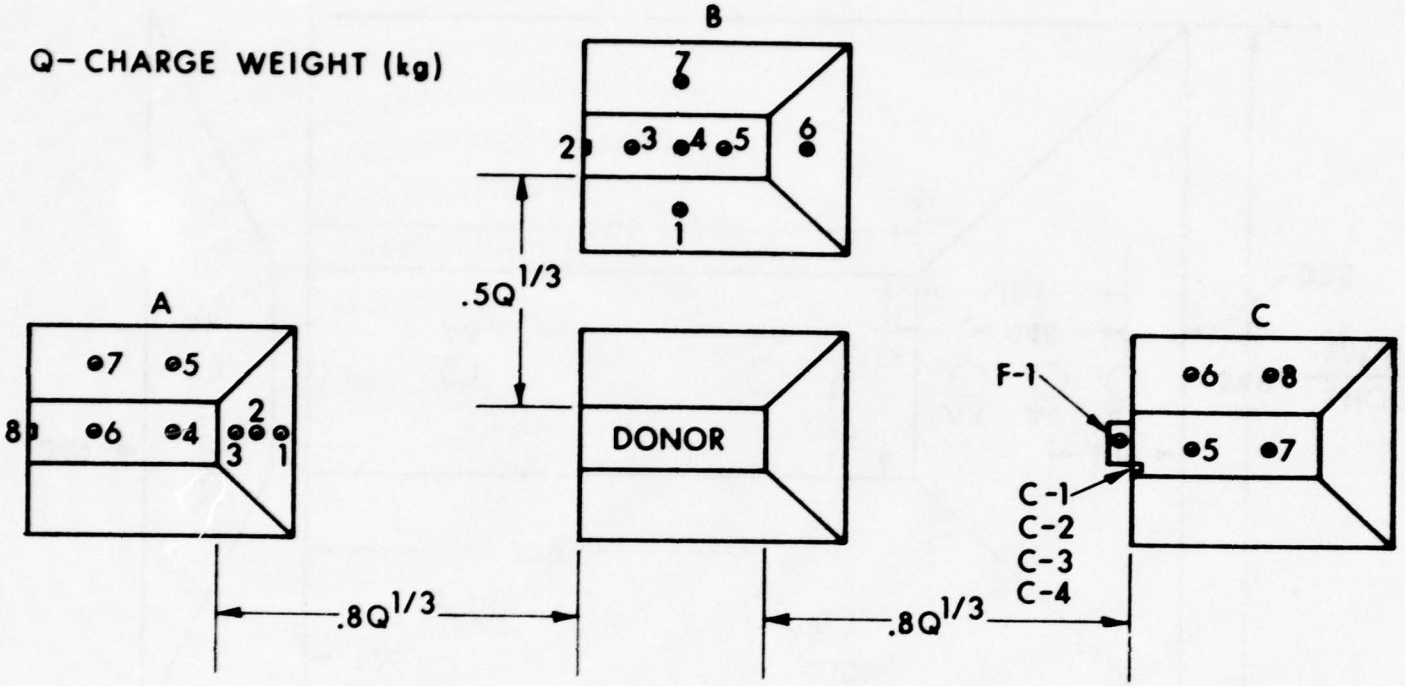

Figure 7. Test Layout

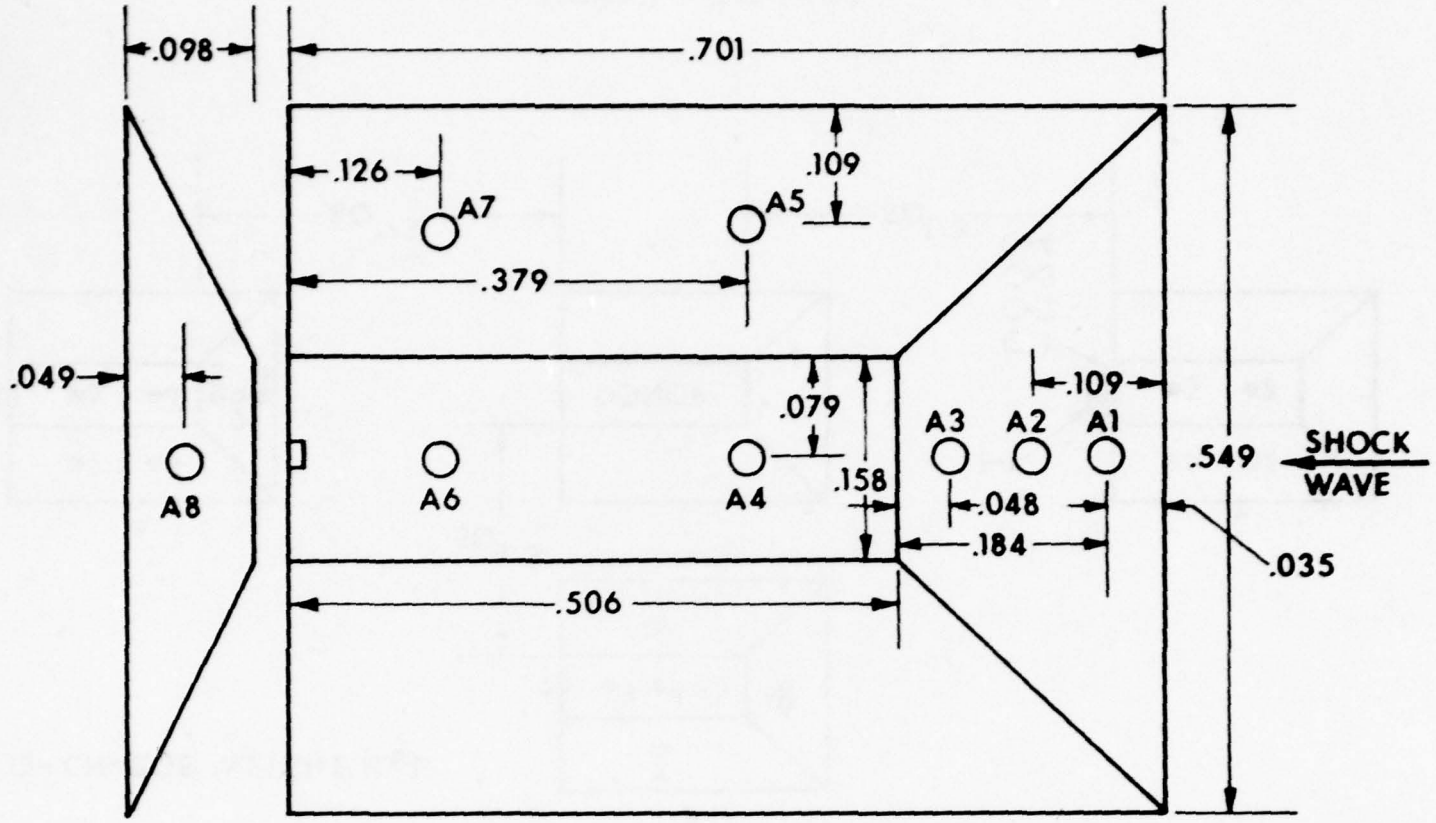

Figure 8. Gauge Station Locations on Structure A

Table II. Gauge Distances from Ground Zero to Locations on Structures A, B, and C

Test Series	I	II	III
Charge Weight	0.363 Kg	1.088 Kg	1.814 kg
Gauge Station	Distance from GZ in Metres		
	m	m	m
A-1	0.630	0.875	1.035
A-2	0.697	0.942	1.102
A-3	0.751	0.996	1.156
A-4	0.920	1.166	1.325
A-5	0.937	1.178	1.337
A-6	1.174	1.419	1.580
A-7	1.187	1.430	1.590
A-8	1.300	1.545	1.706
B-1	0.334	0.496	0.592
B-2	0.569	0.718	0.809
B-3	0.525	0.684	0.779
B-4	0.510	0.672	0.768
B-5	0.525	0.684	0.779
B-6	0.619	0.758	0.845
B-7	0.687	0.849	.946
C-1	0.814	1.082	1.220
C-2	0.814	1.082	1.220
C-3	0.814	1.082	1.220
C-4	0.814	1.082	1.220
C-5	0.940	1.210	1.348
C-6	0.958	1.223	1.360
C-7	1.193	1.461	1.599
C-8	1.206	1.472	1.609
F-1	0.754	1.022	1.160

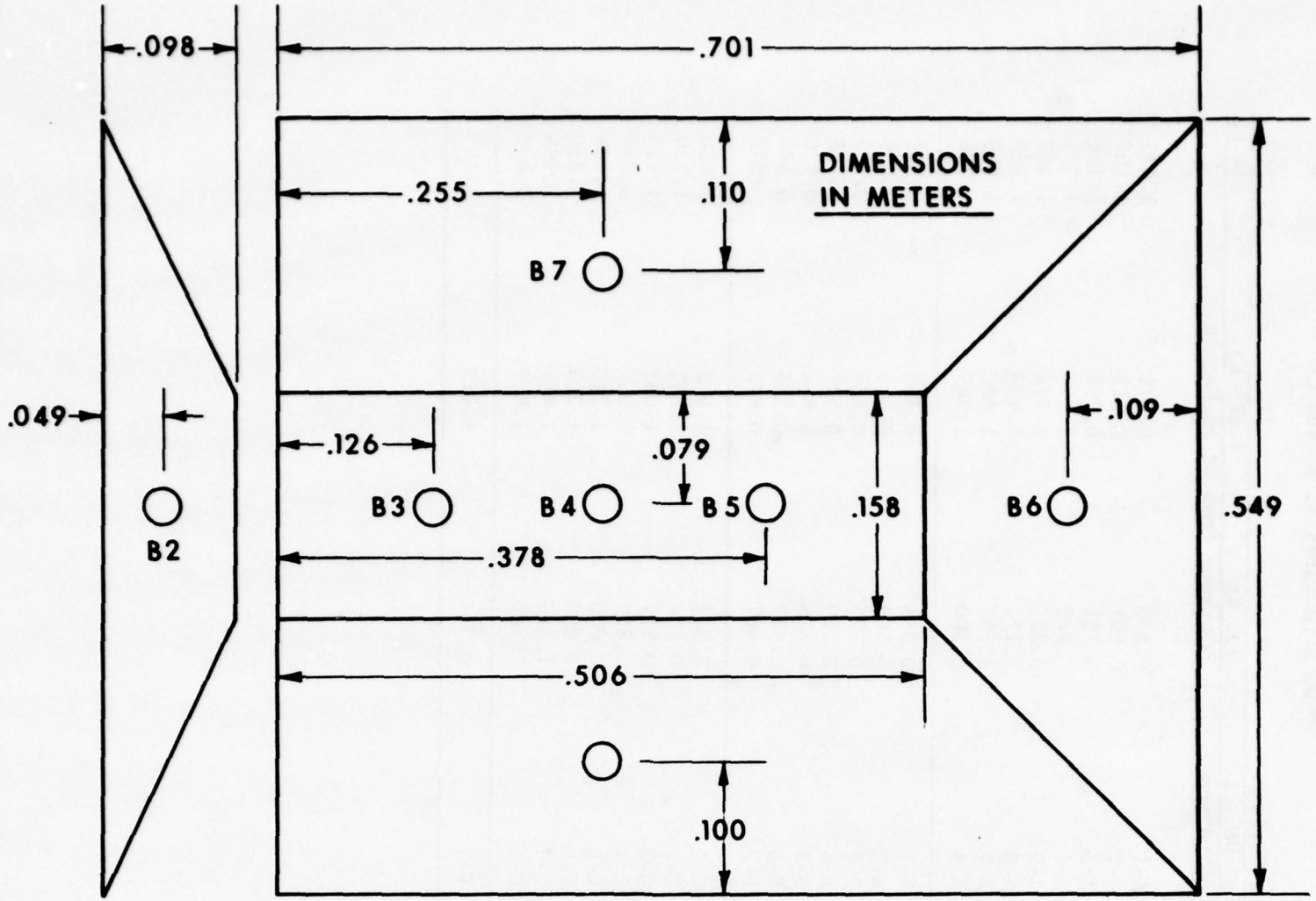

Figure 9. Gauge Station Locations on Structure B

distances were 0.571, 0.823, and 0.976 metres. The distances of the gauge stations from ground zero are listed in Table II. The locations of the gauge stations on acceptor structure C are shown in Figure 10. Each gauge location is preceded by the letter C.

E. Test Matrix

Ten charges were detonated during the field testing phase of the program. The first shot was a calibration test using an uncovered spherical charge weighing 0.082 kg. This shot was fired to check the instrumentation system.

Shots 2, 3 and 4, will be noted as Test Series II. It consisted of covered hemicylindrical charges with an average weight of 1.066 kg.

Shots 5, 6 and 7 are noted as Test Series III. The charges had an average weight of 1.792 kg.

Shots 8, 9 and 10 are noted as Test Series I. The average charge weight was 0.357 kg.

III. RESULTS

The results will be presented in the form of arrival time, peak overpressure, positive impulse, and overpressure duration for each gauge station on the acceptor models. Comparisons with other model tests and full scale data will be made where possible. Three tests were conducted for each charge weight and therefore average values for the three shots will be used in most comparisons. Selected plots of overpressure versus time at specific locations on the models will also be presented.

A. Blast Loading on Structure A

Structure A was located to the front of the donor magazine. The separation distance was $0.8Q^{1/3}$. The test lay-out is shown in Figure 7. The gauge station locations are shown in Figure 8. All stations were instrumented on all shots fired in Test Series I (0.357 kg), II (1.066 kg), and III (1.792 kg). Selected records of overpressure and impulse versus time for all gauge positions are presented in Appendix A.

1. Overpressure on Rear Slope of Structure A. There were three gauge locations on the rear slope of Structure A. Because of the blast focusing to the front of the donor these gauge stations are loaded with high overpressures as well as detonation products and debris. Good overpressure versus time records on the rear slope were not obtained and therefore only the first peak is listed in Table III. It should be noted that although the safe separation distance is a function of charge weight the peak overpressure recorded at specific gauge locations increased as the donor charge was increased.

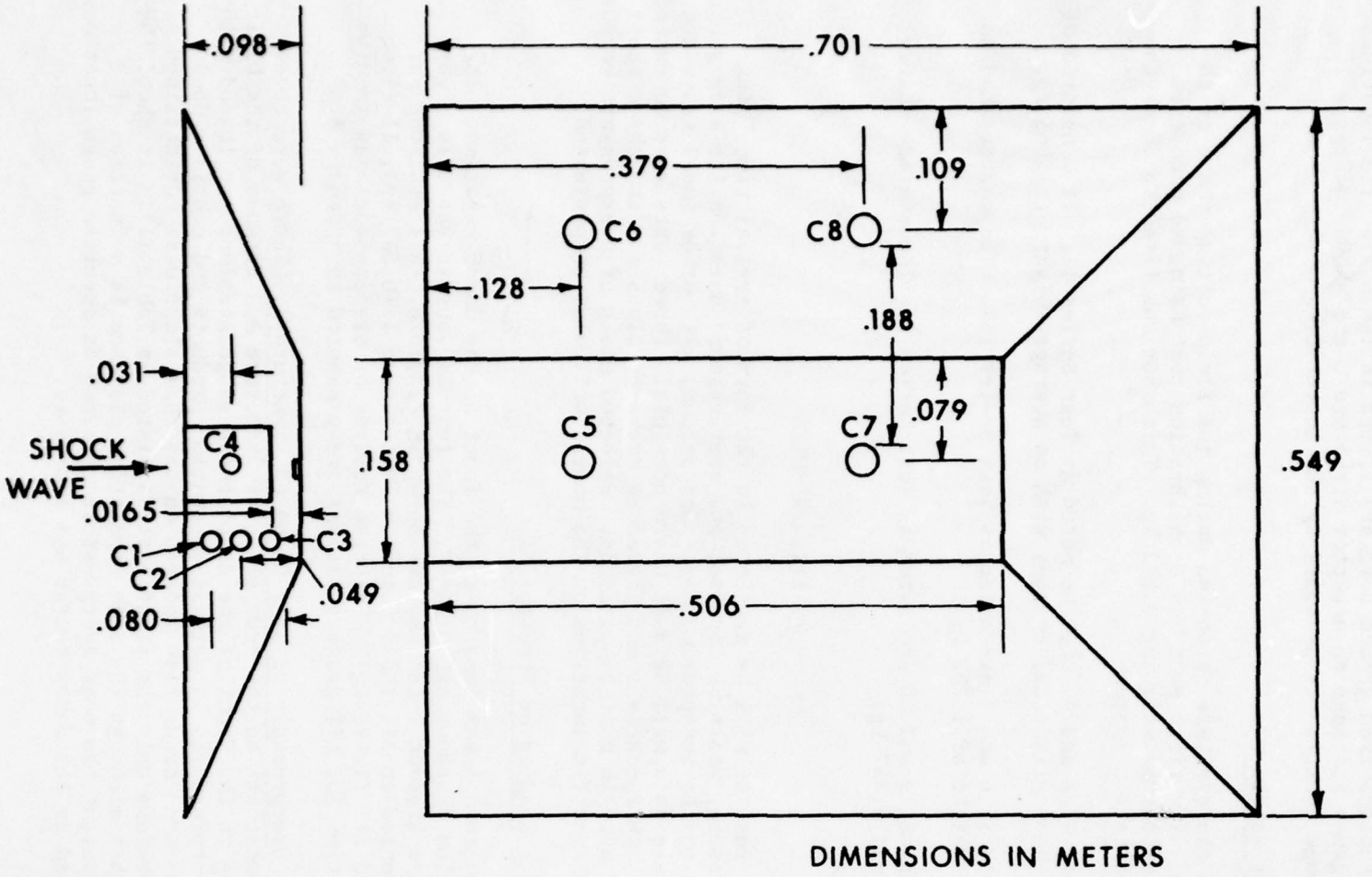

Figure 10. Gauge Station Locations on Structure C

Table III. Blast Parameters Loading Structure A

Charge Weight	Gauge Station	Distance from GZ	Arrival Time	Peak Overpressure			Positive Impulse			Duration Positive Pressure
kg		m	ms	bar	kPa	psi	bar-ms	kPa-ms	psi-msec	ms
0.357	A-1	0.630	0.34	33.0	3300	479	-	-	-	-
	A-2	0.697	0.39	20.2	2020	293	-	-	-	-
	A-3	0.751	0.42	17.5	1750	254	-	-	-	-
	A-4	0.920	0.59	7.26	726	105	0.790	79.0	11.4	0.44
	A-5	0.937	0.65	7.04	704	102	0.933	93.3	13.5	0.81
	A-6	1.174	0.91	3.46	346	50	0.546	54.6	7.9	0.63
	A-7	1.187	0.97	3.92	392	57	0.704	70.4	10.2	0.71
	A-8	1.300	1.19	.57/.76	57/76	8.3/11	0.524	52.4	7.6	1.51
1.066	A-1	0.875	0.38	36.3	3630	526	-	-	-	-
	A-2	0.942	0.43	24.2	2420	351	-	-	-	-
	A-3	0.996	0.44	21.1	2110	306	-	-	-	-
	A-4	1.166	0.60	11.5	1150	167	1.310	131.0	19.0	0.48
	A-5	1.178	0.61	10.5	1050	152	1.674	167.4	24.3	0.89
	A-6	1.419	0.85	6.62	662	96	1.554	155.4	22.5	0.97
	A-7	1.430	0.88	6.02	602	87	2.059	205.9	29.9	1.52
	A-8	1.545	1.10	1.18/2.74	118/274	17/40	1.788	178.8	25.9	1.97
1.792	A-1	1.035	0.41	50.3	5030	729	-	-	-	-
	A-2	1.102	0.44	31.2	3120	452	-	-	-	-
	A-3	1.156	0.47	24.4	2440	354	-	-	-	-
	A-4	1.325	0.62	14.1	1410	204	1.366	136.6	19.8	0.58
	A-5	1.337	0.65	10.8	1080	157	1.848	184.8	26.8	0.89
	A-6	1.580	0.84	10.0	1000	145	1.735	173.5	25.2	0.80
	A-7	1.590	0.91	7.26	726	105	2.310	231.0	33.5	1.31
	A-8	1.706	1.06	1.09/3.08	109/309	16/45	1.934	193.4	28.0	2.39

2. Overpressure and Impulse on the Top and Side of Structure A. As noted in Figure 8, gauge Stations A-4 and A-6 are on the top of magazine A, while Stations A-5 and A-7 are on the side slope. The results obtained from the three different charge weights are listed in Table III. One of the most significant results to be noted in the loading on the top of Structure A is, that while the peak overpressure decreases with distance when traveling from A-4 to A-6 and A-5 to A-7 on all three test series, the positive impulse increases on Test Series II and III.

When the shock front moves up the rear slope and expands over the top and around the sides of the structure, the peak overpressure is greater at Station A-4 than A-5, but the duration and impulse are greater at Station A-5 than A-4. See example from Test Series III in Figure 11. The expansion over the top causes a faster decay of pressure behind the shock front at location A-4 than A-5. Thus A-5 has a longer duration and larger impulse. The positive impulse values are listed in Table III.

As the shock front moves away from the explosive source to Station A-6 (top) and A-7 (side) the peak overpressure is again greater at Station A-6 than A-7, while the positive impulse is greater at Station A-7 than A-6. See example from Test Series III in Figure 12. The positive impulse is greater at Station A-6 than at Station A-4 and greater at Station A-7 than at Station A-5 with the exception of Test Series I (0.357 kg).

It is quite evident in Table III that the peak overpressures and impulses recorded at Stations A-4, A-5, A-6, and A-7 all increase with increasing charge weight. This observation means that if a structure is designed to withstand the blast loading from 224000 kg of explosive at the specified safe separation distance it will be overdesigned for an explosive load of 44625 kg at that specified safe separation distance.

3. Overpressure and Impulse on the Headwall of Structure A. Only one gauge station (A-8) was located on the headwall of this magazine. It was on the centerline near the top where the entrance door would be located. See Figure 8 for dimensions. The initial shock passing down the wall is relatively weak because of the expansion from over the top, but when the reflections from the surface reach the gauge station there is a gradual build-up of pressure which reaches two to three times that of the initial shock. An example of the overpressure versus time recorded at Station A-8 is presented in Figure 13. The values of the initial peak and maximum peak overpressure are listed in Table III. It should be noted in Table III that both the peak overpressures and impulses increased as the donor charge weight is increased.

The positive impulse recorded at Station A-8 on Test Series II and III are of similar magnitude to that recorded on the headwall of Structure C located to the rear of the donor magazine. The build-up

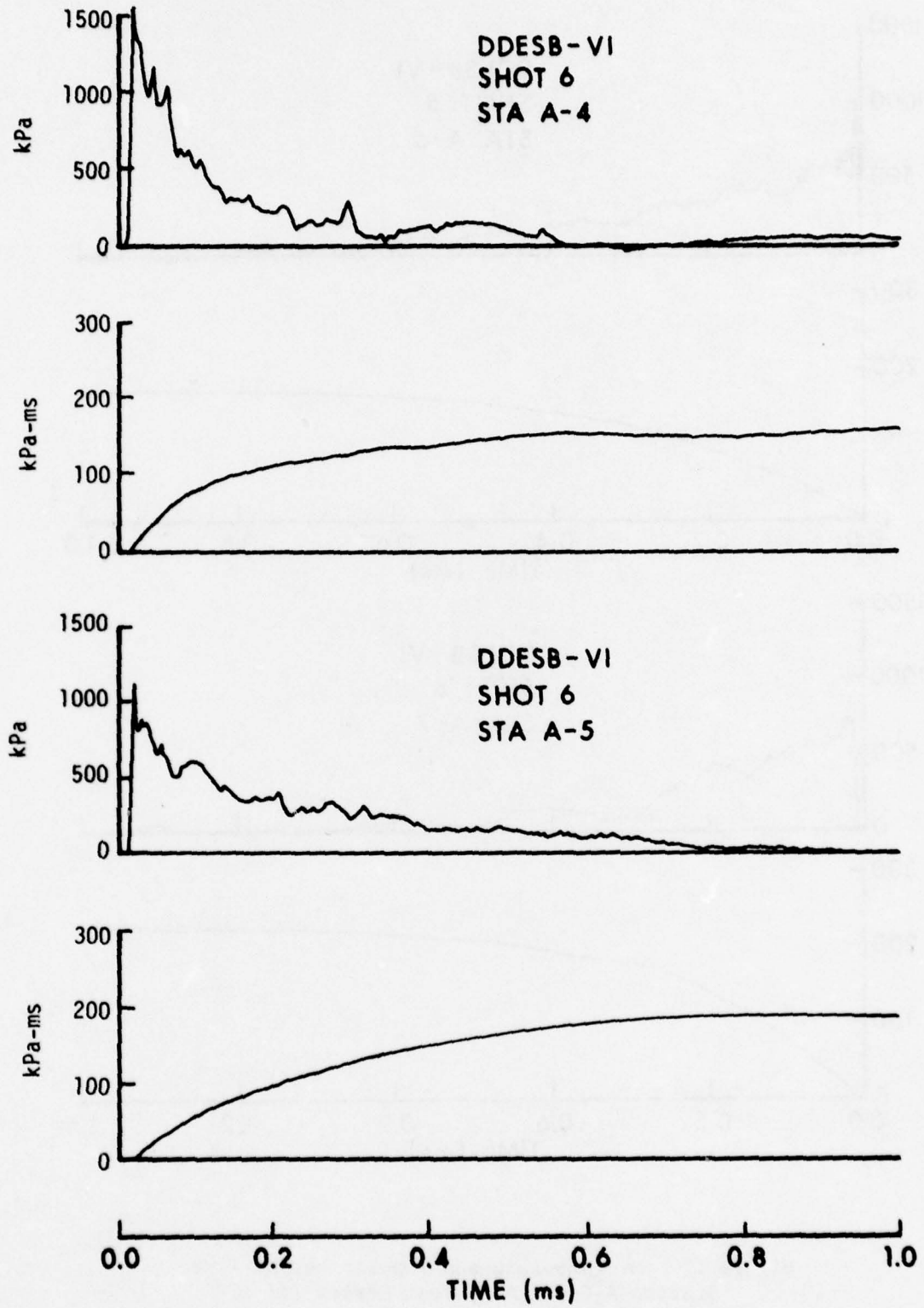

Figure 11. Overpressure and Impulse versus Time, Station A-4 and A-5, Test Series III

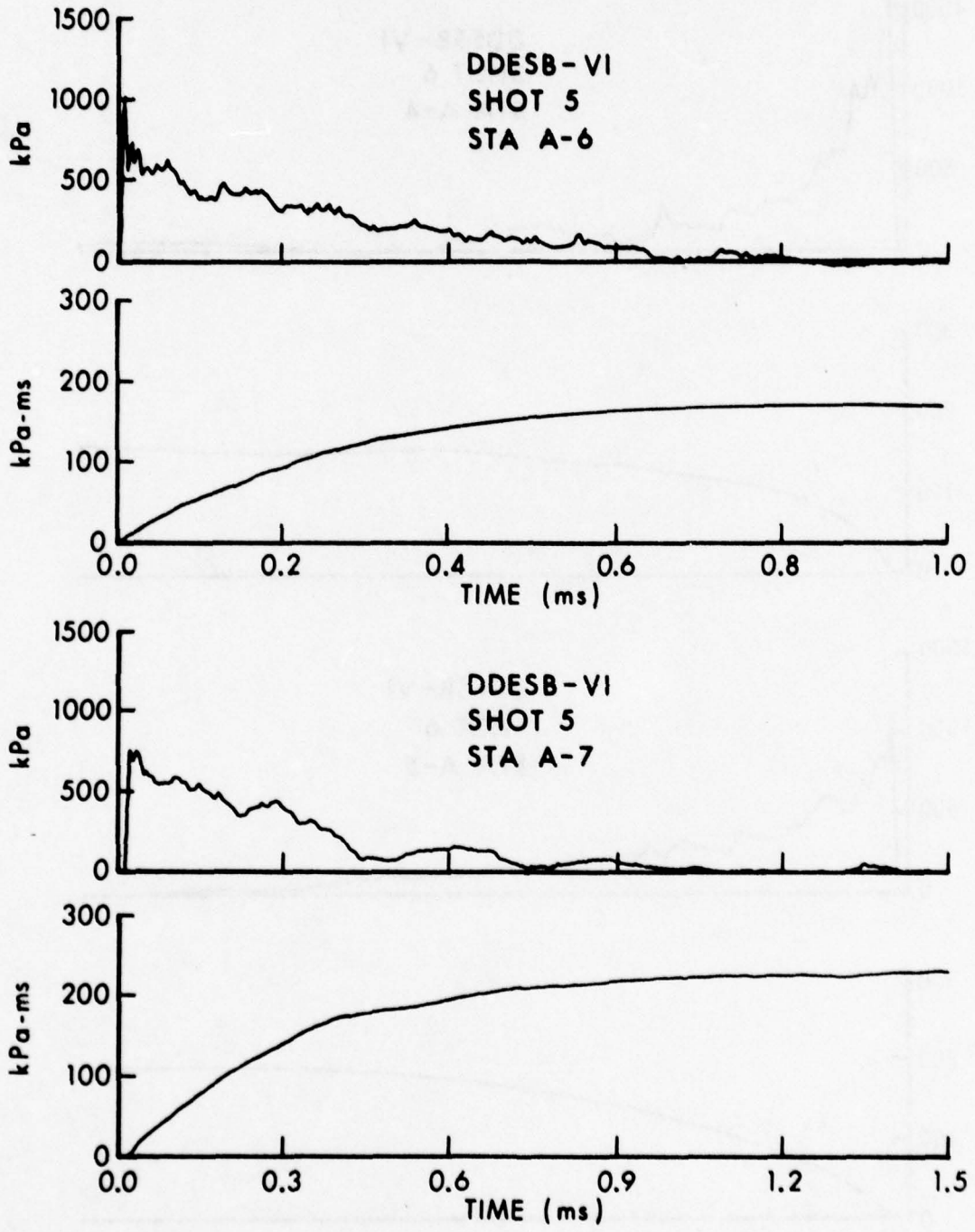

Figure 12. Overpressure and Impulse versus Time, Station A-6 and A-7, Test Series III

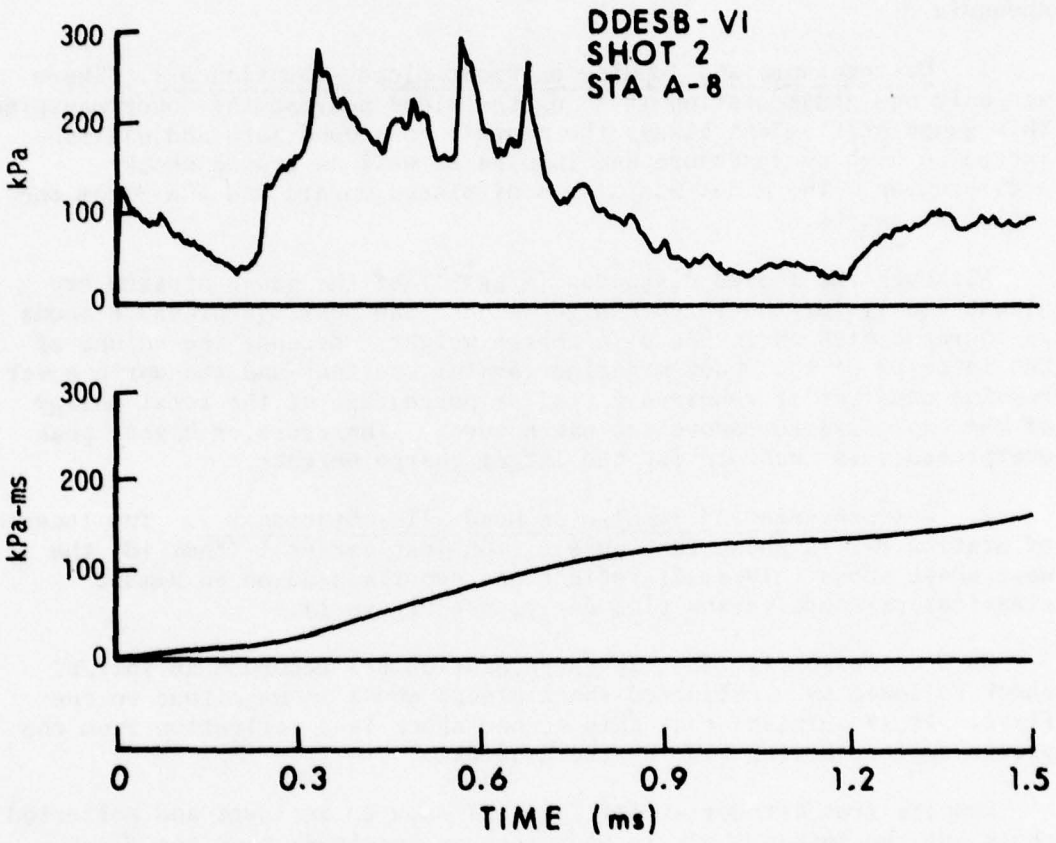

Figure 13. Overpressure and Impulse versus Time, Station A-8, Test Series II

of impulse on the headwall of Structure A is much slower than the build-up on Structure C.

B. Blast Loading on Structure B

Structure B was located at a side-to-side separation distance of $0.5Q^{1/3}$ as shown in Figure 7. There were seven gauge station locations (B-1 through B-7) as shown in Figure 9. Average values of the recorded blast parameters are listed in Table IV. Selected records of the overpressure versus time at each gauge station are presented in Appendix B.

1. Overpressure and Impulse on Front Slope - Station B-1. There was only one gauge station (B-1) on the slope nearest the donor magazine. This gauge station was always the nearest to ground zero and was subjected to high overpressure and impulse as well as ground shock acceleration. The model was always displaced upward and away from the explosive source.

Although the scaled distances ($m/kg^{1/3}$) of the gauge station are almost equal, for the three charge weights the peak overpressure shows an increase with an increase in charge weight. Because the volume of the interior of the donor magazine remains constant and the earth cover remains constant it requires a smaller percentage of the total energy of the explosive to remove the earth cover. Therefore, a higher peak overpressure is recorded for the larger charge weights.

2. Overpressure and Impulse on Headwall - Station B-2. The location of Station B-2 is shown in Figure 9. On Test Series I (Shot 10) the wave shape shows only small reflections superimposed on an almost classical pressure versus time decay; see Figure 14.

On Test Series II (Shot 2) gauge Station B-2 recorded an initial shock followed by a reflected shock almost equal in magnitude to the first. It is surmised that this second shock is a reflection from the ground surface moving back up the headwall.

Results from Test Series III (Shot 7) show an incident and reflected shock but the second shock is much less in magnitude than the first shock. The values of overpressure were quite consistant for the three shots fired in Test Series III.

The positive impulse values were repeatable within each series and show an expected increase with increase in charge weight. Average values of peak overpressure and impulse are listed in Table IV.

3. Overpressure and Impulse on Top of Structure B. The overpressure and impulse loading on the top of Structure B were recorded at three locations, B-3, B-4, and B-5. The results will be presented by describing the loading at each position for a specific test series.

Table IV. Blast Parameters Loading Structure B

Charge Weight	Gauge Station	Distance from GZ	Arrival Time	Peak Overpressure			Positive Impulse			Duration Positive Pressure
kg		m	ms	bar	kPa	psi	bar-ms	kPa-ms	psi-msec	ms
0.357	B-1	0.334	0.42	7.57	757	110	1.405	140.5	20.4	0.85
	B-2	0.569	0.67	3.27	327	47	0.559	55.9	8.1	0.94
	B-3	0.525	0.69	2.66/3.40	266/340	39/49	0.702	70.2	10.2	0.73
	B-4	0.510	0.65	2.67/2.85	267/285	39/41	0.711	71.1	10.3	0.64
	B-5	0.525	0.68	3.06/4.02	306/402	44/58	0.754	75.4	10.9	0.65
	B-6	0.619	0.79	3.09	309	45	0.554	55.4	8.0	0.92
	B-7	0.687	1.02	1.03/1.65	103/165	15/24	0.486	48.6	7.0	1.09
1.066	B-1	0.496	0.57	9.44	944	137	1.941	194.1	28.1	0.83
	B-2	0.718	0.75	3.07/5.24	307/524	44/76	0.929	92.9	13.5	0.95
	B-3	0.684	0.76	4.96	496	72	1.086	108.6	15.8	0.90
	B-4	0.672	0.79	4.32	432	63	1.130	113.0	16.4	0.79
	B-5	0.684	0.78	4.53	453	66	1.070	107.0	15.5	0.83
	B-6	0.758	0.94	3.53	353	51	0.871	87.1	12.6	1.00
	B-7	0.849	1.03	2.41	241	35	0.837	83.7	12.1	1.21
1.792	B-1	0.592	0.55	14.2	1420	206	2.044	204.4	29.6	0.83
	B-2	0.809	0.77	4.28/5.00	428/500	62/72	1.264	126.4	18.3	0.98
	B-3	0.779	0.72	6.64	664	96	1.243	124.3	18.0	0.86
	B-4	0.768	0.71	5.52	552	80	1.289	128.9	18.7	0.94
	B-5	0.779	0.76	5.87	587	85	1.180	118.0	17.1	0.75
	B-6	0.845	0.87	4.69	469	68	1.021	102.1	14.8	1.00
	B-7	0.946	1.02	3.23	323	47	0.868	86.8	12.6	1.20

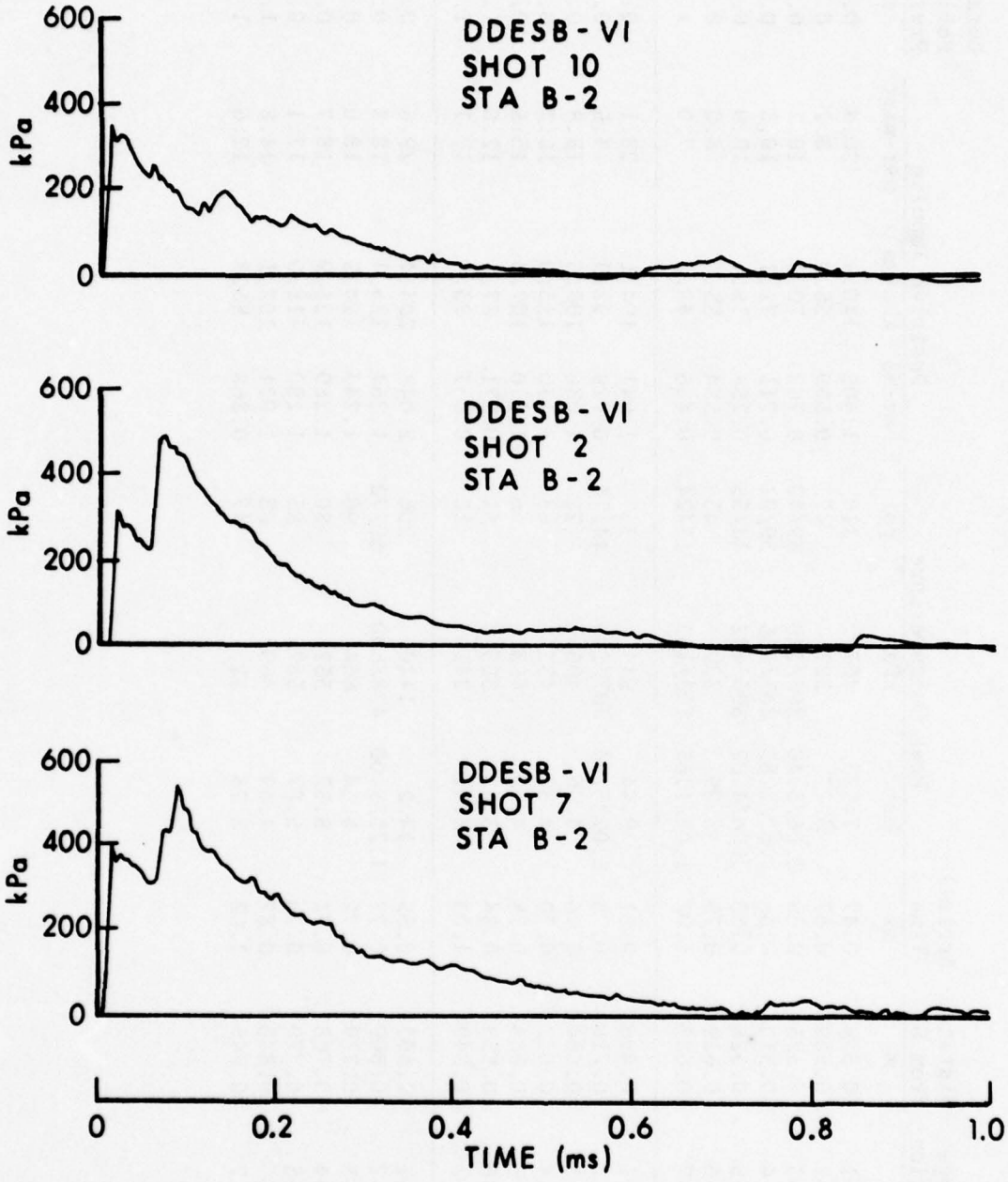

Figure 14. Overpressure versus Time, Station B-2, Test Series I, II, and III

Blast parameters are listed in Table IV.

a. Test Series I. An average charge weight of 0.357 kg was used as the donor charge for this test series. The records of overpressure versus time are not consistent at a given gauge station for similar charge weights. On Shot 8 at Station B-3 a single peak was recorded while on Shots 9 and 10 two peaks were recorded. Gauge Stations B-3 and B-5 were similar while Station B-4 recorded three separate shocks both increasing and decreasing in magnitude. Overpressure versus time records for gauge Stations B-3, B-4, and B-5 for Test Series I are presented in Figure 15.

The positive impulses recorded at the three gauge stations were more repeatable within a test series than the peak overpressures. In test Series I the average impulse from the three gauge stations was 0.722 bar-ms, 72.2 kPa-ms, or 10.47 psi-msec.

b. Test Series II. Test Series II was conducted with an average charge weight of 1.066 kg of pentolite. The records of overpressure versus time were very consistent at the individual gauge stations for the three shots. Data scatter were within plus or minus 6 percent of an arithmetic mean. The average peak overpressure recorded at Station B-3, B-4, and B-5 was 4.60 bar, 460 kPa, or 66.7 psi. Gauge Station B-3 recorded a higher mean value than B-4 or B-5. The records of overpressure versus time presented in Figure 16 show only small variations in the peak values.

The positive impulse recorded at individual gauge stations were within plus or minus 3 percent of an arithmetic mean for the three repeat shots. The positive impulse recorded at the three gauge stations for the three shots of Test Series II fell within a plus or minus 5 percent range of an arithmetic mean. This average overpressure impulse was 1.095 bar-ms, 109.5 kPa-ms or 15.9 psi-msec.

c. Test Series III. In Test Series III the average weight of the three charges was 1.792 kg. The peak overpressures recorded at the individual gauge stations for the three shots were very repeatable with the spread being only a few percent about the mean. The same trend in average pressure values is seen in this series as noted in Series II; i.e., Station B-3 records a higher mean value of peak overpressure than Stations B-4 or B-5. The average peak overpressure recorded at the three stations for the three shots in Test Series III is 6.0 bar, 600 kPa or 87.1 psi. Overpressure versus time recorded at stations B-3, B-4, and B-5 on Shot 6, Test Series III is presented in Figure 17.

Average impulse values determined from Stations B-3, B-4, and B-5 for Test Series III are listed in Table IV. There was very little scatter in the recorded values from shot to shot. The average positive impulse for all stations for the three shots was 1.237 bar-ms, 123.7 kPa-ms, or 17.9 psi-msec.

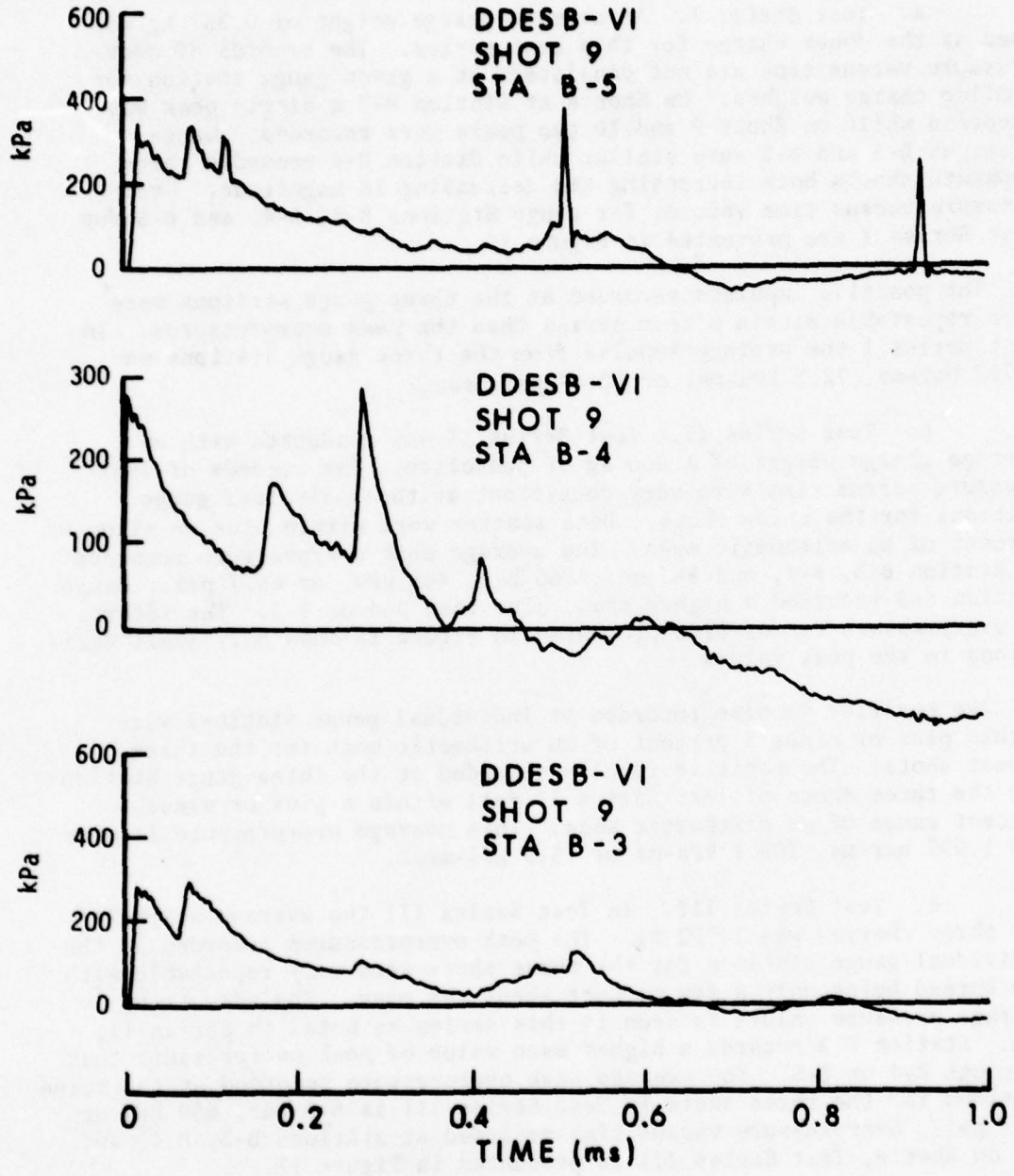

Figure 15. Overpressure versus Time, Station B-3, B-4, and B-5, Shot 9, Test Series I

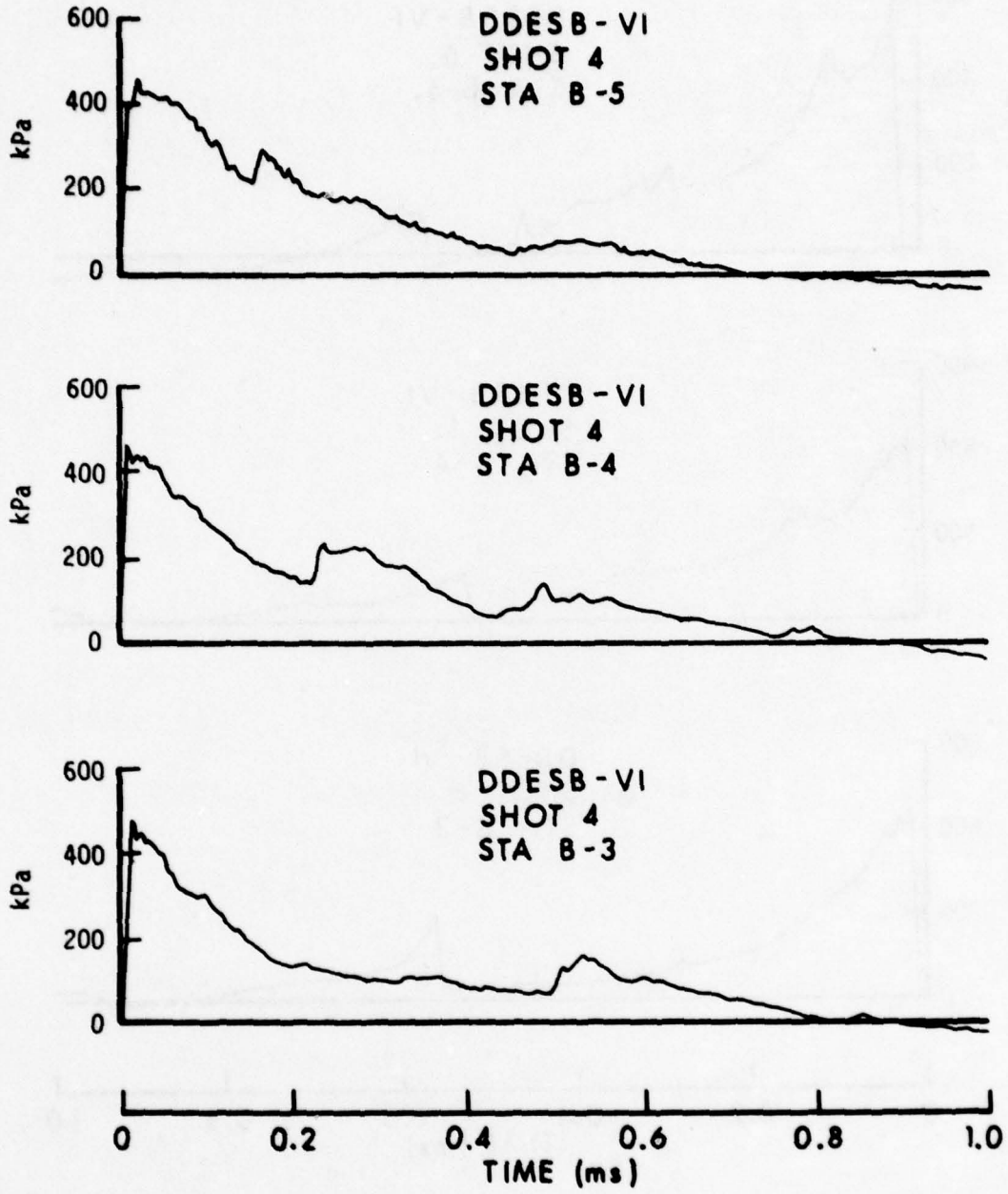

Figure 16. Overpressure versus Time, Station B-3, B-4, and B-5, Shot 4, Test Series II

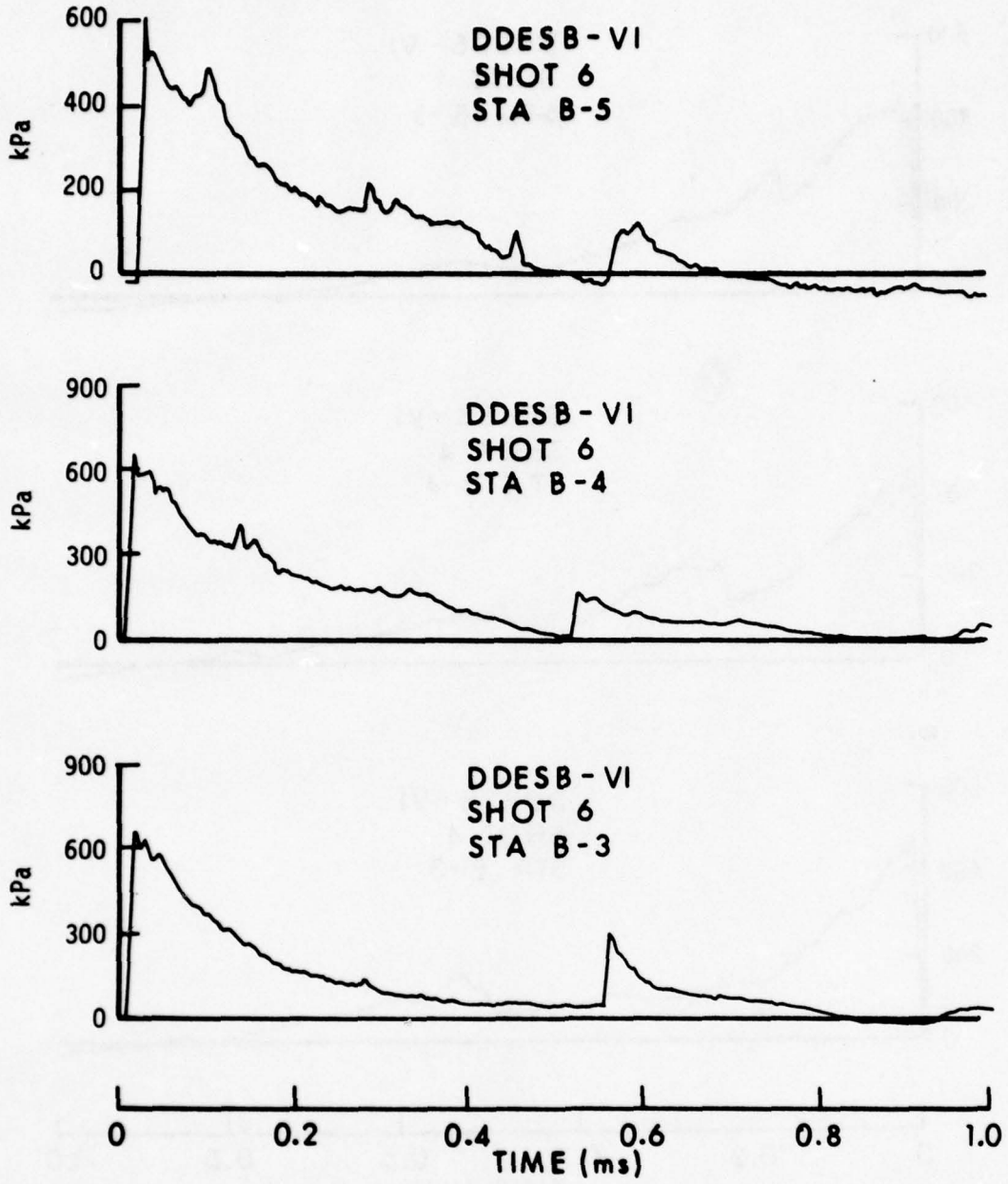

Figure 17. Overpressure versus Time, Station B-3, B-4, and B-5, Shot 6, Test Series III

It should be noted that from gauge Stations B-3, B-4, and B-5, gauge Station B-4 always recorded the lowest average peak overpressure but always recorded the highest average positive impulse value on Test Series II and III.

4. Overpressure and Impulse on End Slope - Station B-6. There was only one gauge station (B-6) located on the end slope of Structure B. All records of overpressure versus time had an initial pressure rise followed by a classical pressure decay behind the shock front. There was very little scatter in peak overpressure or positive impulse values within each series of shots. The results are listed in Table IV, with an example of the recorded overpressure and impulse versus time for Shot 5, Test Series III, presented in Figure 18.

5. Overpressure and Impulse on the Back Slope - Station B-7. The side of the structure away from the donor was instrumented with one gauge station (B-7). Location is shown in Figure 9. There are multiple peaks in the records of overpressure versus time from Test Series I. The multiple reflections are similar to those recorded at Station B-4 on Test Series I, and may have propagated back to Station B-7; see example from Shot 9, Figure 19.

On test Series II the peak overpressure and positive impulse both show excellent repeatability. The variation in the three shots was less than plus or minus 2 percent of the mean values. Example of overpressure versus time is given in Figure 19, for Shot 4.

Results from Test Series III also show good repeatability from shot to shot. The records of overpressure versus time from the three shots are quite similar. An example of the overpressure versus time recorded on Shot 6 is presented in Figure 19. Recorded values of the positive impulse are well within acceptable accuracy of ± 10 percent.

Average values of the blast parameters for gauge Station B-7 are listed in Table IV.

C. Blast Loading on Structure C

The blast loading on Structure C will be treated in two phases. Phase 1 will include the loading on the headwall and door while Phase 2 will cover the loading on the top and side of the structure. The safe separation distance was $0.8Q^{1/3}$ for the structure to the rear of the donor. There were eight gauge stations. The locations are shown in Figure 10. Average values of the blast parameters recorded for the three shots in each test series are listed for the eight gauge stations in Table V.

1. Overpressure and Impulse on Headwall of Structure C. The blast loading on the headwall and door of Structure C consist of incident and reflected shocks striking the upper two thirds of the headwall while a

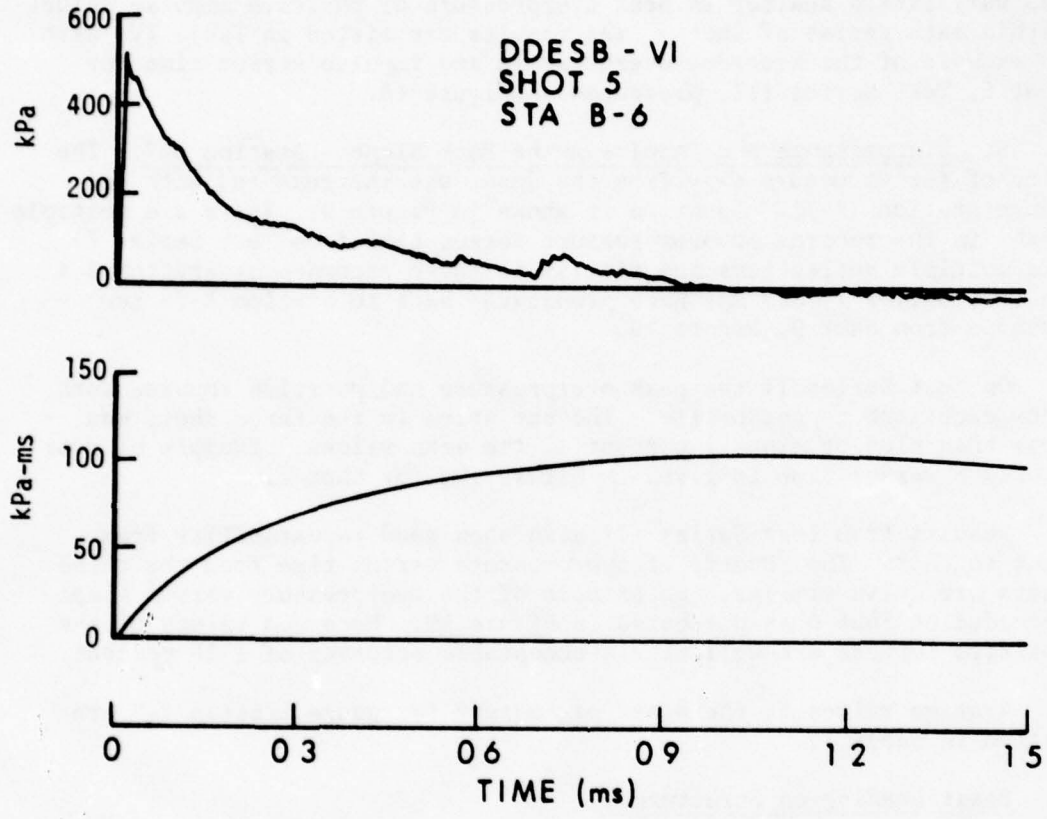

Figure 18. Overpressure and Impulse versus Time, Station B-6, Shot 5, Test Series III

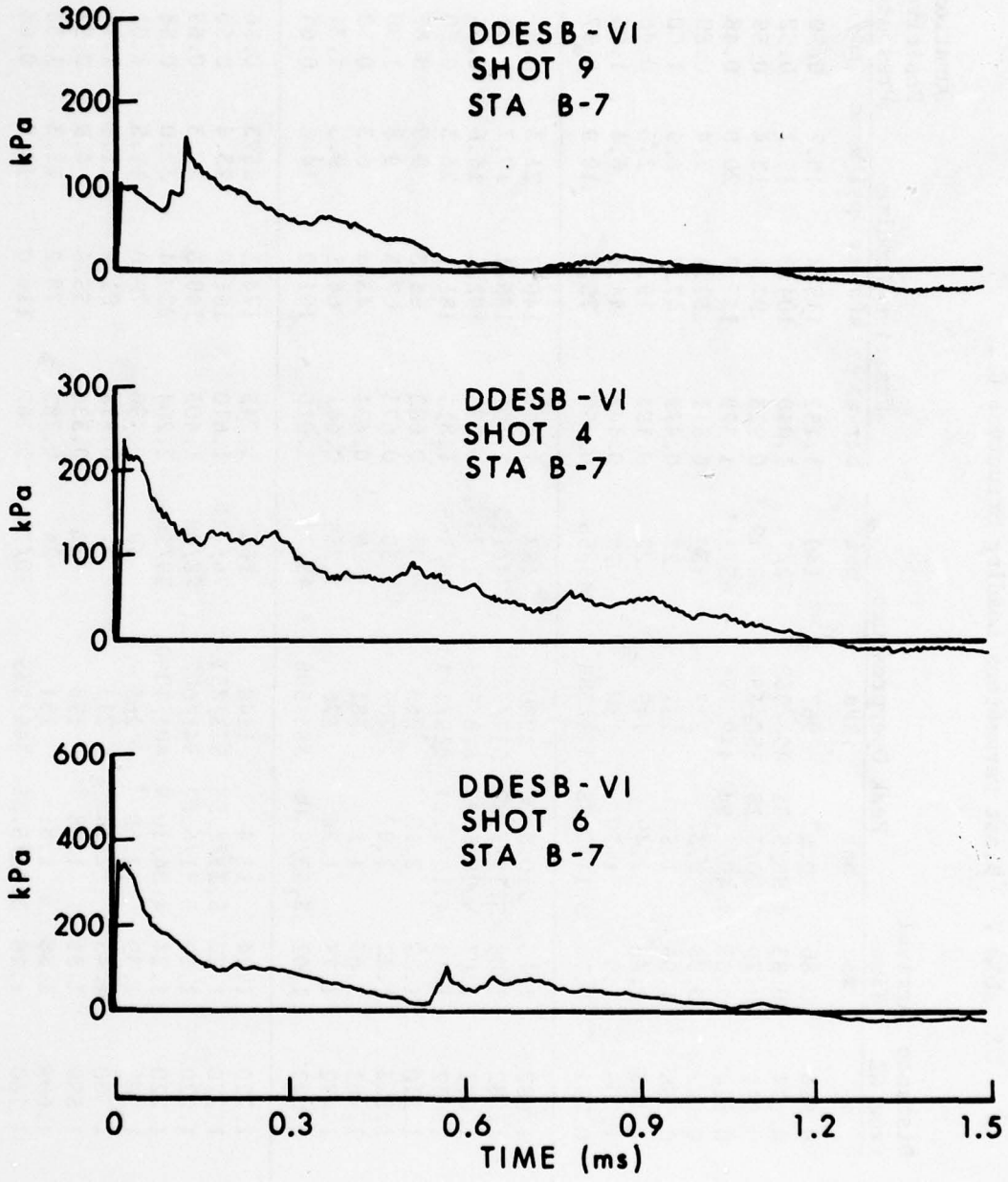

Figure 19. Overpressure versus Time, Station B-7, Test Series I, II, and III

Table V. Blast Parameters Loading Structure C

Charge Weight	Gauge Station	Distance from GZ	Arrival Time	Peak Overpressure			Positive Impulse			Duration Positive Pressure
kg		m	ms	bar	kPa	psi	bar-ms	kPa-ms	psi-msec	ms
0.357	C-1	0.814	0.86	9.67	967	140	1.152	115.2	16.7	0.50
	C-2	0.814	0.83	4.96/5.38	496/538	72/78	1.040	104.0	15.1	0.52
	C-3	0.814	0.79	5.50/3.39	550/339	80/49	0.923	92.3	13.4	0.59
	C-4	0.814	0.83	4.49/7.94	449/794	65/115	1.379	137.9	20.0	0.48
	C-5	0.942	0.98	2.37	237	34	0.511	51.1	7.4	0.89
	C-6	0.958	1.06	1.57	157	23	0.479	47.9	6.9	1.00
	C-7	1.193	1.43	1.49	149	22	0.194	19.4	2.8	0.46
	C-8	1.206	1.51	1.30	130	19	0.444	44.4	6.4	1.05
	F-1	0.754	0.74	3.11/3.88	311/388	45/56	0.750	75.0	10.9	0.57
1.066	C-1	1.082	1.10	10.8	1080	157	1.467	146.7	21.3	0.51
	C-2	1.082	1.08	5.11/7.82	511/782	74/113	1.361	136.1	19.7	0.51
	C-3	1.082	1.07	5.28/5.03	528/503	77/73	1.026	102.6	14.9	0.55
	C-4	1.082	1.10	4.15/11.4	415/1140	60/165	1.815	181.5	26.3	0.50
	C-5	1.210	1.25	2.63	263	38	0.683	68.3	9.9	0.87
	C-6	1.223	1.32	2.07	207	30	0.673	67.3	9.8	1.00
	C-7	1.461	1.67	1.81	181	26	0.434	43.4	6.3	0.79
	C-8	1.472	1.75	1.76	176	25	0.641	64.1	9.3	1.31
	F-1	1.022	1.02	3.33/5.06	333/506	48/73	1.010	101.0	14.6	0.64
1.792	C-1	1.220	1.24	11.4	1140	165	1.745	174.5	25.3	0.56
	C-2	1.220	1.22	5.23/8.53	523/853	76/124	1.610	161.0	23.4	0.53
	C-3	1.220	1.19	5.41/6.07	541/607	78/88	1.403	140.3	20.3	0.65
	C-4	1.220	1.24	4.04/10.9	404/1090	59/158	2.204	220.4	32.0	0.58
	C-5	1.348	1.39	2.68	268	39	0.790	79.0	11.5	1.01
	C-6	1.360	1.45	2.13	213	31	0.814	81.4	11.8	1.11
	C-7	1.599	1.81	1.98	198	29	0.336	33.6	4.9	0.52
	C-8	1.609	1.88	1.81	181	26	0.782	78.2	11.3	1.38
	F-1	1.160	1.16	3.45/5.35	345/535	50/78	1.160	116.0	16.8	0.66

Mach stem shock strikes the lower third. Gauge Station F-1 was located 0.060 metres to the front of the structure and mounted flush with the ground surface. A general description of the shock loading will be given, which will apply to the three test series.

If we assume that when the blast wave propagates out of the rear of the donor magazine and travels down the 26.6 degree rear slope, it tends to become perpendicular to the slope as shown in Figure 20. Upon reaching the ground surface, if the angle of incidence is assumed to be 63.4 degrees, then a Mach stem will form and the ground surface will be in the Mach reflection region while above the triple point there will be an incident and reflected shock. Upon shock arrival at the acceptor structure the headwall and door will be subjected to a very complex loading with the reflection of the incident wave, reflected wave, and Mach stem wave. The assumed interactions are shown in Figure 21. The height of the triple point on the headwall and door can be determined by extrapolating the time of arrival between the incident and reflected shocks at gauge Stations C-3 and C-2 to zero time. On five shots, incident and reflected shocks were recorded at gauge Station C-4 which means on these five shots it was above the triple point and on four shots it was below the triple point. At gauge Station C-1 a single shock was always recorded showing it was always below the triple point and that the Mach stem pressure was being reflected on the lower portion of the headwall. The overpressure versus time recorded at the four gauge stations is presented in Figure 22 for Shot 8, Test Series I.

Some general observations noted concerning the reflected overpressure recorded on the front wall of Structure C are discussed as follows. At Gauge Station C-3 the first reflected overpressure was higher than the first reflected overpressure recorded at Gauge Station C-2, and the first reflected overpressure recorded at Gauge Station C-2 is greater than the first reflected overpressure recorded at Gauge Station C-4. This observation is shown in Figure 22. The magnitude of the second reflected peak overpressure is a function of the time interval between the two shocks. This phenomenon is shown on Test Series II, in Figure 23, where it can be seen that as the time interval between the two shocks decreases the magnitude of the second reflected shock increases. The time interval between the two shocks is a function of the height of the triple point. The lower the triple point, the larger the time interval. At Station C-2 (Figure 23) the time interval between the two shocks is the largest on Shot 2 and on that shot the triple point was below Station C-4. The magnitudes of the first reflected shock overpressures will be discussed in a later section.

The magnitude of the positive impulse recorded on the headwall of Structure C is a function of the donor charge weight and the gauge station location. The closer a gauge station location is to the top or side slope of the structure the sooner a rarefaction wave will reach the gauge station causing a more rapid relief of the reflected overpressure. Following this reasoning the positive impulse should increase

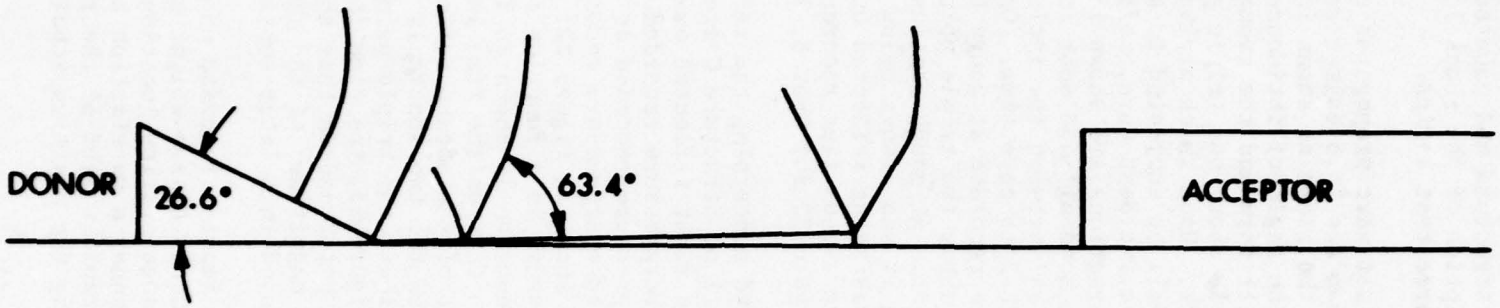

Figure 20. Blast Wave Profiles to Rear of Donor Magazine

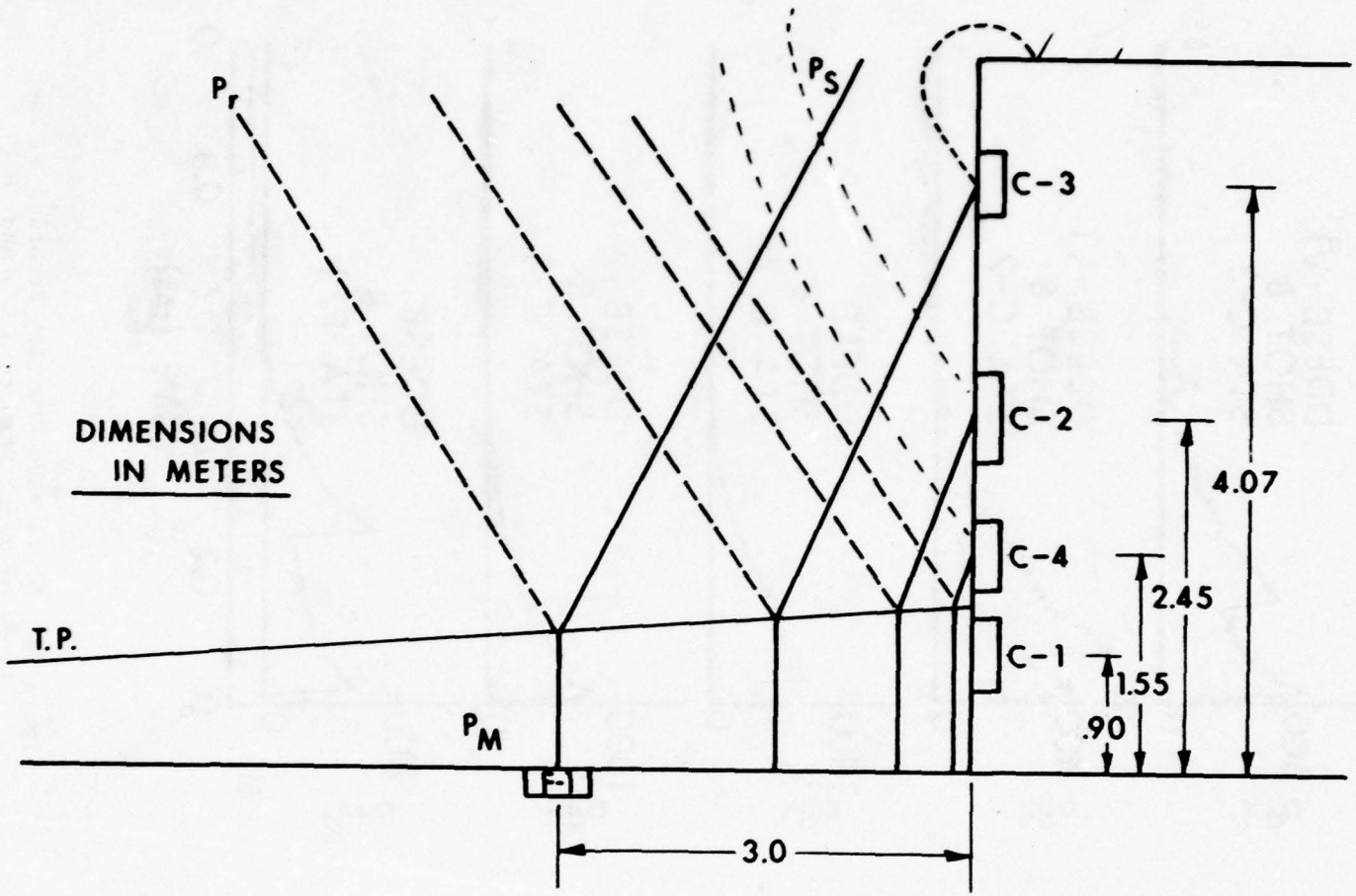

Figure 21. Shock Interactions on Headwall of Structure C

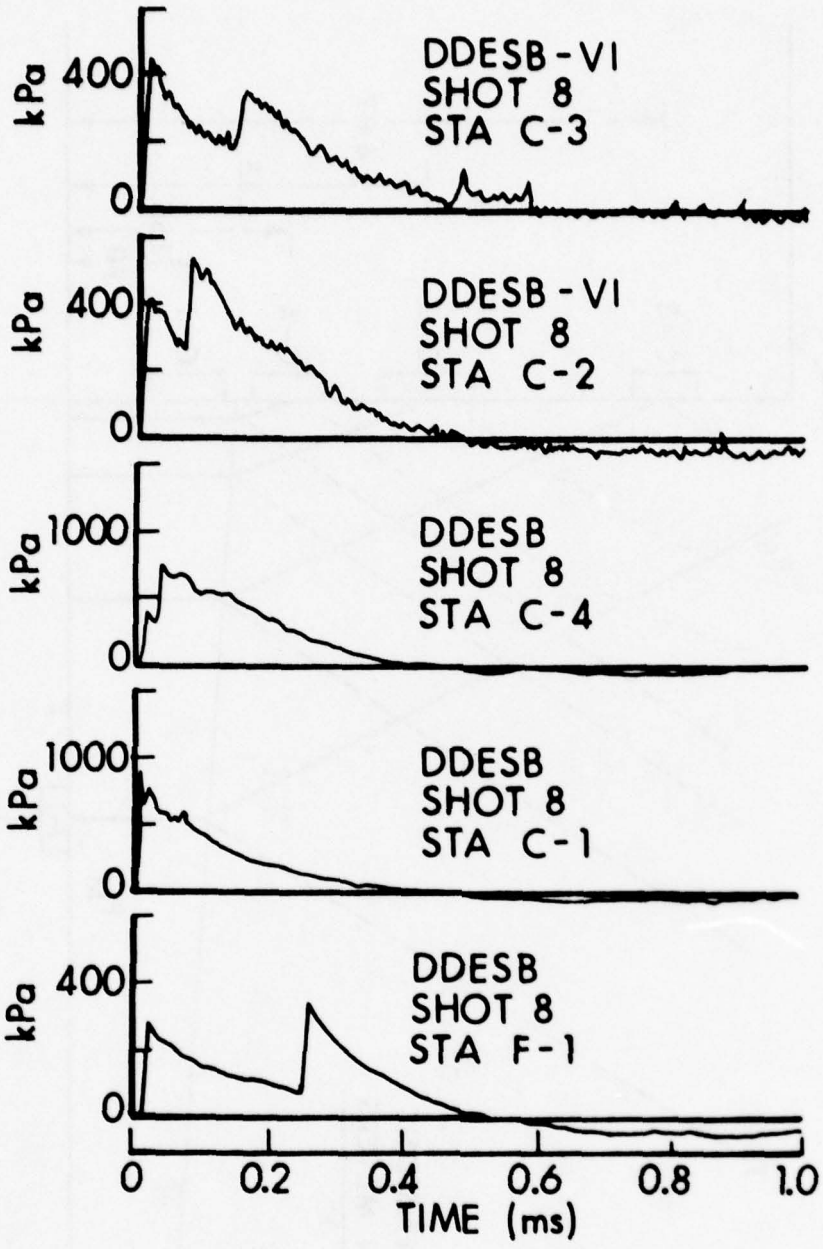

Figure 22. Shock Wave Profiles Recorded on the Front of Model Structure C - Shot 8

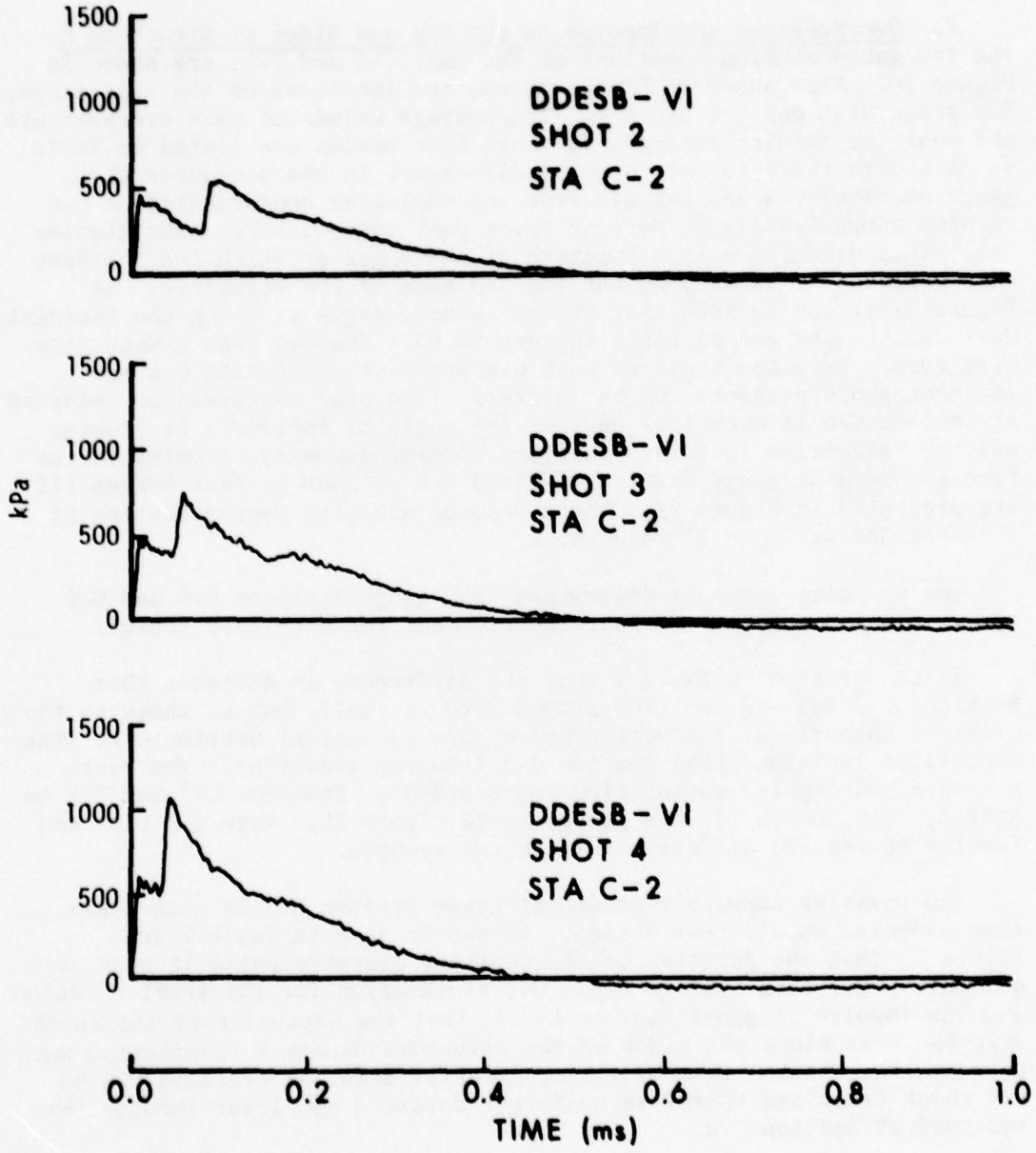

Figure 23. Effect of Arrival Time on Magnitude of Second Reflected Shock

in magnitude from Station C-3 to, C-2, to C-1, and be the largest at Station C-4. In Table V it can be seen that this is the trend that was established for each test series.

2. Overpressure and Impulse on the Top and Sides of Structure C. The two gauge station locations on the top, C-5 and C-7, are shown in Figure 10. Also shown in Figure 10 are the locations on the side slope, for gauge Stations C-6 and C-8. The average values of peak overpressure and positive impulse recorded for each test series are listed in Table V. Although there is only a small difference in the distances that gauge Stations C-5 and C-6 are from the explosive center, Station C-6 records approximately 20 percent lower peak overpressures than Station C-5. This difference is a function of the angle at which the incident wave strikes the surface of the top and side of the structure. In Figure 21 it can be seen that if the assumed angle at which the incident wave strikes the top of the structure is 63.4 degrees then a Mach stem will form. From the measured peak overpressure at Station C-5 the incident shock pressure can be inferred. The peak overpressure recorded at Station C-6 is much less because the angle of incidence is greater and the refiection factor is smaller. Overpressure and impulse versus time recorded at gauge Stations C-5 and C-6 on Shot 6, Test Series III are presented in Figure 24. These records are also representative of the Test Series I and II results.

The positive impulses determined from gauge Stations C-5 and C-6 are within ± 3 percent of an arithmetic mean for each test series.

It can be seen in Table V that the difference in distance that Stations C-7 and C-8 are from ground zero is small, but as shown in the previous comparison, the peak overpressure is less at Station C-8, (the side slope location) than Station C-7 (the top location). The overpressure and impulse versus time as recorded at Stations C-7 and C-8 on Shot 3, Test Series II, are presented in Figure 25. Note the time and impulse scales are different for the two records.

The positive impulse recorded at gauge Station C-7 is much lower than expected on all test series. It can be seen in Table V and Figure 25 that the duration of the positive pressure pulse is much less at Station C-7 than Station C-8. One explanation for the short duration and low impulse at gauge Station C-7 is that the expansion of the shock down the rear slope and sides of the structure causes a rarefaction wave to reach the station thereby giving a faster decay of pressure behind the shock front and therefore a shorter duration and lower impulse than recorded at Station C-8.

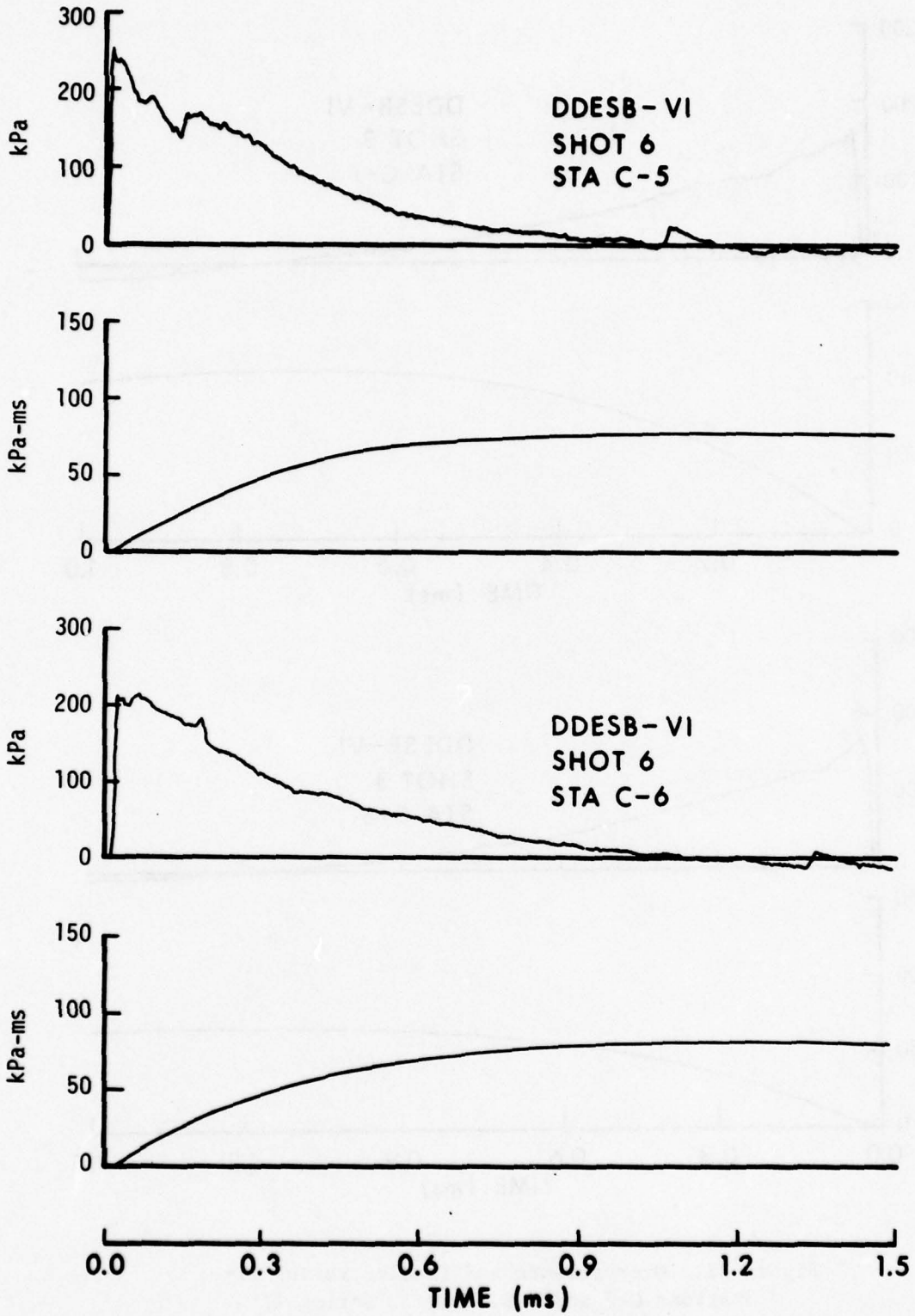

Figure 24. Overpressure and Impulse versus Time, Station C-5, and C-6, Shot 6, Test Series III

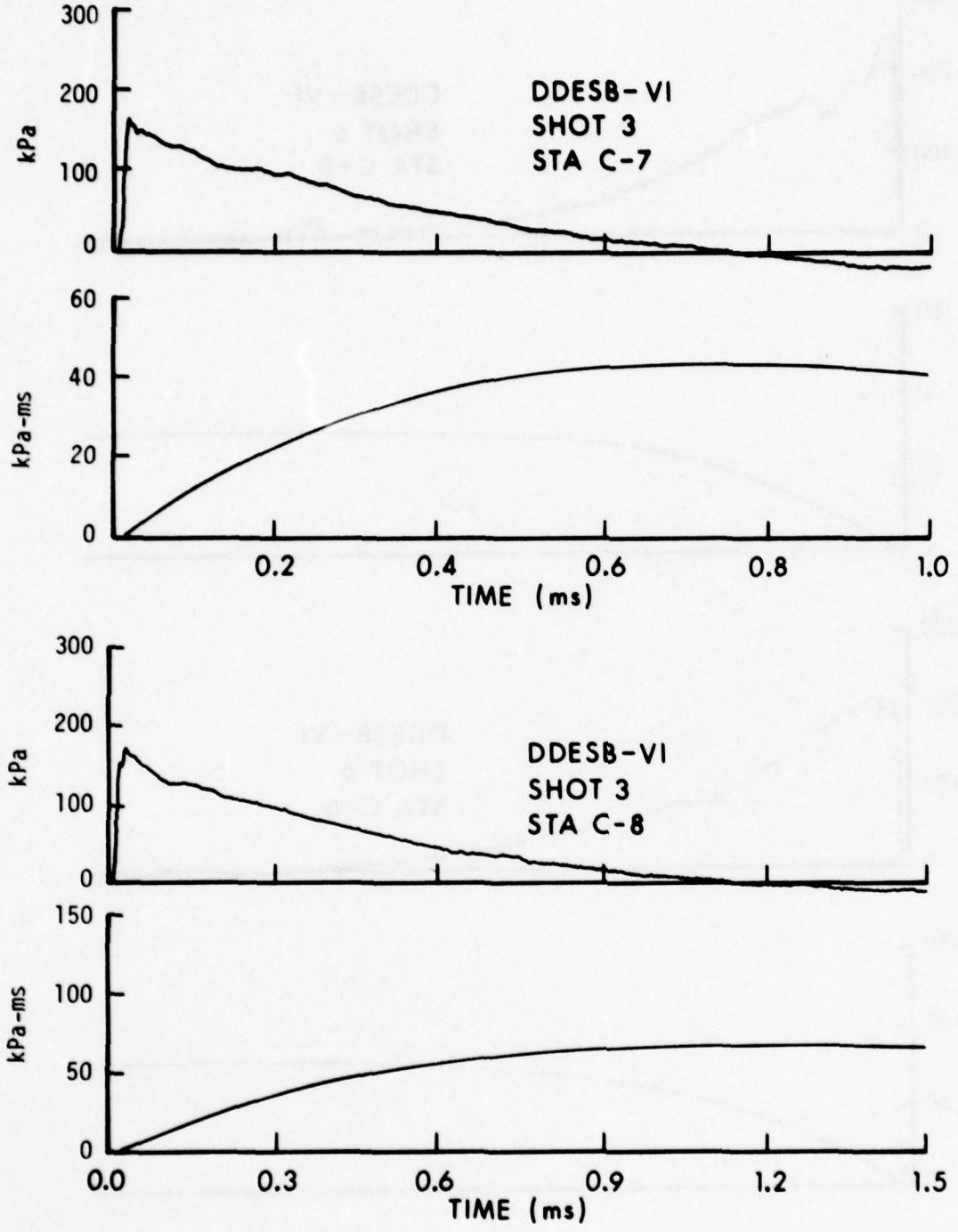

Figure 25. Overpressure and Impulse versus Time, Stations C-7 and C-8, Shot 3, Series II

IV. COMPARISON OF RESULTS

The comparison of the data from this series of tests with other scaled model tests and available full-scale tests results will be done on a full-scale test basis. In order to compare the U.S., 1/50th model results with the UK, 1/10th scale results[2] both will be scaled to full-size.

A. Comparison of Blast Loading on Structure A

A comparison of peak overpressure and positive impulse recorded on the US model will be made with the same parameters recorded on the UK model. The UK and US relative gauge locations are shown in Figure 26. They remain constant on the models for all charge weights. The UK donor model had a rectangular cross-section rather than an arch cross-section as the US model shown in Figure 1. A sketch of the UK 1/10 scale donor model is shown in Figure 27. Because of the difference in the length of the donor models, the scaled-up or full size distances from the center of the donor charge to the recording stations vary for each charge weight. The interior volume of the US donor would be 660 m^3 and the UK donor 729 m^3. The scaled-up charge weights, distances, peak overpressures, and positive impulses for UK gauge Stations 3 and 4, and US gauge Stations A-4 and A-6 are listed in Table VI. It appears in Table VI that the peak overpressure recorded on both models are charge weight dependent; i.e., as the charge weight increases the overpressure values listed increase. One reason for this dependency is the definition of "safe separation" distances as the distance from the rear interior of the acceptor to the front wall of the donor rather than the center of the explosive source within the donor. Note that as the charge weight increases the scaled distance from the center of the explosive source (GZ) decreases within the UK and US tests. Therefore higher peak overpressure would be expected at the smaller scaled distances.

Although the donor magazine used in the UK and US test series were quite different in scale, interior design, and structural materials, similar trends are noted in comparisons of peak overpressure and positive impulse made in Table VI.

As noted in the Results Chapter, Section A.2, for charge weights greater than 44625 kg, there is a significant increase in positive impulse as the shock wave moves from gauge Station A-4 to A-6. This trend was also recorded on the UK test series as the shock wave moved from Station 3 to Station 4.

---

[2] *UK Report, "Blast and Projections from Model Igloos," Report No. ETN 124-76, Proof and Experimental Establishment, Shoeburgness*

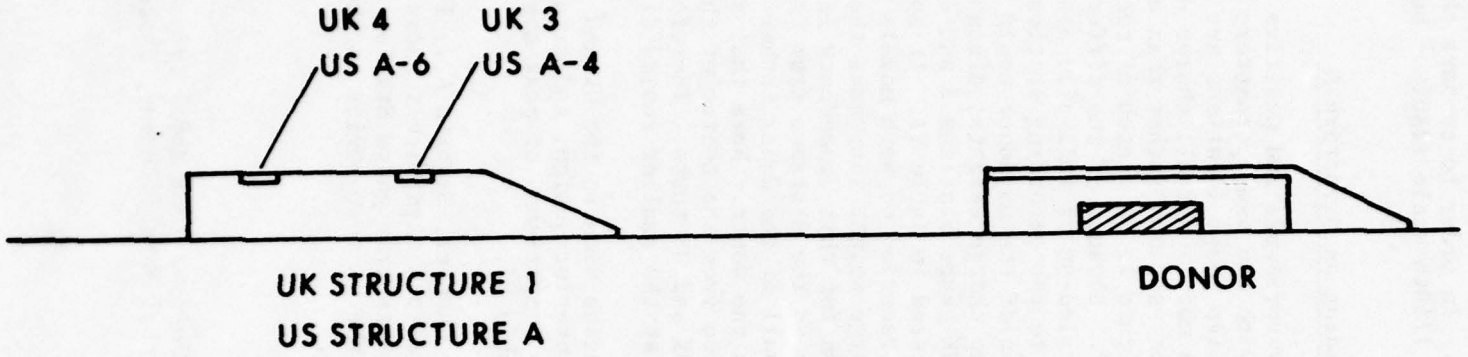

Figure 26. UK and US Gauge Locations - Structure A

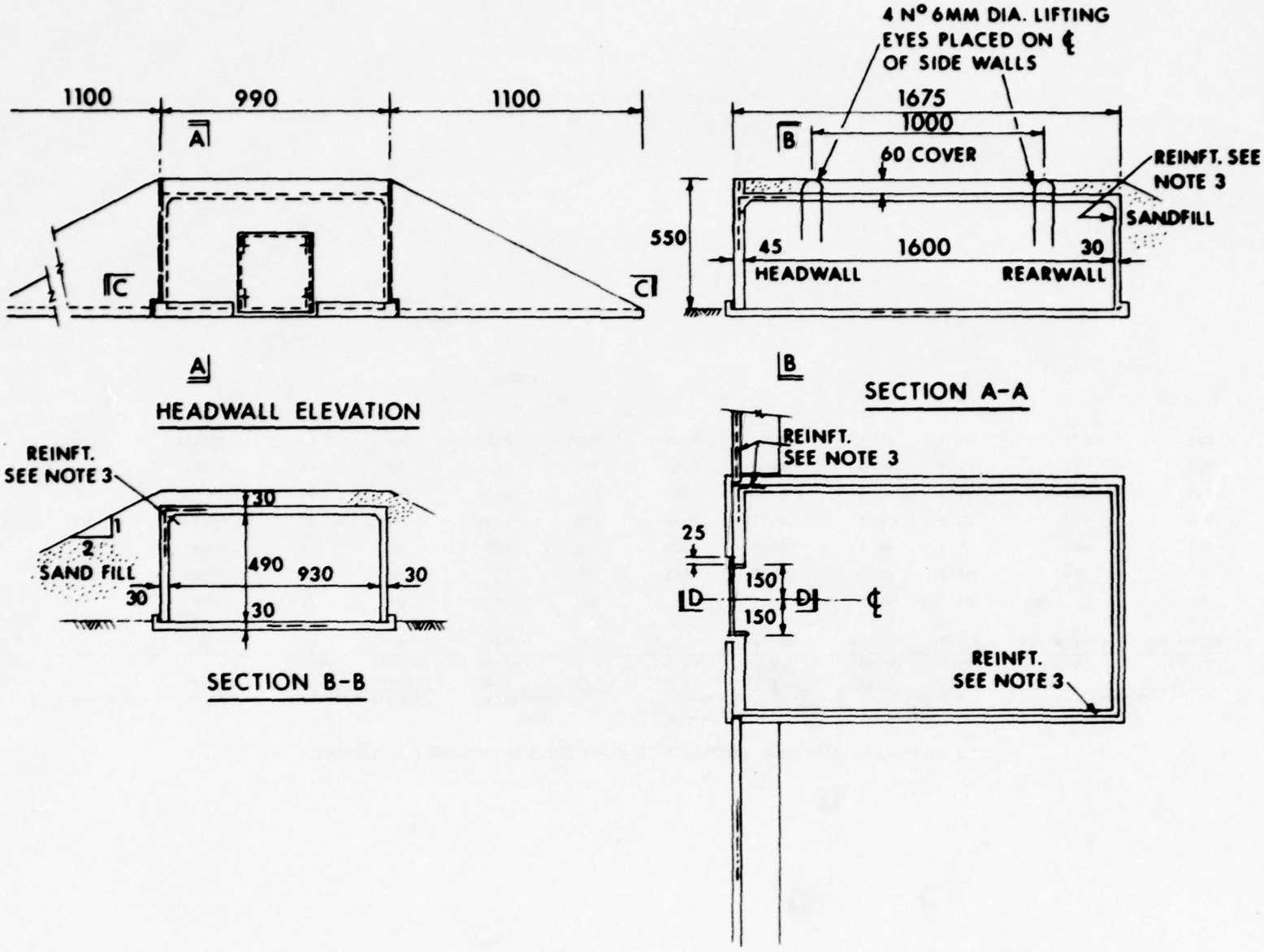

Figure 27. UK, 1/10th Scale Donor Model

Table VI. Comparison of Blast Loading on Acceptor Structure in Front of Donor

Reference	Charge Weight	Distance from GZ		Peak Overpressure		Overpressure Impulse		Scaled Distance		Scaled Impulse	
		UK-3 US-A4	UK-4 US-A6	UK-3 US-A4	UK-4 US-A6	UK-3 US-A4	UK-4 US-A6	UK-3 US-A4	UK-4 US-A6	UK-3 US-A4	UK-4 US-A6
	kg	m	m	kPa	kPa	kPa-ms	kPa-ms	$m/kg^{1/3}$	$m/kg^{1/3}$	$kPa-ms/kg^{1/3}$	$kPa-ms/kg^{1/3}$
UK	8000	27	42	303	76	-	1380	1.35	2.10	-	69
US	44625	46	59	726	346	3950	2730	1.30	1.66	111	77
UK	64000	43	58	855	503	4000	6960	1.08	1.45	100	174
UK	125000	51	66	1117	621	4830	5390	1.02	1.32	97	108
US	133250	58	71	1150	662	6550	7770	1.14	1.39	128	152
UK	216000	59	74	910	1331	7520	7580	0.98	1.23	125	126
US	224000	66	79	1410	1000	6830	8670	1.09	1.30	112	143

B. Comparison of Blast Loading on Structure B

Data that can be used for comparing the blast loading on Structure B with full-scale or other model tests are quite limited. A comparison will be made between the results recorded on ESKIMO III[3]. The donor charge consisted of 158900 kg of Tritonal encased in M117 bombs. A reduction factor of 0.753, presented in Reference 3, was used to account for bomb casing, giving 119652 kg Tritonal equivalent. Therefore a comparison will be made with model test data from Test Series II (1.066 kg) pentolite scaled to full size (133250 kg). The location of the gauge positions on ESKIMO III are shown in Figure 28. Gauge locations on model Structure B were shown in Figure 9.

The values of peak overpressure and positive impulse reported in Reference 3 are listed in Table VII along with the values of peak overpressure and positive impulse listed in Table IV for the 1.066 kg charge scaled up to full scale (133250 kg). In general the peak overpressures recorded on the ESKIMO III structures were higher than those recorded on the model structure but the positive impulse values show a fair agreement.

A comparison of the peak overpressures and positive impulses over the full scale structure is made in Figures 29 and 30.

C. Comparison of Blast Loading on Structure C

A discussion of the comparison of blast loads on a storage magazine located to the rear of the donor will be divided into two areas. The first will be the headwall and door while the second area will be the blast load on the top surface of the structure.

1. Comparison of UK and US Model Results on Headwall of Structure to Rear of Donor. Four US gauge locations were installed on the headwall of Structure C. These locations are shown in Figure 31. The relative locations of three UK gauge positions, 18, 19, and 20, taken from Reference 2, are also shown in Figure 31. For a direct comparison, the results from the US 1/50th scaled model and the UK 1/10th scaled model have been scaled to full size. There were four charge weights used in the UK test series. They were 8, 64, 125, and 216 kg. The scale factor is 10^3 for full size. Results of the peak overpressure on the front headwall and door of a full size structure are presented in Table VIII. The positive impulses on the same full size structure are presented in Table IX.

Because of the sensitivity of the peak values of the reflected shocks to arrival times and the height of the Mach stem the comparison of overpressure impulse loading on the headwall and door is much better

[3] *F. H. Weals, "ESKIMO III Magazine Separation Tests," Naval Weapons Center Report NWC TP 5771, February 1976.*

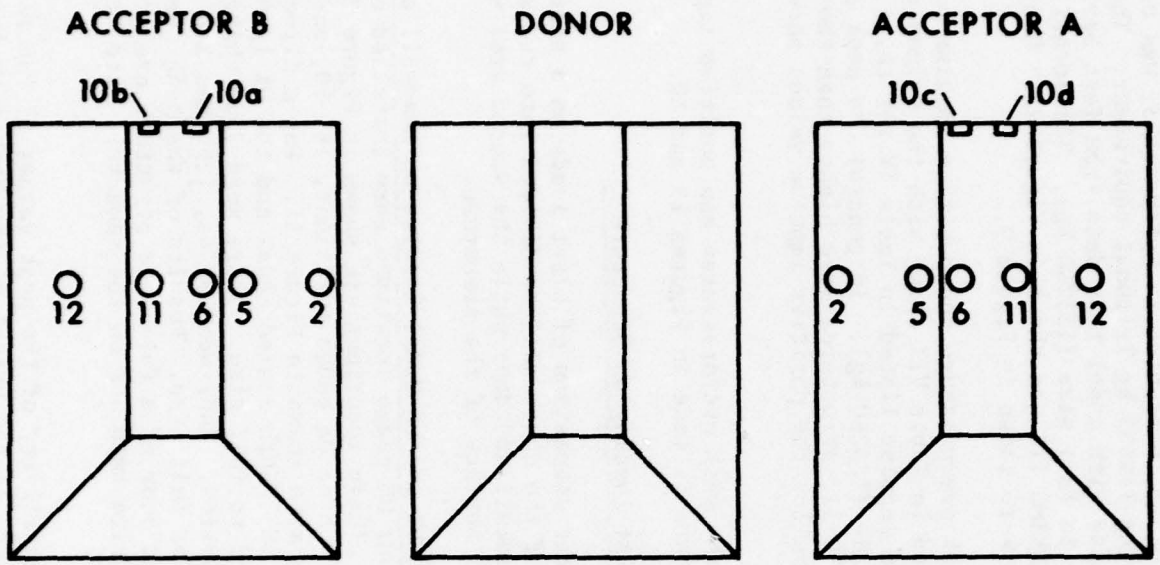

Figure 28. Gauge Locations on ESKIMO III

Table VII. Comparison of Blast Loading on Acceptor to Side of Donor

Reference	Gauge Location	Distance from GZ	Peak Overpressure			Overpressure Impulse		
		m	bar	kPa	psi	bar-ms	kPa-ms	psi-msec
E III	2a	22.6	7.6	760	110	-	-	-
	2b	22.6	8.3	830	120	55.4	5540	803
M	B-1	24.8	9.4	940	136	70.2	7020	1018
E III	5a	28.7	11.4	1140	165	46.7	4670	677
E III	10a	33.8	5.1	510	74	42.5	4250	616
	10c	33.8	3.8	380	55	41.4	4140	600
M	B-2	35.9	5.2	520	75	46.6	4640	673
E III	10b	39.6	4.1	410	59	40.9	4090	593
	10d	39.6	2.8	280	41	54.8	5480	795
E III	6a	31.7	5.5	550	80	36.5	3650	529
	6b	31.7	6.6	660	96	55.6	5560	806
M	B-3	34.2	5.0	500	72	54.3	5430	787
M	B-4	33.6	4.3	430	62	56.5	5650	819
M	B-5	34.2	4.5	450	65	53.5	5350	776
E III	11a	37.8	5.6	560	81	42.9	4290	622
	11b	37.8	5.9	590	86	44.3	4430	642
M	B-6	37.9	3.5	350	51	43.6	4360	632
M	B-7	42.5	2.4	240	35	41.8	4180	606
E III	12a	43.5	2.8	280	41	33.4	3340	484

Reference E III - ESKIMO III (119 652 kg Tritonal)

M - Model scaled to full size (133 250 kg Pentolite)

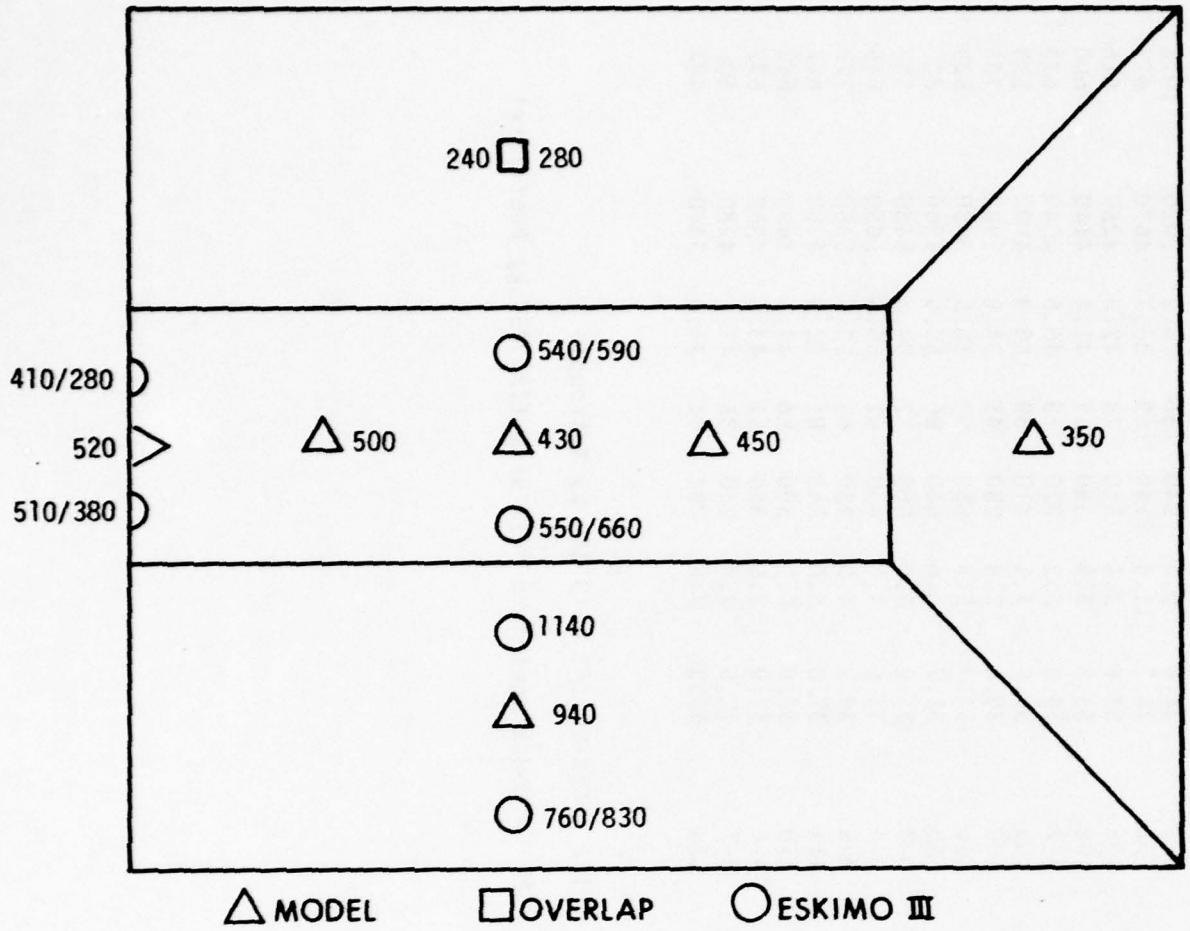

Figure 29. Peak Overpressure (kPa) Comparison, Model versus ESKIMO III

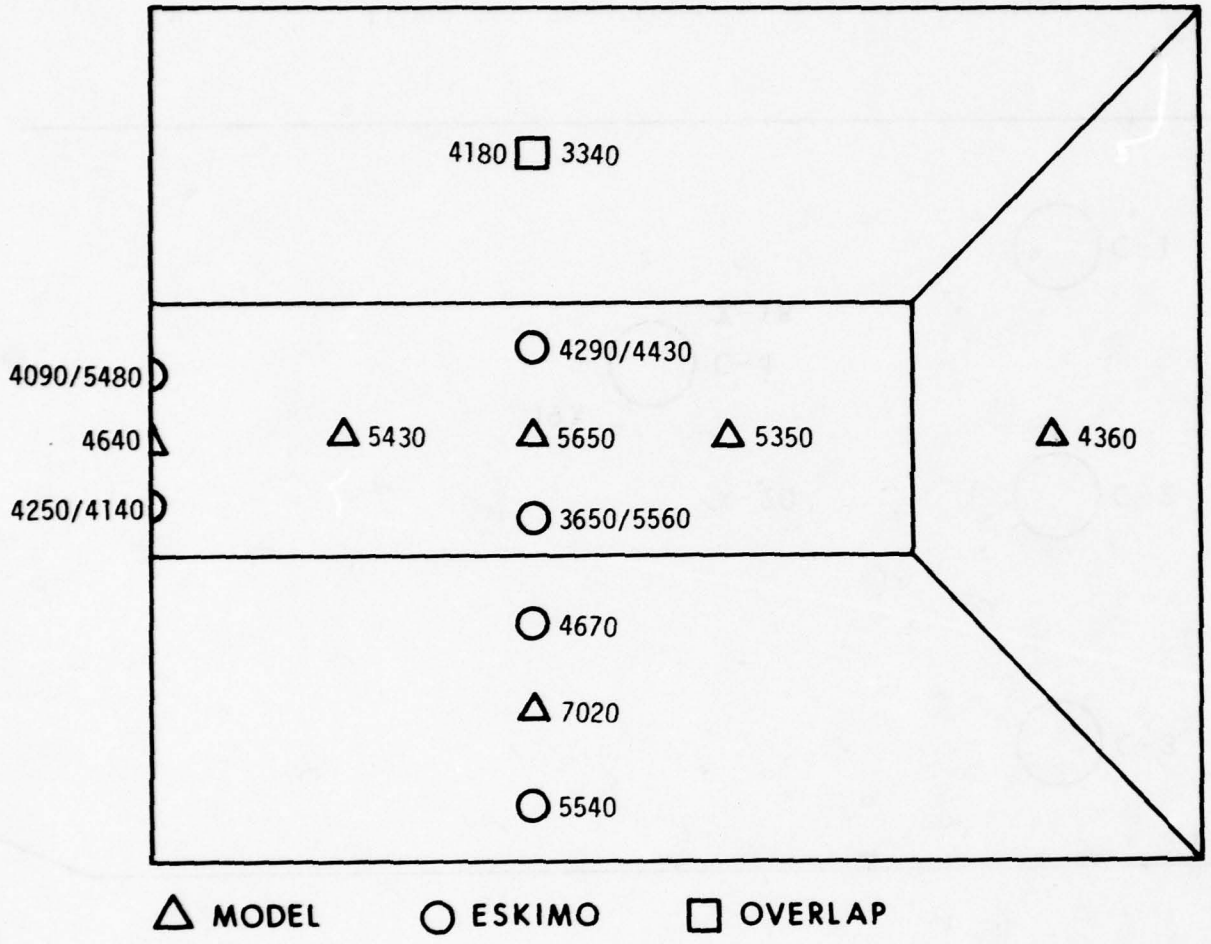

Figure 30. Positive Impulse (kPa-ms) Comparison, Model versus ESKIMO III

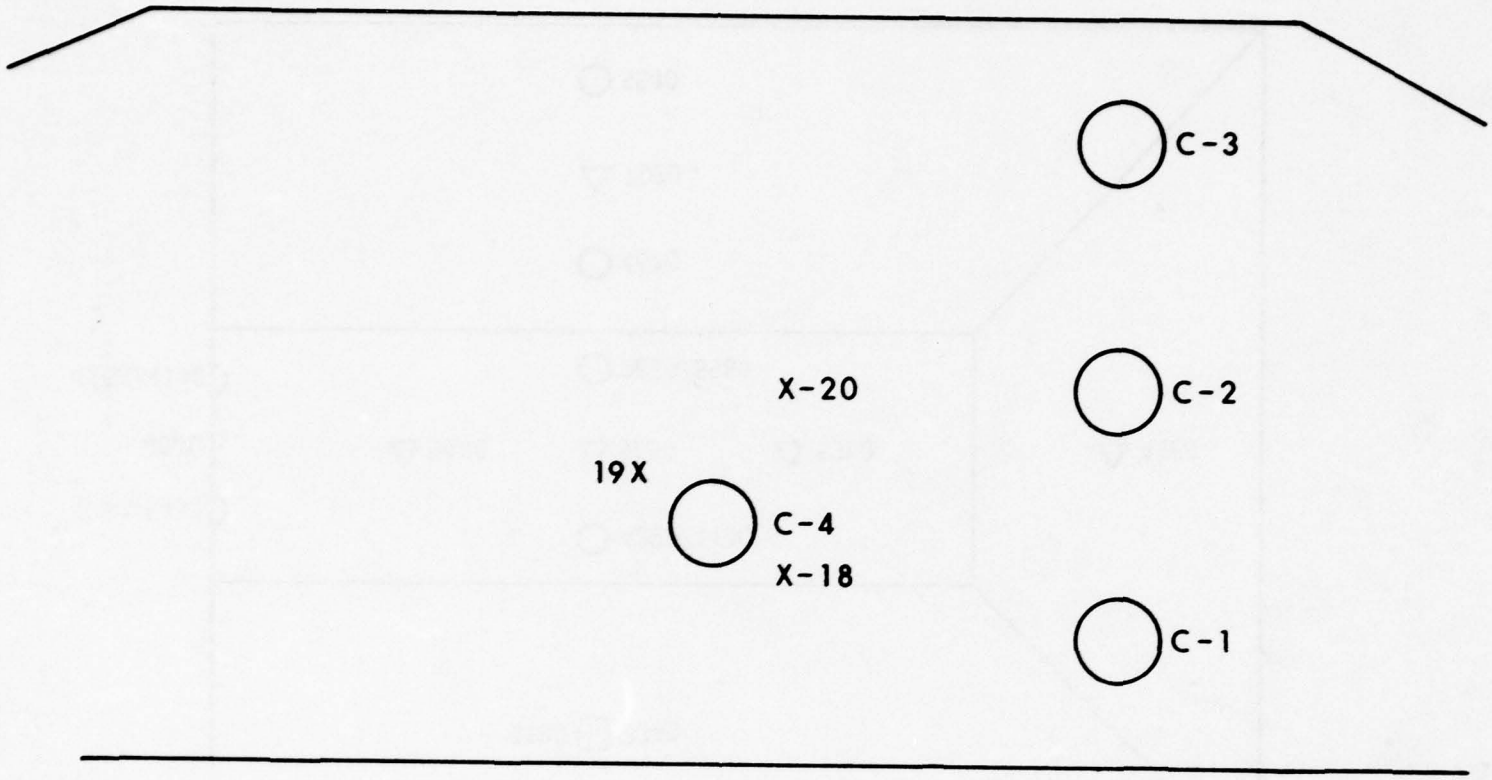

Figure 31. Gauge Locations on Front of US Model Structure C and UK Model Structure 3

Table VIII. Peak Overpressure on Headwall of Structure to Rear of Donor

UK Results

Charge Weight kg	GZ to Headwall m	Gauge Stations 17 kPa	18 kPa	19 kPa	20 kPa
8000	24	225/170	97/145	200/248	214/172
64000	40	300/326	862	317/621	331/493
125000	45	350/448	448/848	400/793	428/690
216000	53	360/665	1630	421/834	462/745

US Results

Charge Weight kg	GZ to Headwall m	Gauge Stations F-1 kPa	C-1 kPa	C-2 kPa	C-3 kPa	C-4 kPa
44625	38	311/388	967	496/538	550/339	449/794
133250	51	333/506	1075	511/782	528/503	415/1140*
224000	58	345/525	1144	523/853	541/607	404/1092*

NOTE: 1. Values separated by / indicates an initial shock followed by a reflected shock.

2. UK gauge Station 17 and US gauge Station F-1 are mounted flush with the ground surface 3 metres (full-scale) in front of the headwall.

*Two shocks occurred on one of three shots.

Table IX. Positive Impulse on Headwall of Structure to Rear of Donor

UK Results

Charge Weight kg	GZ to Headwall m	Gauge Stations 17 kPa-ms	18 kPa-ms	19 kPa-ms	20 kPa-ms
8000	24	2010	1850	2270	2190
64000	40	3780	5770	5120	5030
125000	45	5720	8370	7810	7830
216000	53	6880	10780	9640	9430

US Results

Charge Weight kg	GZ to Headwall m	Gauge Stations F-1 kPa-ms	C-1 kPa-ms	C-2 kPa-ms	C-3 kPa-ms	C-4 kPa-ms
44625	38	3750	5760	5200	4610	6900
133250	51	5050	7340	7280	5130	9080
224000	58	5800	8720	8050	7010	11020

See Note 2 of Table VIII.

than the peak overpressure values. The UK gauge stations are rather closely grouped and there is only a small spread in the three impulse values recorded on each shot. The US gauge stations are widly spaced and since the impulse is a function of gauge location it can be seen that Station C-4 always recorded the largest overpressure impulse values and Station C-3, because it was closest to the source of a rarefaction wave, always recorded the smallest positive impulse for specific yields.

2. Comparison of Predictions with Experimental Results. If the phenomenon as described in Section III, Paragraph C-1 and shown in Figures 20 and 21 is valid then it should be possible to predict the initial shock reflecting on the headwall and door of the Structure C. Based on experimental data presented in Reference 4, and the Whitham Theory[5], the pressure along the Mach stem can be predicted if the angle of incidence and strength of the incident shock are known. Conversly, if the Mach pressure and angle of the incident shock are known, then the strength of the incident shock can be predicted. In Figure 32, incident pressure as a function of the measured Mach pressure at an assumed angle of 63.4 degrees is presented (see Figure 20).

If we assume that the angle of incidence of the shock striking the headwall of the structure is 26.6 degrees, (see Figure 21) then the strength of the shock can be determined from regular reflection theory[6]. A plot of the incident pressure as a function of the measured reflected pressure on the front surface of the headwall for an assumed angle of incidence of 26.6 degrees is presented in Figure 33.

A comparison of the predicted incident peak overpressure determined from the measured Mach pressure and reflected pressure at US gauge Station F-1 and UK gauge Station 17, US gauge Station C-4 and UK gauge Stations 19 and 20, and US gauge Station C-5 and UK gauge Station 21, for the various charge weights scaled to full size is presented in Table X. It must be remembered that reflection factors are very sensitive to angle of incidence of the shock front and the actual angles of incidence may be quite different from those chosen in this analysis. From Table X it can be seen that for charge weights greater than 64000 kg the average inferred incident shock overpressure at US F-1 and UK 17 is 1.99 bar, 199 kPa, or 28.9 psi. When this shock reaches US Station C-4 or UK Stations 19 - 20 it has decayed to 1.47 bar, 147 kPa, or 21.3 psi. This is approximately a 25 percent decay in the peak overpressure in traveling from US Station F-1 to C-4. US gauge Station C-3

---

[4] *R. J. Arave and N. R. Wallace, "Dynamic Pressure from Blast Waves: Methods for Predicting the Effects of Terrain," DASA-1732, February 1966.*

[5] *C. B. Whitham, "A New Approach to Problems of Shock Dynamics," J. Fluid Mech., Vol. 2, 1957, p. 145.*

[6] *C. N. Kingery and B. F. Pannill, "Parametric Analysis of the Regular Reflection of Air Blast," BRL Report No. 1249, June 1964.*

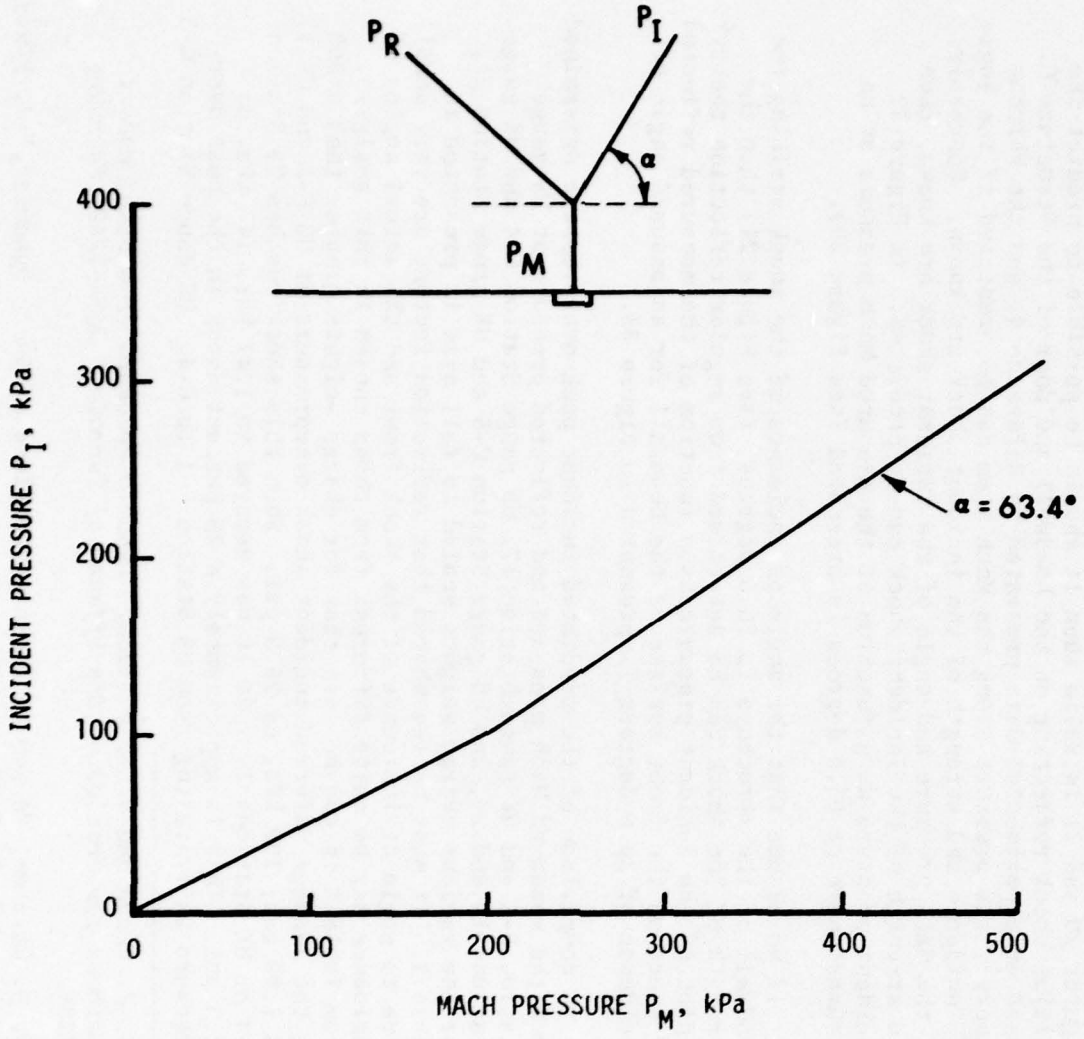

Figure 32. Incident Peak Overpressure versus Mach Overpressure for an Angle of 63.4 Degrees

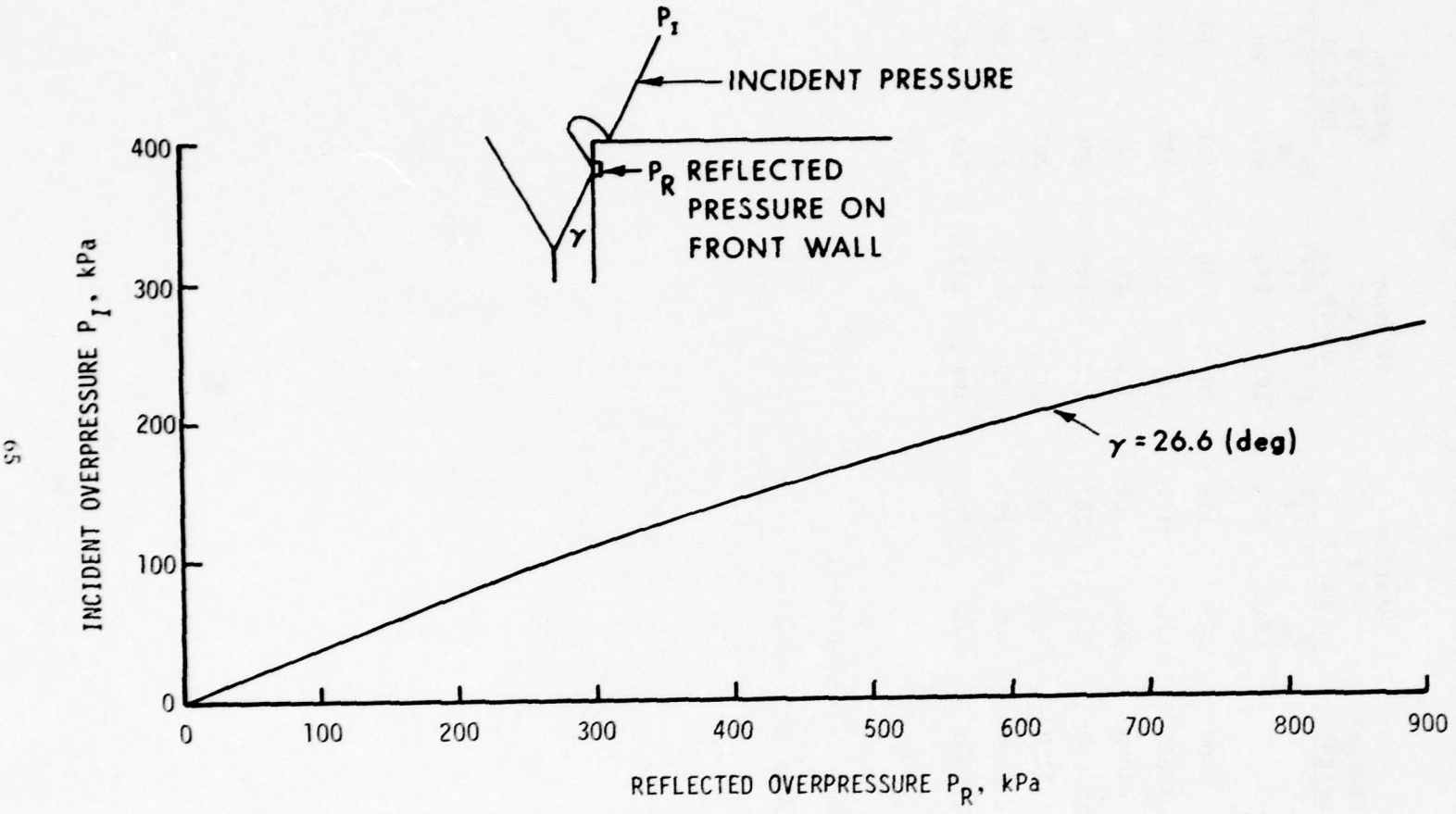

Figure 33. Incident Overpressure versus Reflected Overpressure for an Angle of 26.6 Degrees

Table X. Predicted Incident Peak Overpressure

Reference	Charge Weight	Station US F-1 UK 17		Station US C-4 UK 19-20		Station US C-5 UK C-21	
		P_m kPa	P_I* kPa	P_R kPa	P_I** kPa	P_m kPa	P_I* kPa
UK	8000	225	118	207	78	101	50
US	44625	311	175	449	154	237	128
UK	64000	300	167	324	118	-	-
UK	125000	350	201	412	145	258	140
US	133250	333	190	415	146	263	142
UK	216000	360	207	442	154	287	158
US	224000	345	197	404	142	268	145

*From Figure 32 (Predicted)

**From Figure 33 (Predicted)

recorded an average reflected peak overpressure of 540 kPa and from Figure 33 would predict an incident peak overpressure of 181 kPa which is in the right order of magnitude. US gauge Station C-2 (see Figure 31 for location) recorded an average reflected peak overpressure of 510 kPa and from Figure 33 this would predict an incident pressure of 174 kPa. The inferred incident overpressure has decayed from F-1, to C-3, to C-2, to C-4, values of 199 kPa to 181 kPa, to 174 kPa, to 147 kPa, or from 28.9 psi to 21.3 psi.

US gauge Station C-1 was always below the triple point and recorded a single peak reflected overpressure. From Reference 6, the incident pressure can be determined if the head-on reflected peak overpressure is known. In Figure 34, the incident peak overpressure versus the head-on reflected peak overpressure is presented. In Table VIII peak reflected overpressures recorded at Station C-1 for Test Series I, II and III are listed as 967, 1075, and 1144 kPa. From Figure 34 this would imply a Mach stem pressure of 269, 288, and 301 kPa should be striking the lower portion of the structure. These values are consistent with the initial shock overpressures of 311, 333, and 345 kPa recorded at US Station F-1. A decay in peak overpressure of approximately 13 percent would be inferred in traveling from Station F-1 to Station C-1.

From the preceding discussion it should be possible to predict the initial reflected shock loading on the headwall, and door, of an acceptor magazine located to the rear of a donor magazine from a free field measurement made flush with the surface of the ground at a distance in front of the structure less than the height of the magazine. It should also be possible to predict the same initial shock loading from a free field measurement made at a distance of $0.8Q^{1/3}$ and at one structure height above the surface. It is of interest to note that in Reference 2, UK Station 16 was located a distance of $0.8Q^{1/3}$ along a 118 degree line at a full scale height of 6.1 metres above the ground surface. The incident peak overpressures for the four tests were 55, 156, 227, and 224 kPa versus predicted values from UK gauge Station 17 of 120, 167, 202, and 208 kPa as presented in Table X. One measurement was made on the ground surface at Station 33. The Mach pressure measured was 101 kPa and from Figure 32 an incident shock pressure of 52 kPa would be predicted. The value recorded at UK Station 16 located at the same distance as Station 33 was 55 kPa.

It must be noted again that the comparisons have been made from data recorded on tests conducted with different model designs, different model scales, different model materials, different explosive charges, and different charge configuration. But with all of the above differences, certain trends have been noted, and a better understanding of the blast loading on acceptor magazines has been established.

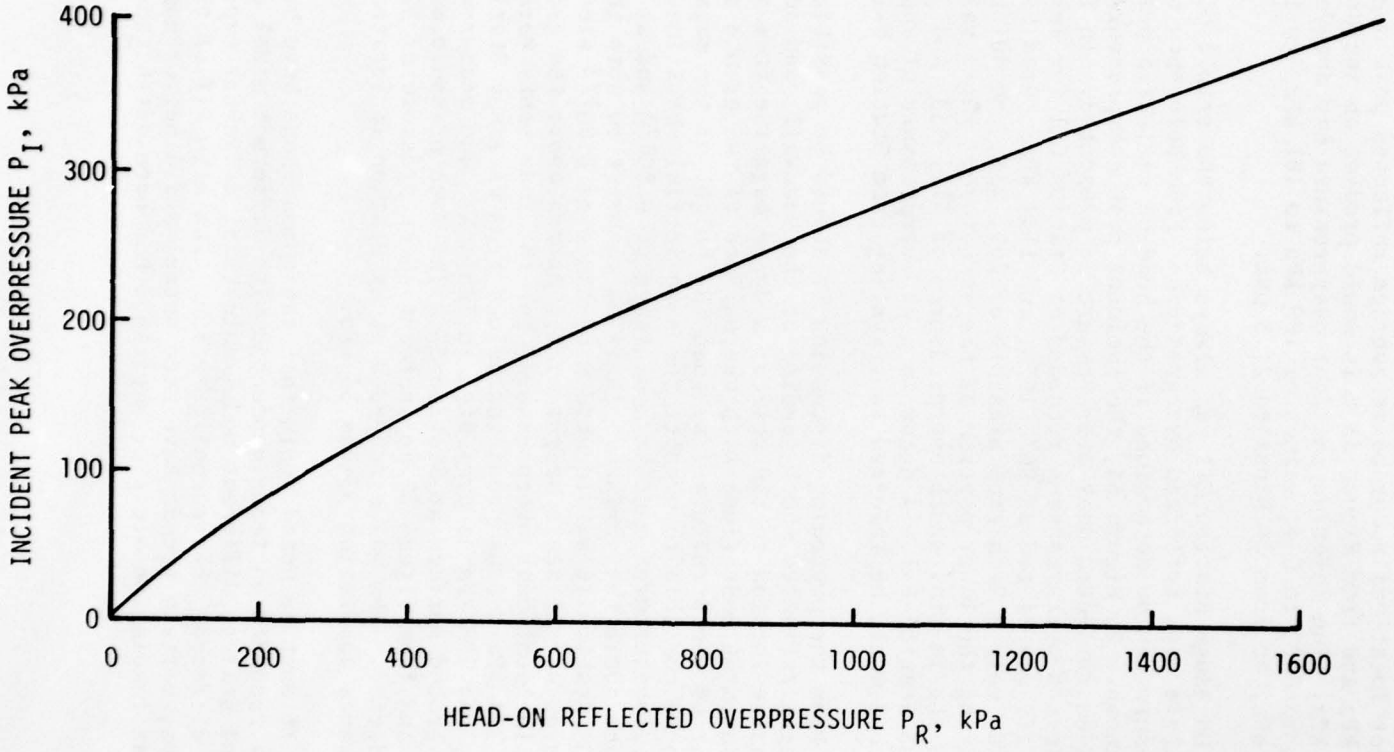

Figure 34. Incident Peak Overpressure versus Head-On Reflected Peak Overpressure

3. Comparison of Results from Top of UK Structure 3 and US Structure C. In this section a comparison of results from UK acceptor Magazine 3 and US acceptor Magazine C will be made using data from UK gauge Stations 21 and 22, and US gauge Stations C-5 and C-7. The relative gauge station locations are shown in Figure 35. The values of peak overpressure and positive impulse for full scale charge weights are listed in Table XI. In the bottom half of Table XI the data have been scaled to 1 kg for a better observation of the trends relative to scaled distance. At UK Station 21 and US Station C-5 the peak overpressure shows a decrease with increasing scaled distance while the positive impulse has a mixed trend. The overall average scaled impulse for UK-21 and US C-5 is 67.8 kPa-ms/$kg^{1/3}$ with a scatter of $\pm$ 11 percent about an arithmetic mean.

If it is assumed that US gauge Station C-5 and UK gauge Station 21 are in the Mach reflection region, then the incident shock overpressure can be predicted from Figure 32. The measured Mach overpressure and predicted peak overpressure are listed in Table X. An average of Mach reflection values recorded for charge weights greater than 64000 kg is 269 kPa. From Figure 32 an average value of predicted incident peak overpressure of 146 kPa was determined. This agrees with the 147 kPa determined from gauge Station C-4.

The trend established for US gauge Station C-7 and UK gauge Station 22 is, that within the individual series of tests the peak overpressure decreased with increasing scaled distance. The overall correlation of the US and UK results of the recorded peak overpressure at these two stations is good.

The positive impulses recorded at US gauge Station C-7 and UK gauge Station 22 are quite different. The positive impulse values recorded at the US gauge Station C-7 are much lower than expected and it is difficult to give a rational explanation. A post shot calibration test indicated no problem with the time constant of the gauge. Test Series I and III give the largest variations from an expected positive impulse.

The decay in impulse recorded at gauge Station C-7 on Test Series I, II, and III was 62, 36, and 57 percent of that recorded at C-5. The decay in impulse recorded at UK Station 22 for Test 2, 3 and 4 was 22, 34, and 30 percent of that recorded at UK Station 21.

V. CONCLUSIONS AND RECOMMENDATIONS

Based on the comparisons made between the results from the UK 1/10th scaled models, the ESKIMO III full-size structure, and the US 1/50th scale models, it can be concluded that blast loading on full size structures can be reasonably well predicted. Trends can be established that might be expected from accidental explosions in munition storage magazines when the earth cover, separation distances or amounts of munition stored are varied.

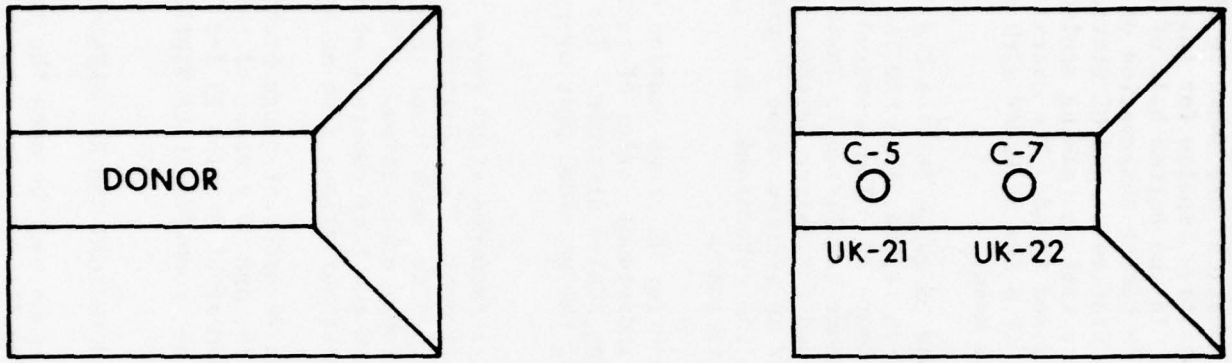

Figure 35. Gauge Locations on US Model Structure C and UK Model Structure 3

Table XI. Roof Loading on Acceptor to Rear of Donor

Reference	Charge Weight kg	Full Scale Distance Metres C-5/21	Full Scale Distance Metres C-7/22	Peak Overpressure kPa C-5/21	Peak Overpressure kPa C-7/22	Impulse kPa-ms C-5/21	Impulse kPa-ms C-7/22
UK 4	8000	27.0	42.3	101	43	1240	860
US I	44625	46.9	59.6	237	149	2560	970
UK 1	64000	43.0	58.3	-	120	-	2480
UK 2	125000	51.0	66.3	258	169	3260	2550
US II	133250	60.4	73.1	263	181	3420	2170
UK 3	216000	59.0	74.3	287	197	4510	2970
US III	224000	67.2	79.8	268	198	3950	1690

Scaled to 1 Kilogram

		$m/kg^{1/3}$		kPa		$kPa\text{-}ms/kg^{1/3}$	
UK 4	1	1.35	2.12	101	43	62.0	43.0
US I	1	1.32	1.68	237	149	72.0	27.3
UK 1	1	1.08	1.46	-	120	-	62.0
UK 2	1	1.02	1.33	258	169	65.2	51.0
US II	1	1.19	1.43	263	181	67.0	42.5
UK 3	1	0.98	1.24	287	197	75.2	49.5
US III	1	1.11	1.30	268	198	65.0	27.8

Model tests of this scale (1/50th) can not be used as a substitute for full scale tests where the response and proof testing of design changes are being studied, but they can be used for establishing guidelines in planning tests and predicting the blast loading that might be expected.

APPENDIXES

OVERPRESSURE AND IMPULSE VERSUS TIME

The Appendixes A, B, and C will present overpressure and positive impulse versus time recorded on US model Structures A, B, and C. Results from one shot only on Test Series II will be presented for each structure.

Appendix A - Overpressure and Positive Impulse versus Time from Gauge Stations A-1 through A-8, Test Series II, Shot 4.

Appendix B - Overpressure and Positive Impulse versus Time from Gauge Stations B-1 through B-7, Test Series II, Shot 3.

Appendix C - Overpressure and Positive Impulse versus Time from Gauge Stations F-1 and C-1 through C-8, Test Series II, Shot 3.

See Figure 7 for the Test Layout, and Table II for gauge station distances from ground zero.

APPENDIX A

OVERPRESSURE AND POSITIVE IMPULSE VERSUS TIME FROM GAUGE STATION A-1 THROUGH A-8, TEST SERIES II, SHOT 4

PRECEDING PAGE BLANK

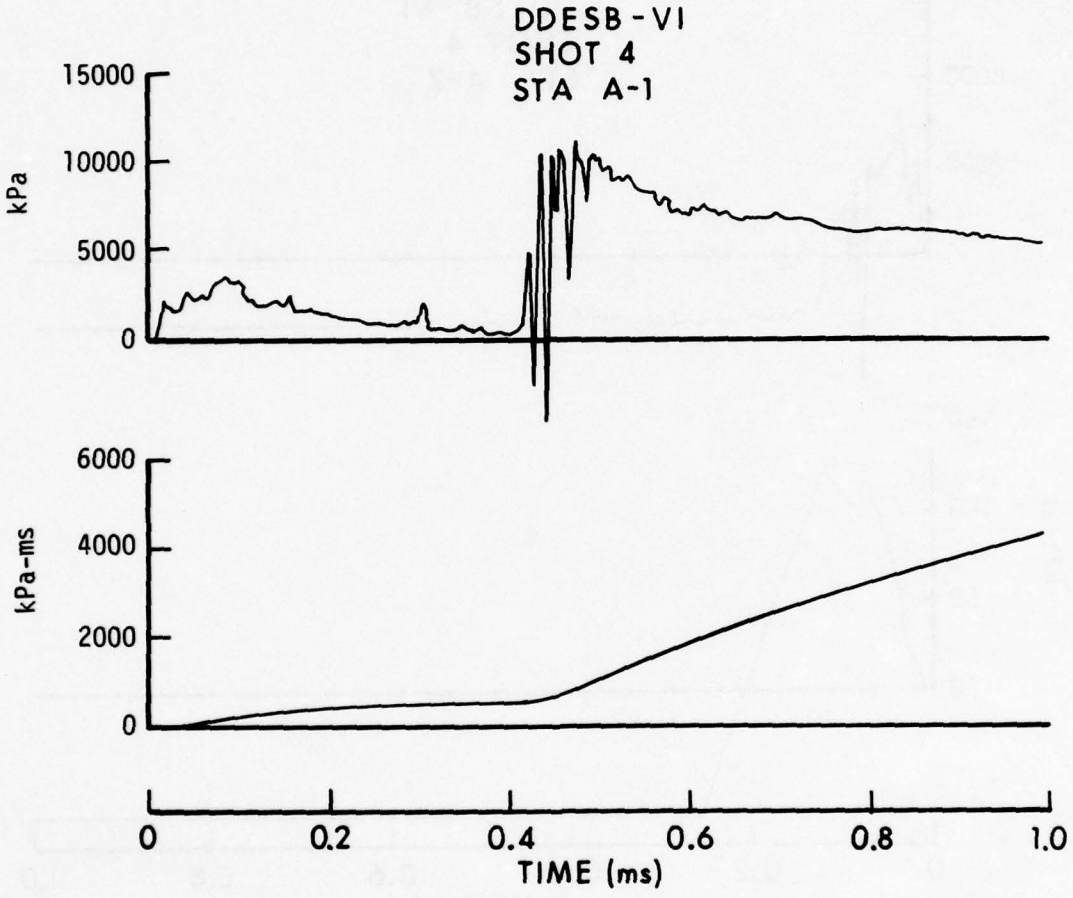

Figure A-1. Overpressure and Impulse versus Time, Station A-1

PRECEDING PAGE BLANK

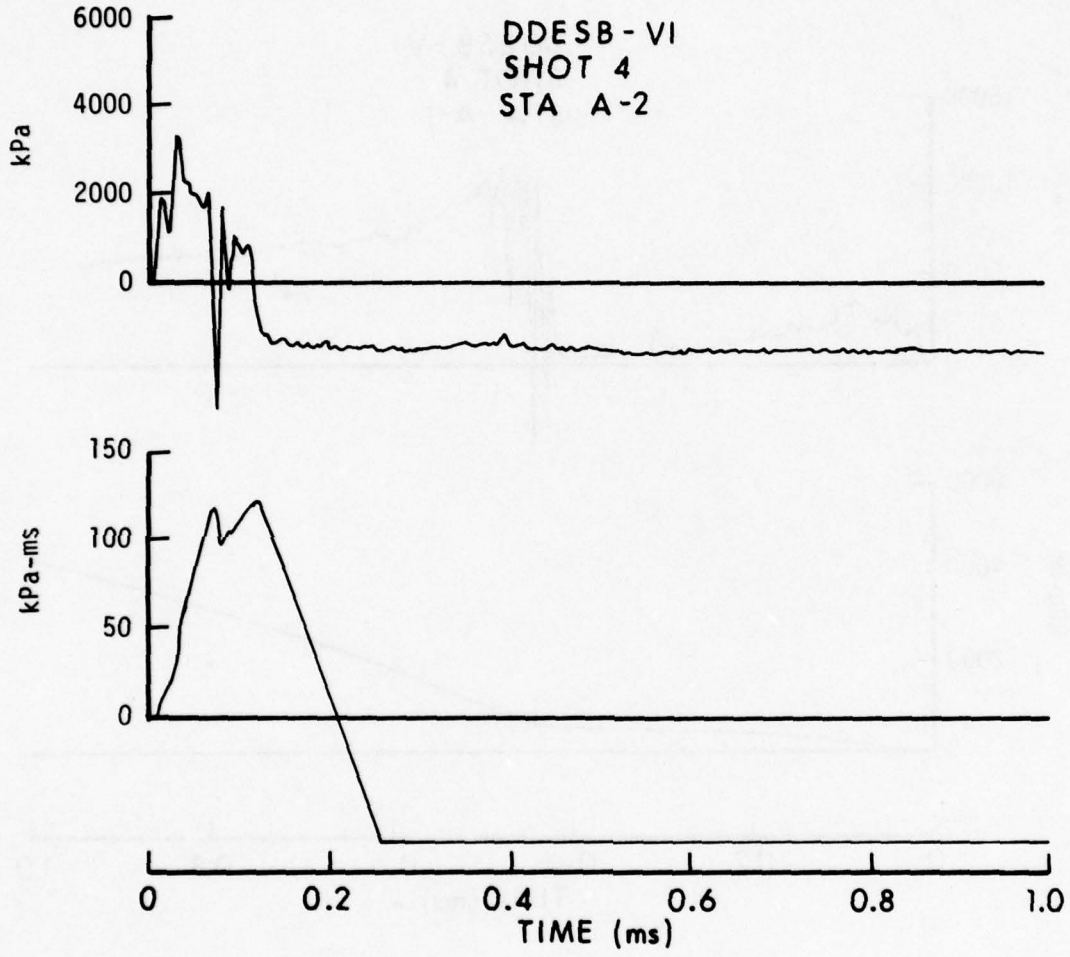

Figure A-2. Overpressure and Impulse versus Time, Station A-2

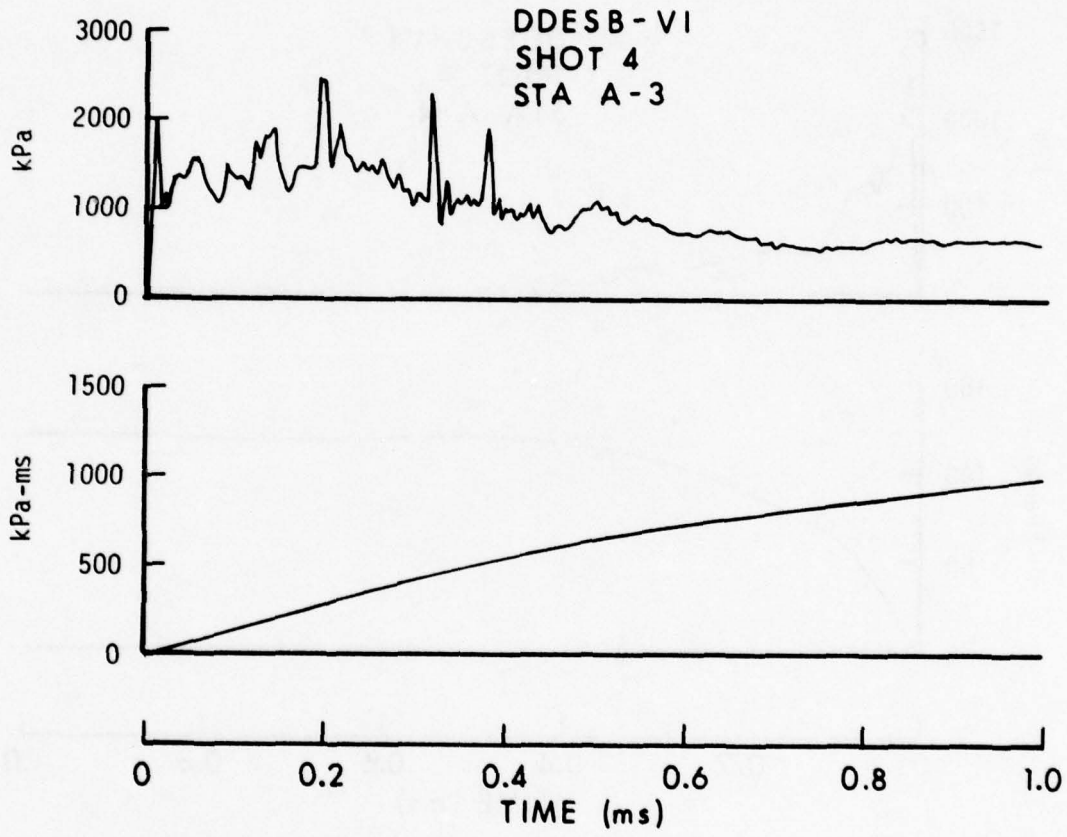

Figure A-3. Overpressure and Impulse versus Time, Station A-3

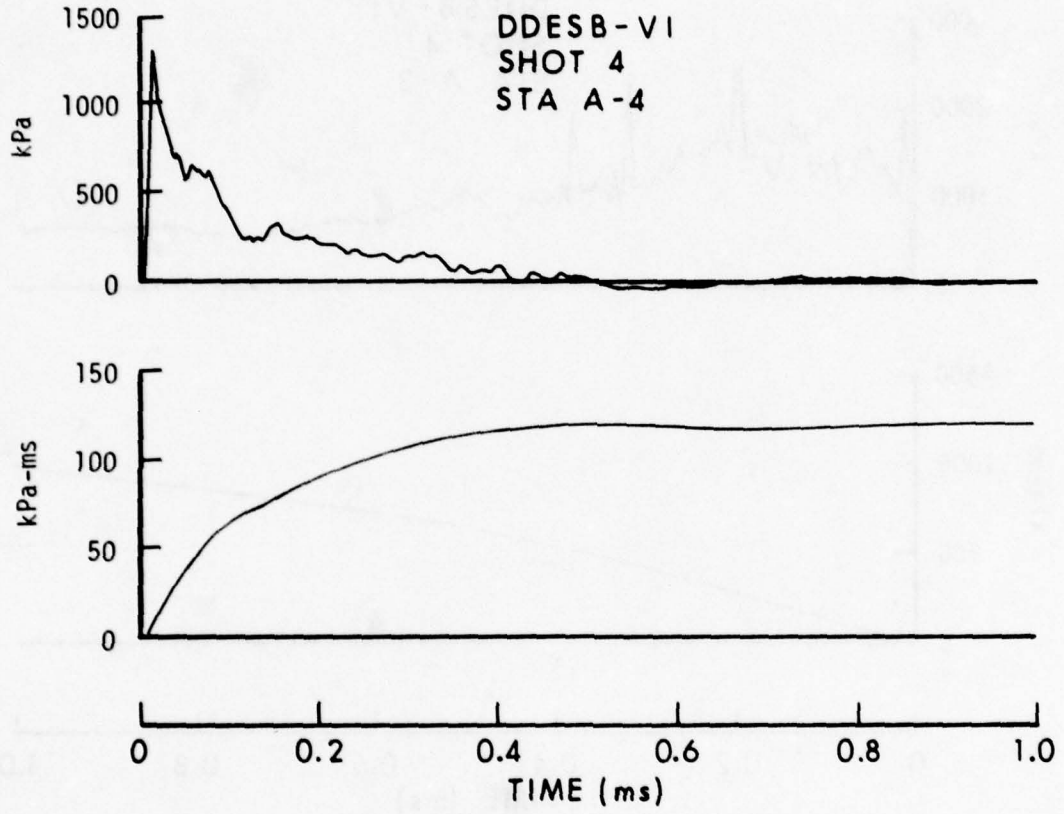

Figure A-4. Overpressure and Impulse versus Time, Station A-4

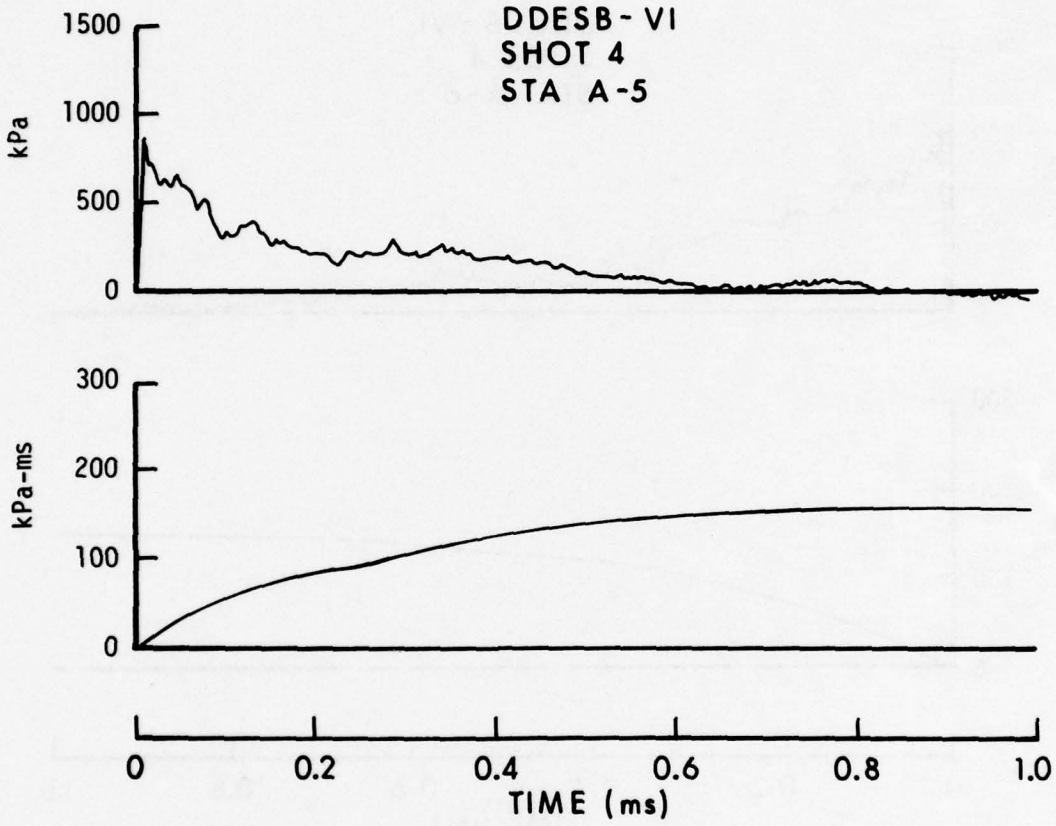

Figure A-5. Overpressure and Impulse versus Time, Station A-5

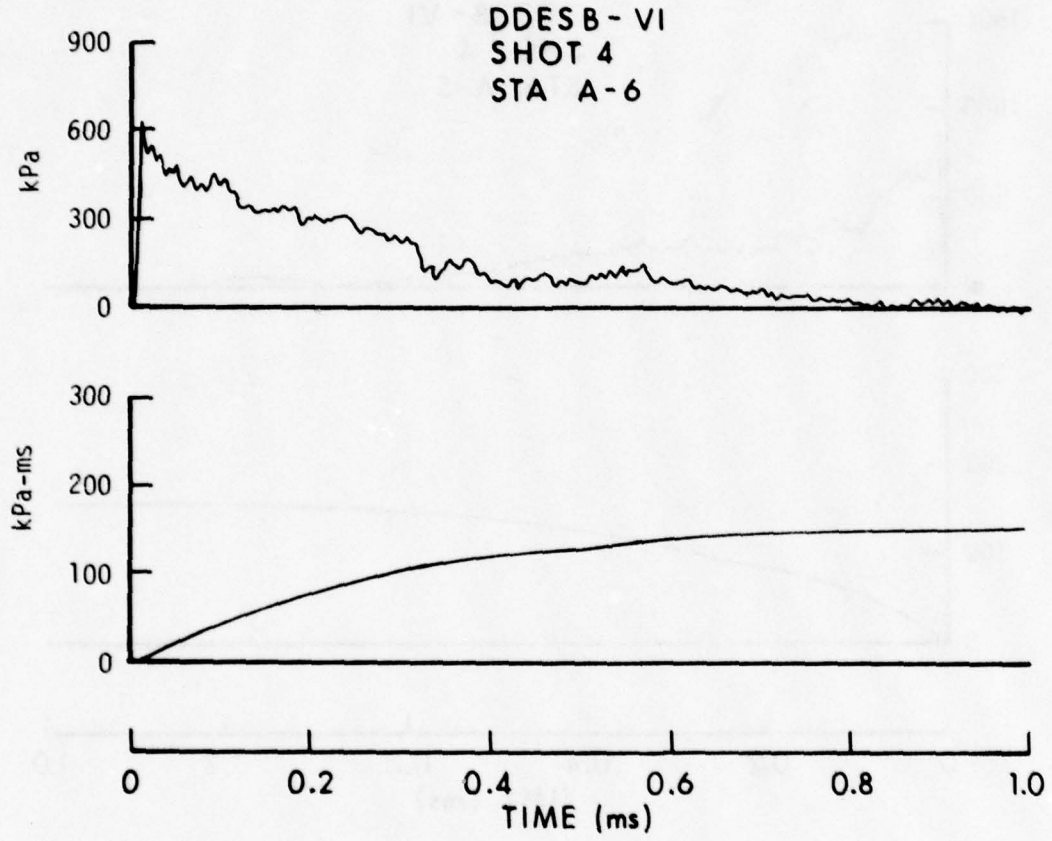

Figure A-6. Overpressure and Impulse versus Time, Station A-6

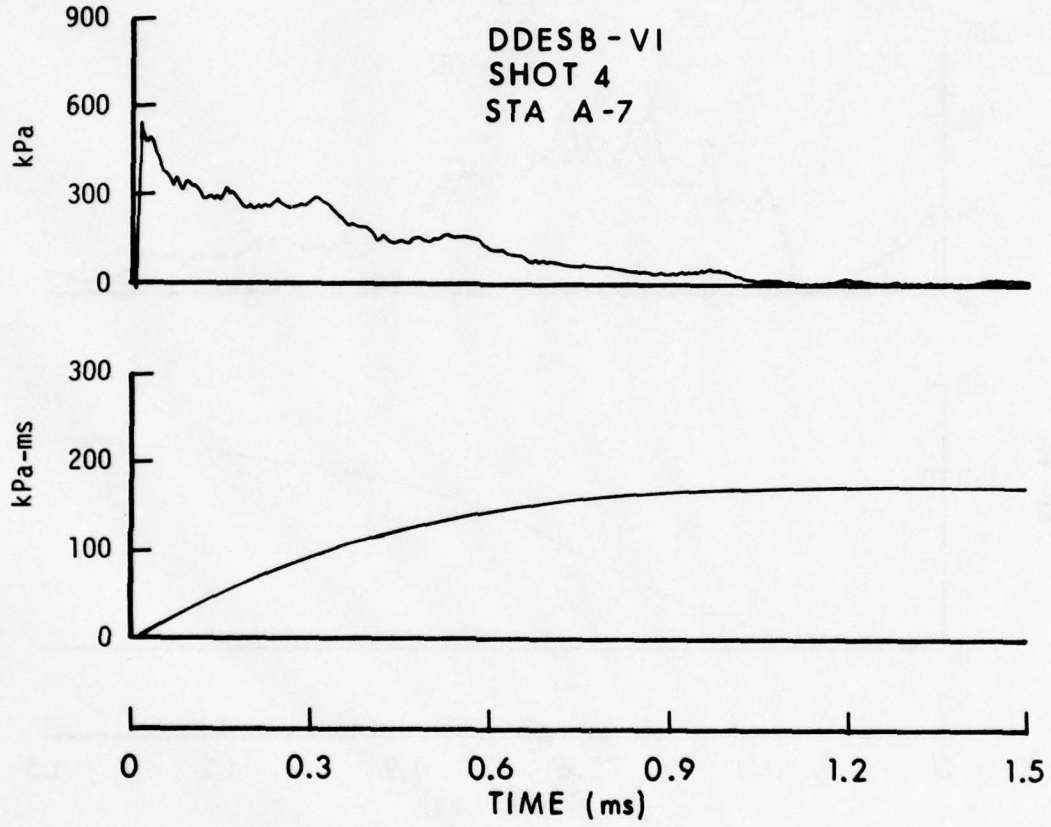

Figure A-7. Overpressure and Impulse versus Time, Station A-7

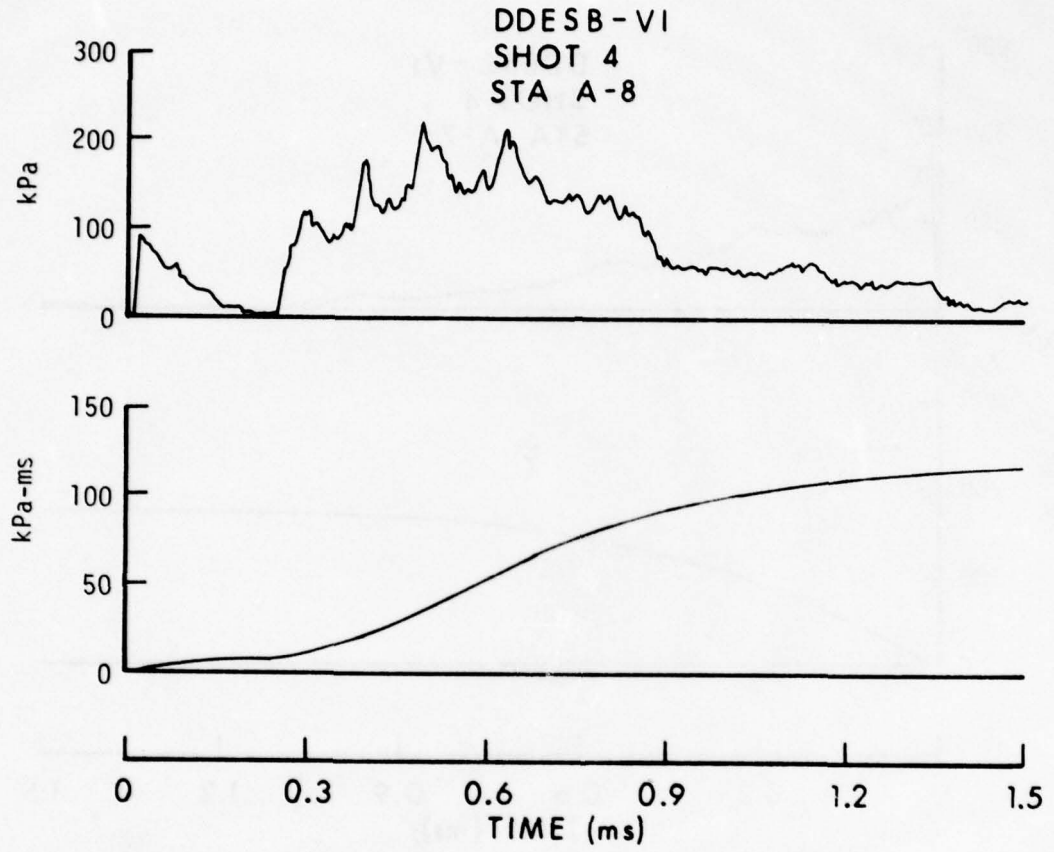

Figure A-8. Overpressure and Impulse versus Time, Station A-8

APPENDIX B

OVERPRESSURE AND POSITIVE IMPULSE VERSUS TIME FROM GAUGE STATIONS B-1 THROUGH B-7, TEST SERIES II, SHOT 3

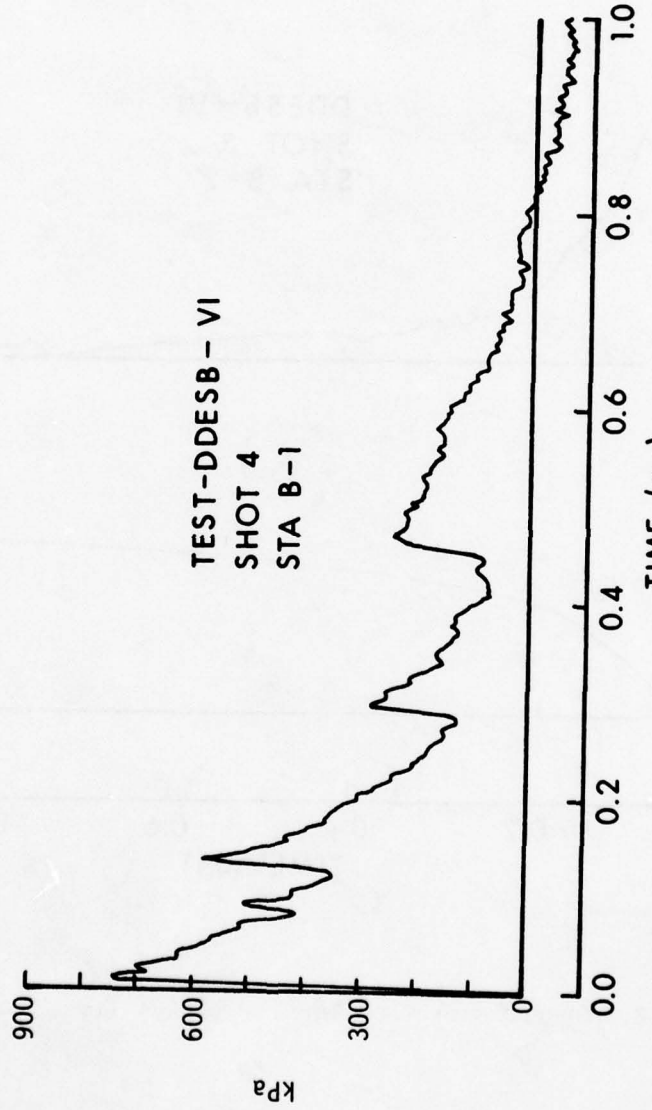

Figure B-1. Overpressure versus Time, Station B-1

PRECEDING PAGE BLANK

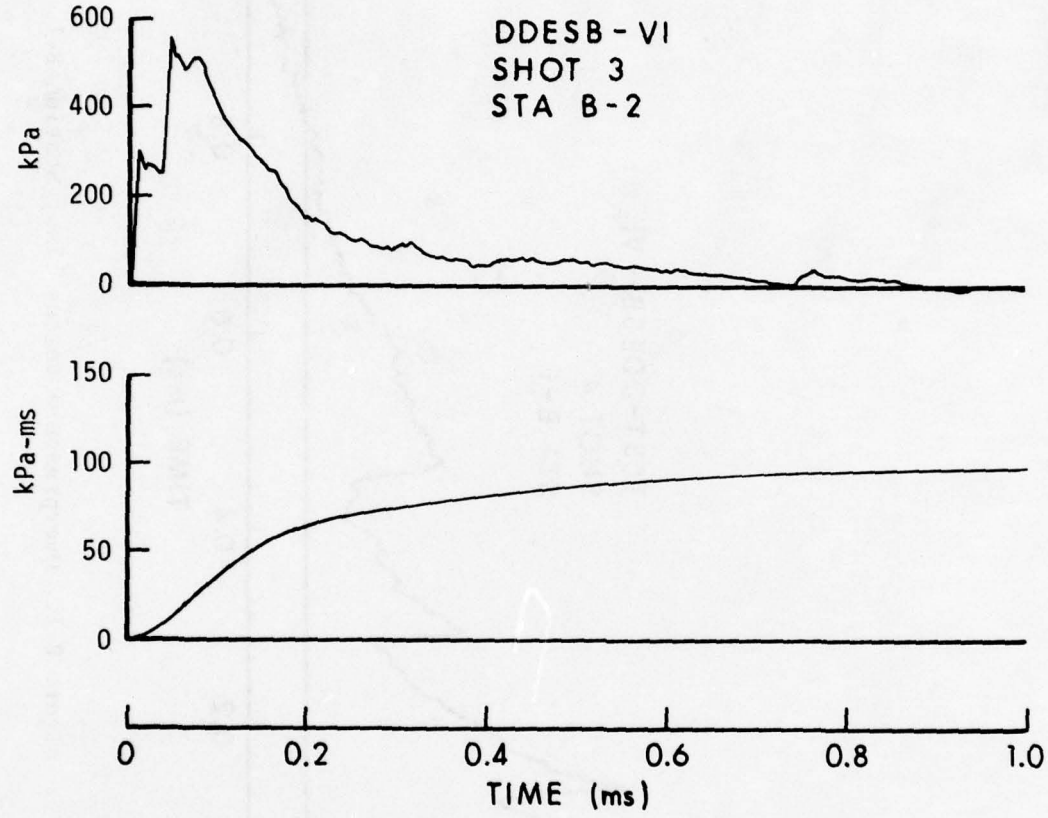

Figure B-2. Overpressure and Impulse versus Time, Station B-2

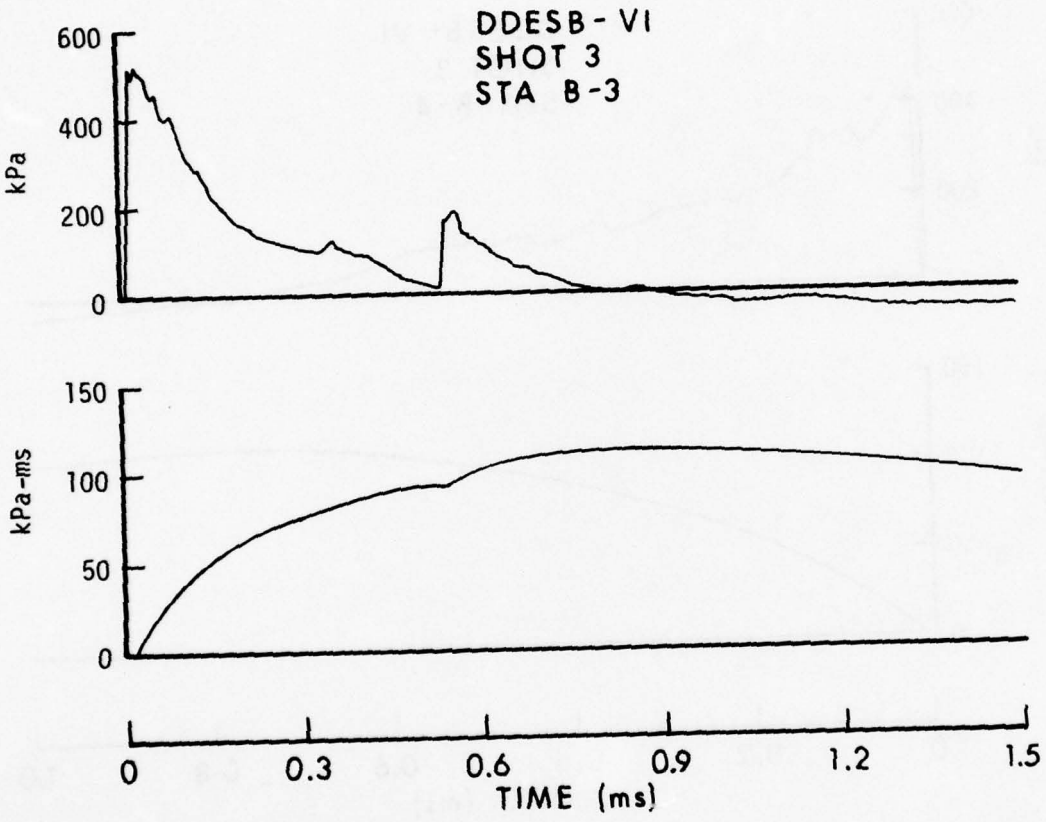

Figure B-3. Overpressure and Impulse versus Time, Station B-3

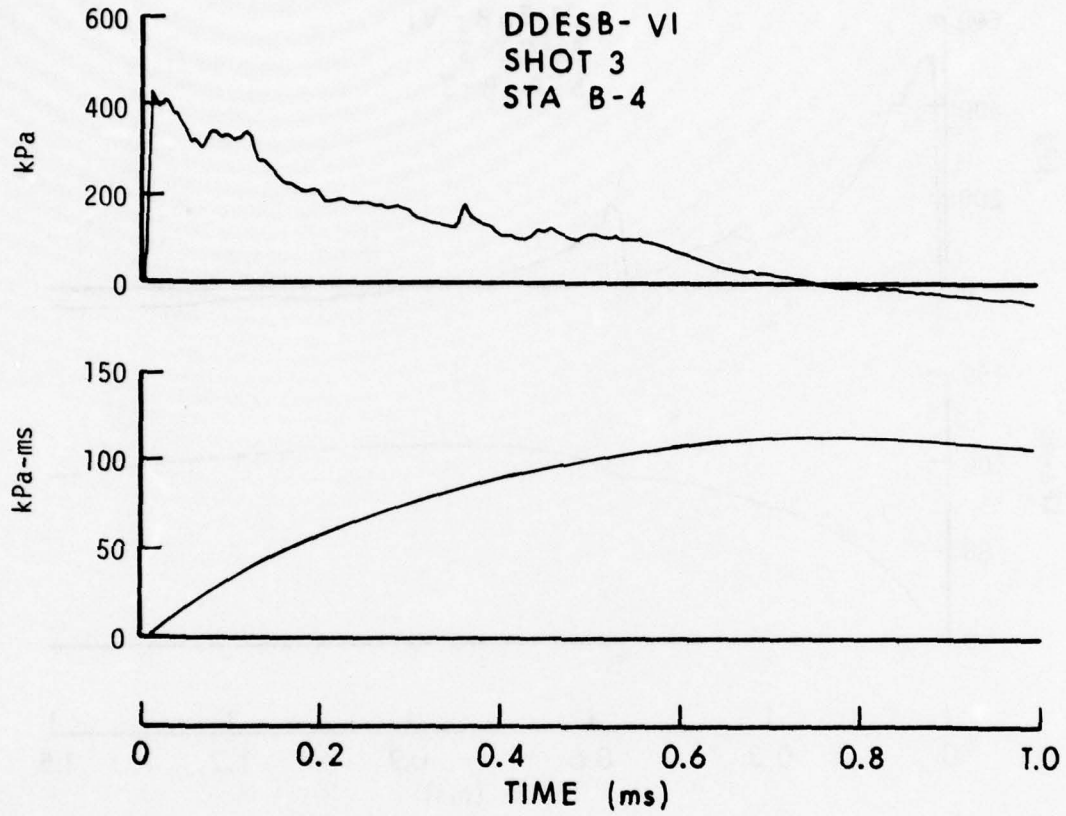

Figure B-4. Overpressure and Impulse versus Time, B-4

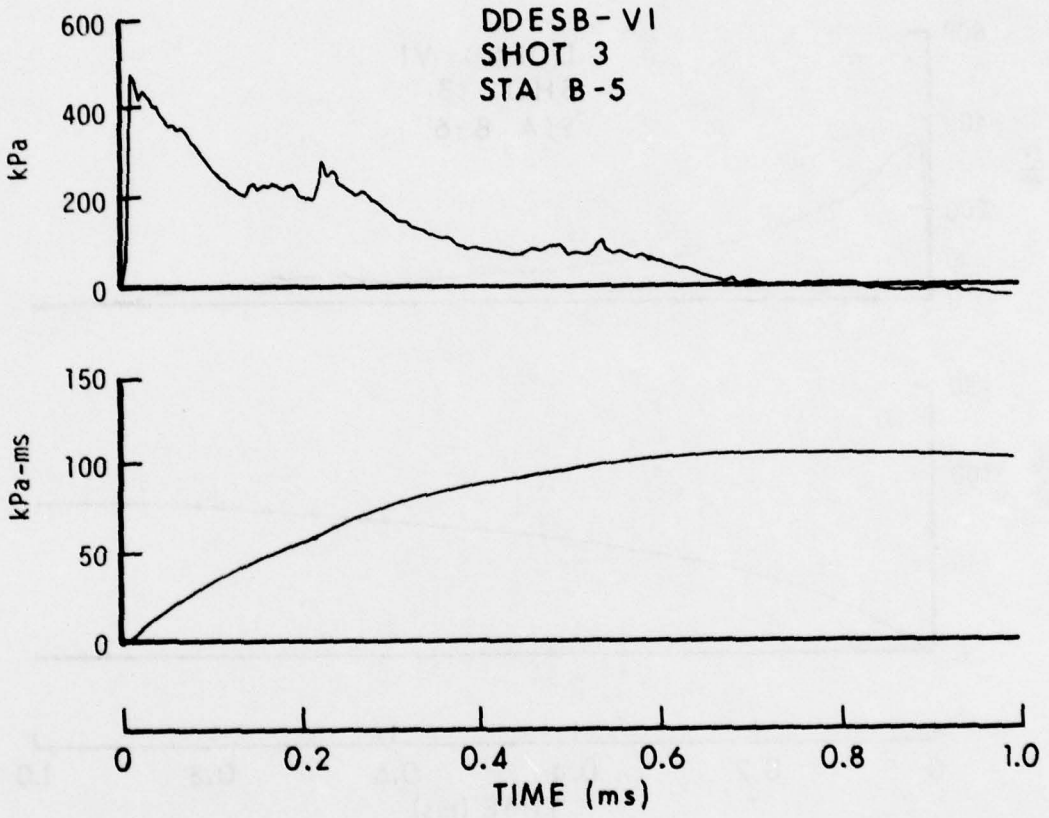

Figure B-5. Overpressure and Impulse versus Time, B-5

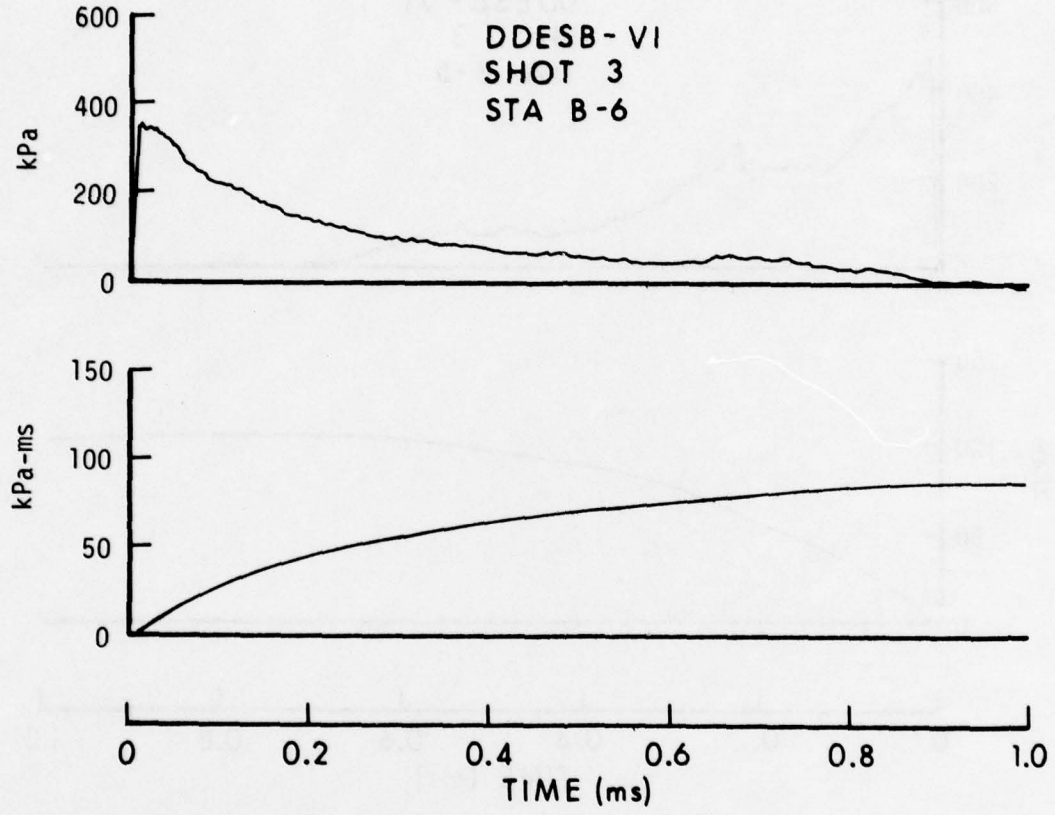

Figure B-6. Overpressure and Impulse versus Time, B-6

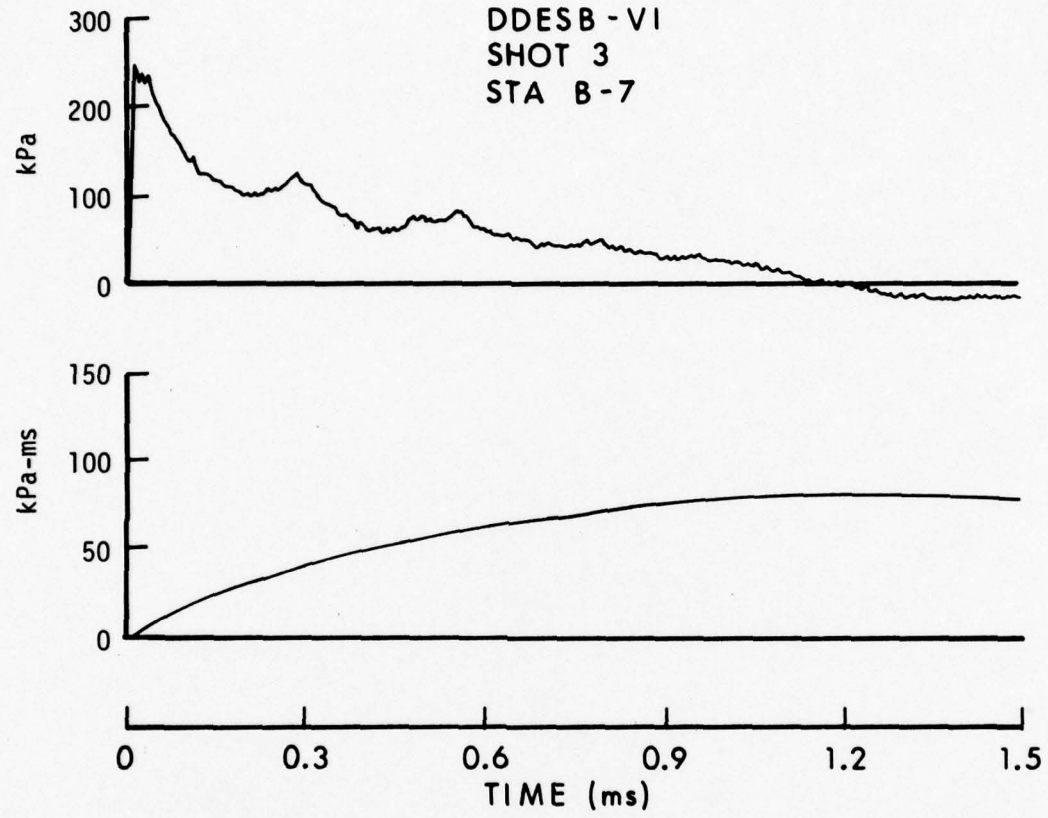

Figure B-7. Overpressure and Impulse versus Time, B-7

APPENDIX C

OVERPRESSURE AND POSITIVE IMPULSE VERSUS TIME FROM GAUGE STATION C-1 THROUGH C-8 AND F-1, TEST SERIES II, SHOT 3

PRECEDING PAGE BLANK

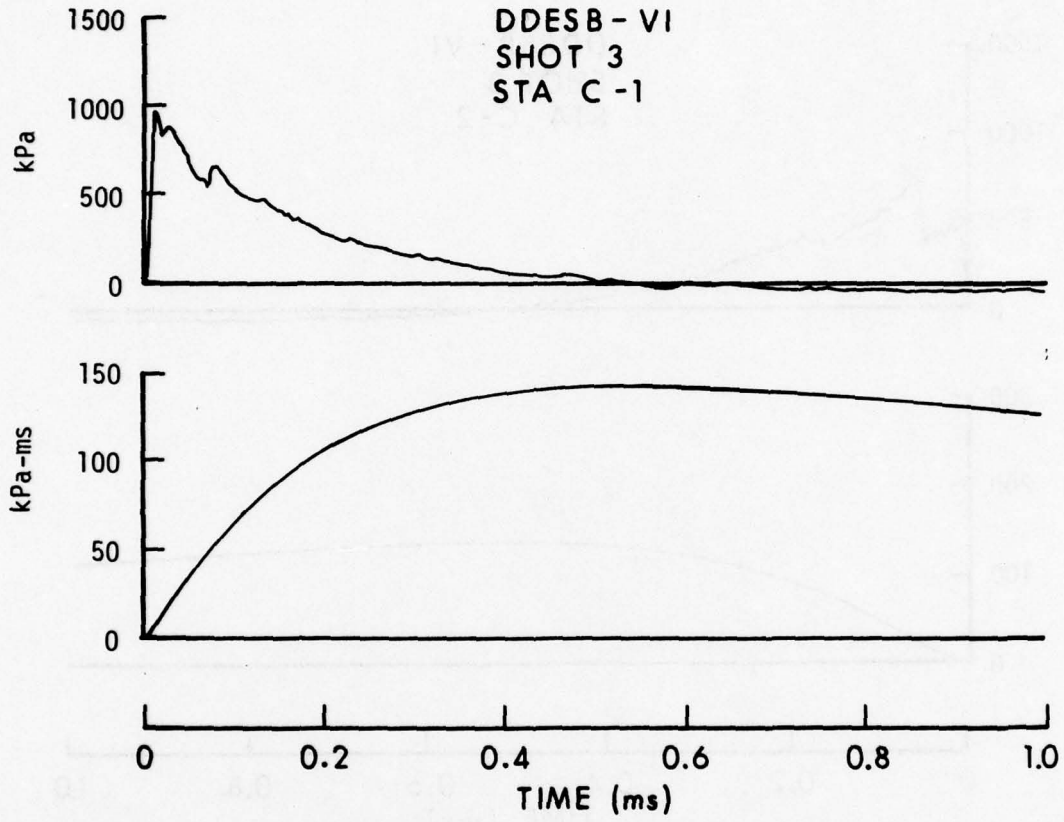

Figure C-1. Overpressure and Impulse versus Time, Station C-1

PRECEDING PAGE BLANK

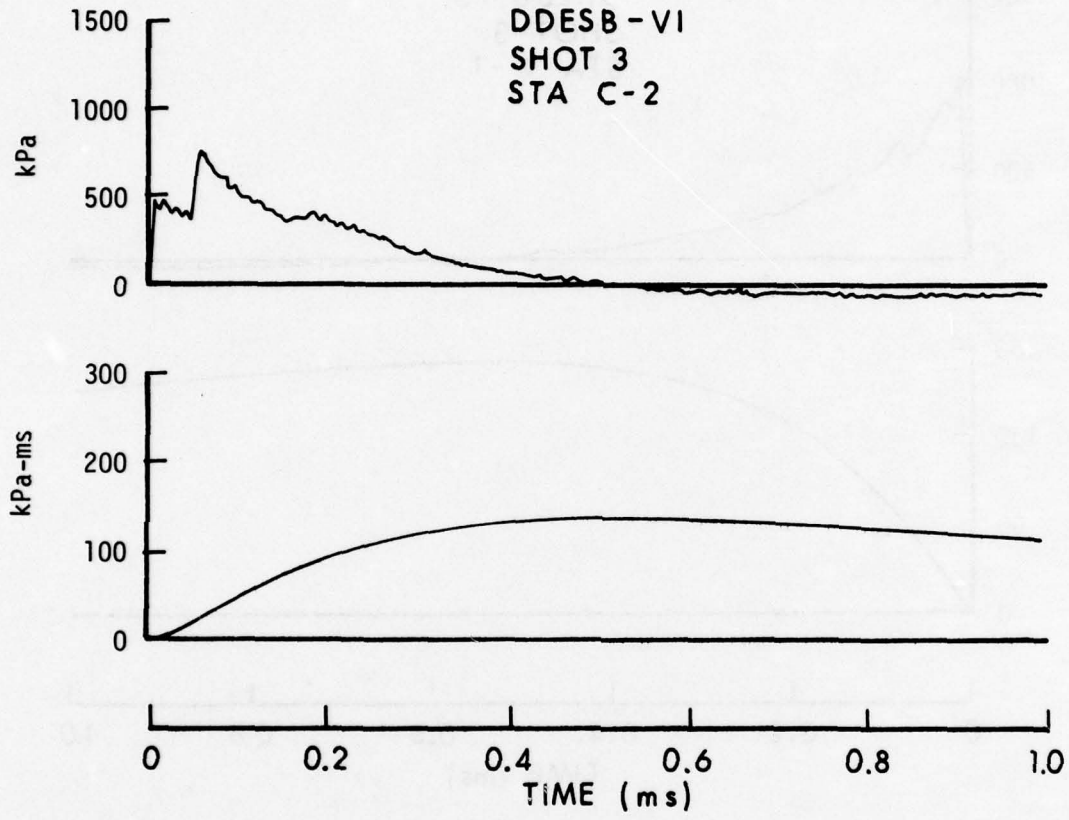

Figure C-2. Overpressure and Impulse versus Time, Station C-2

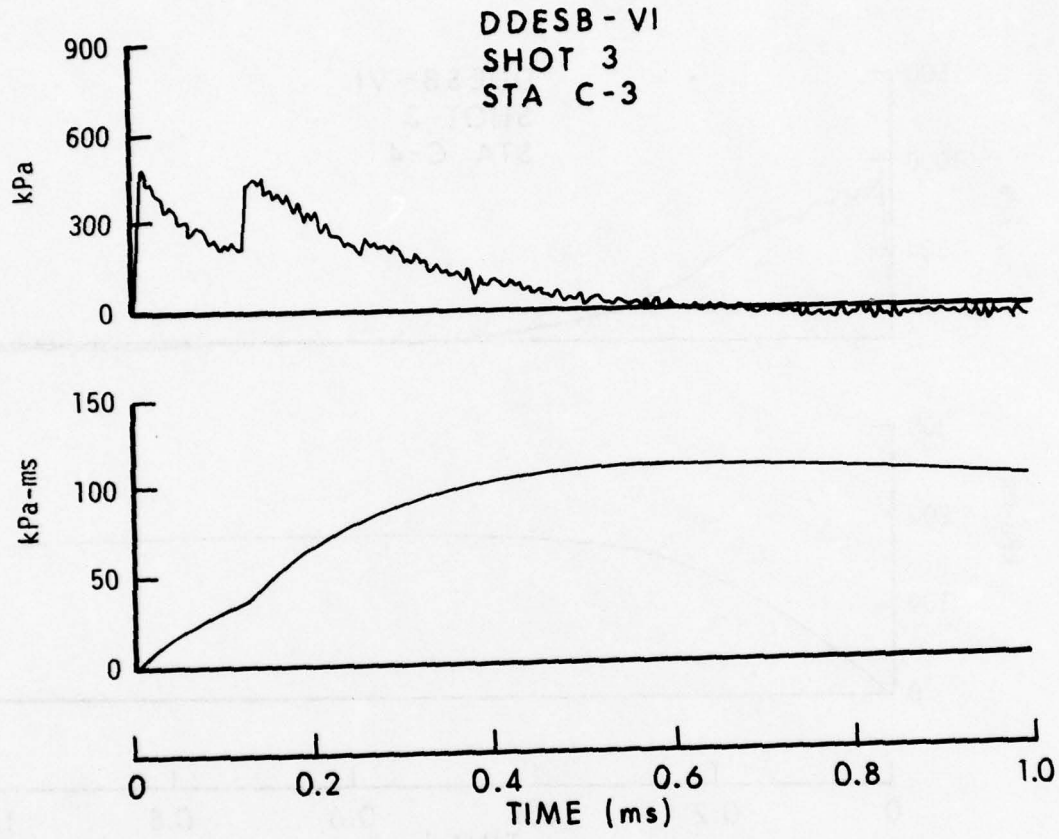

Figure C-3. Overpressure and Impulse versus Time, Station C-3

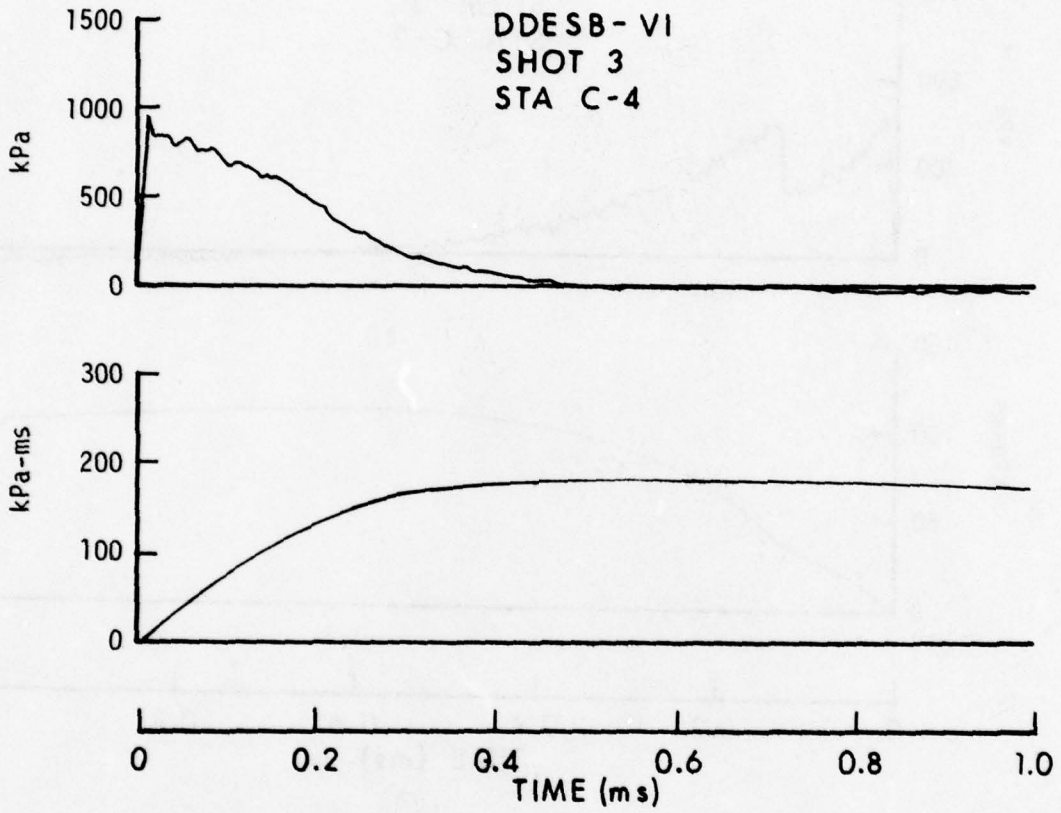

Figure C-4. Overpressure and Impulse versus Time, Station C-4

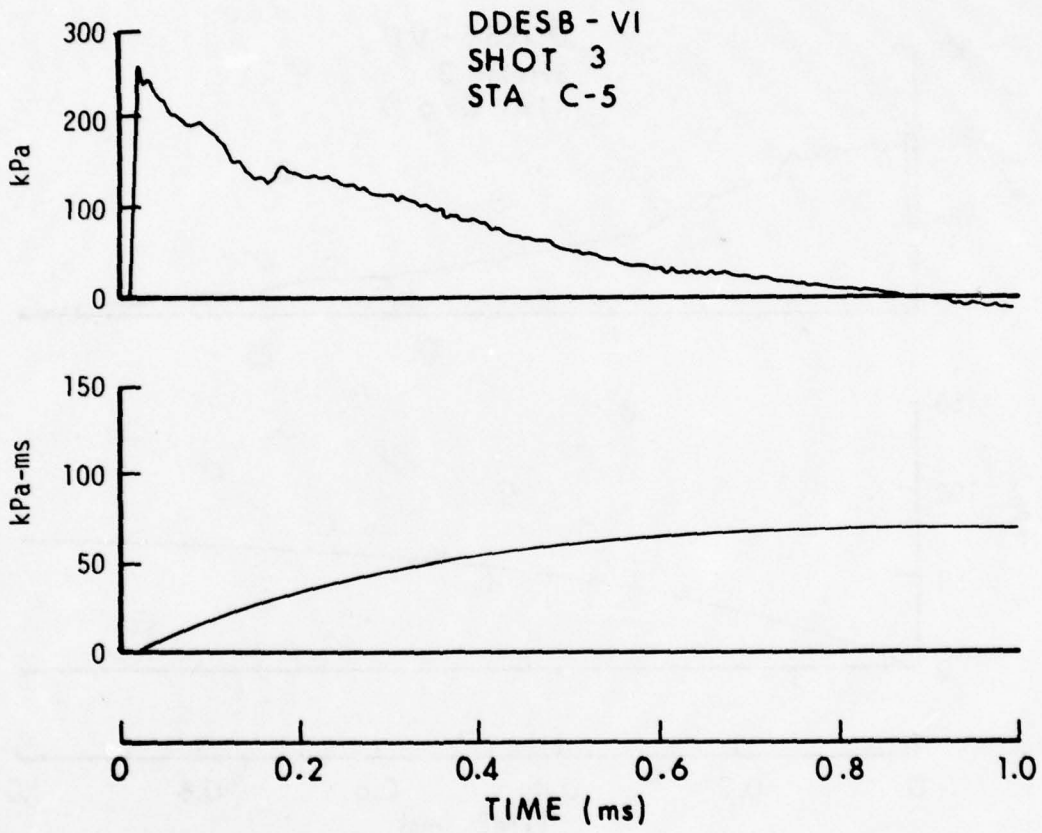

Figure C-5. Overpressure and Impulse versus Time, Station C-5

AD-A069 086 ARMY ARMAMENT RESEARCH AND DEVELOPMENT COMMAND ABERD--ETC F/G 19/4
BLAST LOADING ON MODEL MUNITION STORAGE MAGAZINES.(U)
FEB 79 C N KINGERY, G A COULTER, G T WATSON

UNCLASSIFIED ARBRL-TR-02140 SBIE-AD-E430 224 NL

2 OF 2
AD
A069086

END
DATE
FILMED
6-79
DDC

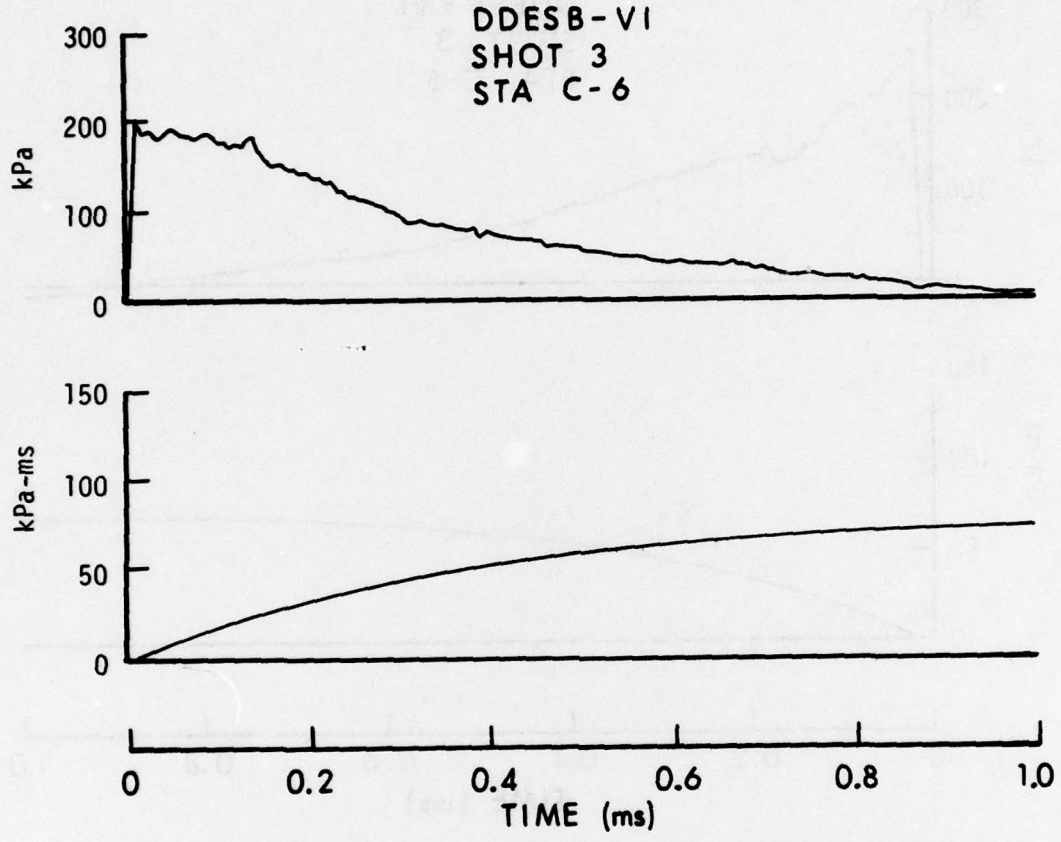

Figure C-6. Overpressure and Impulse versus Time, Station C-6

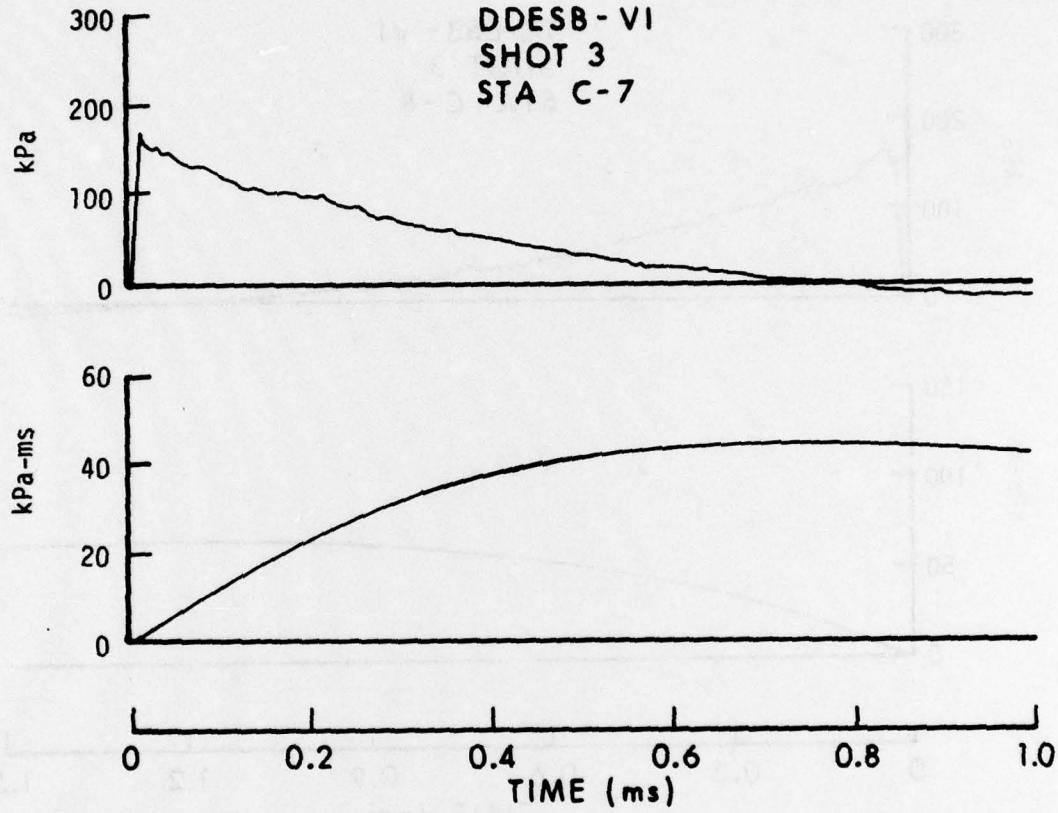

Figure C-7. Overpressure and Impulse versus Time, Station C-7

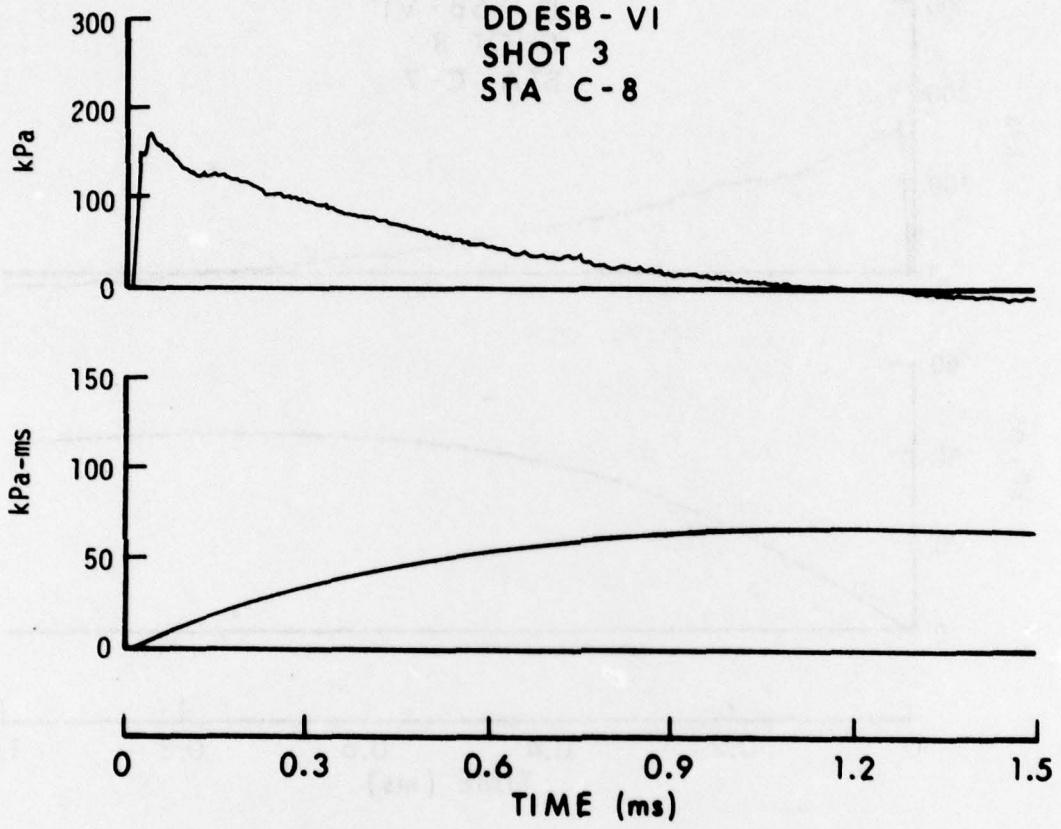

Figure C-8. Overpressure and Impulse versus Time, Station C-8

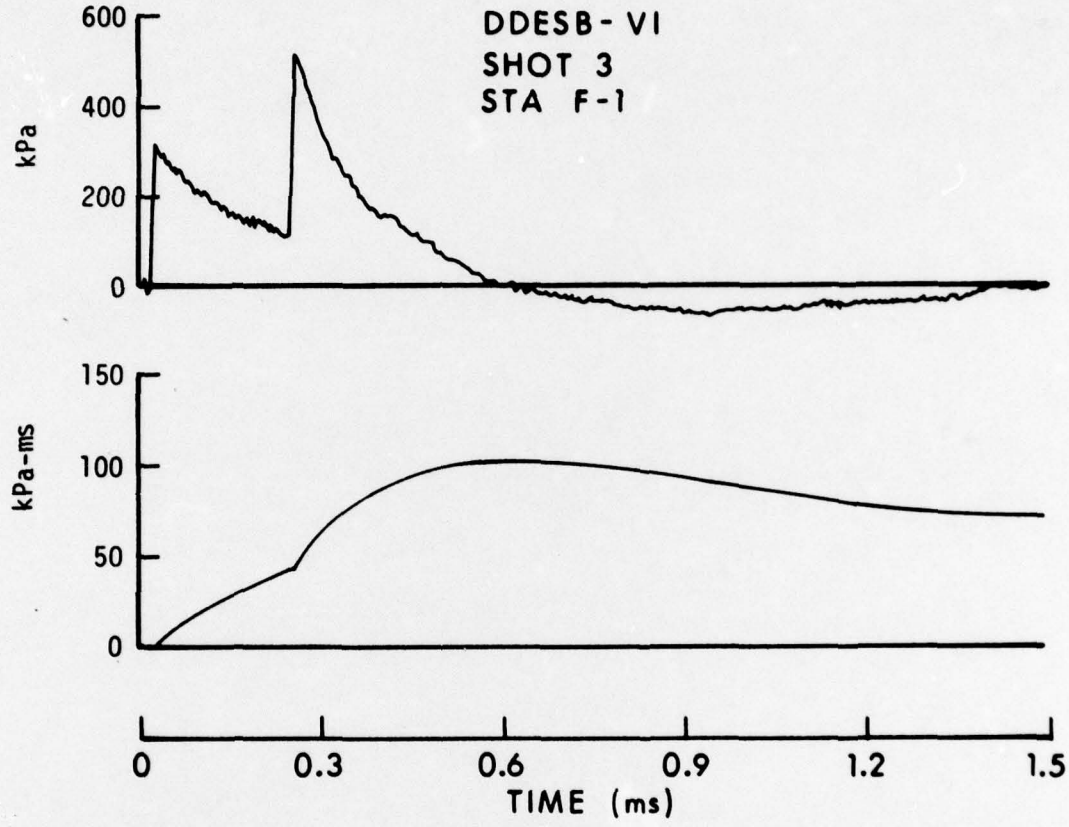

Figure F-1. Overpressure and Impulse versus Time, Station F-1

DISTRIBUTION LIST

No. of Copies	Organization
12	Commander Defense Documentation Center ATTN: DDC-DDA Cameron Station Alexandria, VA 22314
1	Office Secretary of Defense Office DDR&E ATTN: Mr. J. Persh, Staff Specialist, Materials and Structures Washington, DC 20301
1	Assistant Secretary of Defense (MRA&L) ATTN: ID (Mr. H. Metcalf) Washington, DC 20301
1	Assistant to the Secretary of Defense (Atomic Energy) ATTN: Document Control Washington, DC 20301
1	Director of Defense Research and Engineering Department of Defense Washington, DC 20301
1	Director Defense Advanced Research Projects Agency 1400 Wilson Boulevard Arlington, VA 22209
3	Director Institute for Defense Analysis ATTN: Dr. J. Menkes Dr. J. Bengston Tech Info Ofc 400 Army-Navy Drive Arlington, VA 22202
1	Director Weapons Systems Evaluation Group ATTN: CPT Donald E. McCoy Washington, DC 20305
1	Director Defense Communications Agency ATTN: NMCSSC (Code 510) Washington, DC 20305
2	Director Defense Intelligence Agency ATTN: DT-1B, Dr. J. Vorona DIR-4C3, R. Sauer Washington, DC 20301
3	Director Defense Nuclear Agency ATTN: Mr. J. F. Moulton, SPAS Dr. E. Sevin, SPSS Mr. T. P. Jeffers, OLAG Washington, DC 20305
4	Director Defense Nuclear Agency ATTN: SPTL Tech Lib (2 cys) APSI (ARCHIVES) LGLS, Mr. E. L. Eagles Washington, DC 20305
1	Commander Field Command Defense Nuclear Agency ATTN: Tech Lib, FCWS-SC Kirtland AFB, NM 87115
1	DNA Information and Analysis Center TEMPO, General Electric Co. ATTN: DASIAC 816 State Street Santa Barbara, CA 93102

PRECEDING PAGE BLANK

DISTRIBUTION LIST

No. of Copies	Organization
1	Defense Civil Prepardness Agency ATTN: David W. Bensen Washington, DC 20301
5	Chairman Department of Defense Explosives Safety Board 2461 Eisenhower Avenue Alexandria, VA 22331
2	Chairman Joint Chiefs of Staff ATTN: J-3, Operations J-5, Plans & Policy (R&D Division) Washington, DC 20301
2	Director Joint Strategic Target Planning Staff ATTN: JLTW TPTP Offutt AFB Omaha, NB 68113
1	Commander US Army Materiel Development and Readiness Command ATTN: DRCDMD-ST 5001 Eisenhower Avenue Alexandria, VA 22333
1	Commander US Army Materiel Development and Readiness Command ATTN: Mr. W. G. Queen, DRCSF 5001 Eisenhower Avenue Alexandria, VA 22333
1	Commander US Army Aviation Research and Development Command ATTN: DRSAV-E 12th and Spruce Streets St. Louis, MO 63166
1	Director US Army Air Mobility Research and Development Laboratory Ames Research Center Moffett Field, CA 94035
2	Director Lewis Directorate US Army Air Mobility Research and Development Command Lewis Research Center ATTN: Mail Stop 77-5 21000 Brookpark Road Cleveland, OH 44135
1	Commander US Army Electronics Research and Development Command Technical Support Activity ATTN: DELSD-L Fort Monmouth, NJ 07703
1	Commander US Army Communications Research and Development Command ATTN: DRDCO-PPA-SA Fort Monmouth, NJ 07703
2	Commander US Army Missile Research and Development Command ATTN: DRDMI-R DRDMI-RSS, Mr. B. Cobb Redstone Arsenal, AL 35809
2	Commander US Army Missile Research and Development Command ATTN: DRSMI-RX, Mr. W. Thomas DRSMI-RR, Mr. L. Lively Redstone Arsenal, AL 35809

DISTRIBUTION LIST

No. of Copies	Organization
1	Commander US Army Missile Materiel Readiness Command ATTN: DRSMI-AOM Redstone Arsenal, AL 35809
2	Commander US Army Tank Automotive Development Command ATTN: DRDTA DRDTA-UL Warren, MI 48090
1	Commander US Army Mobility Equipment Research & Development Command ATTN: DRDFB-ND Fort Belvoir, VA 22060
3	Commander US Army Armament Research and Development Command ATTN: DRDAR-LC DRDAR-TSS (2 cys) Dover, NJ 07801
2	Commander US Army Armament Material Readiness Command ATTN: DRSAR-LEP-L, Tech Lib DRSAR-SA Rock Island IL 61299
3	Commander US Army Armament Material Readiness Command ATTN: Joint Army-Navy-Air Force Conventional Ammunition Prof Coord GP/E. Jordan Rock Island, IL 61299
1	Commander US Army Rock Island Arsenal Rock Island, IL 61299
2	Commander US Army Watervliet Arsenal ATTN: DRDAR-LCB-TL Watervliet, NY 12189
1	Commander Dugway Proving Ground ATTN: STEDP-TO-H, Mr. Miller Dugway, UT 84022
1	Commander Pine Bluff Arsenal Pine Bluff, AR 71601
1	Commander Cornhusker Army Ammunition Plant Grand Island, NE 68801
1	Commander Indiana Army Ammunition Plant Charlestown, IN 47111
1	Commander Iowa Army Ammunition Plant Burlington, IA 52502
1	Commander Joliet Army Ammunition Plant Joliet, IL 60436
1	Commander Kansas Army Ammunition Plant Parsons, KS 67357
1	Commander Lone Star Army Ammunition Plant Texarkana, TX 75502
1	Commander Longhorn Army Ammunition Plant Marshall, TX 75671

DISTRIBUTION LIST

No. of Copies	Organization
1	Commander Louisiana Army Ammunition Plant Shreveport, LA 71102
1	Commander Milan Army Ammunition Plant Miland, TN 38358
1	Commander Radford Army Ammunition Plant Radford, VA 24141
1	Commander Ravenna Army Ammunition Plant Ravenna, OH 44266
1	Commander US Army Harry Diamond Labs ATTN: DELHD-TI 2800 Powder Mill Road Adelphi, MD 20783
1	Commander US Army Materials and Mechanics Research Center ATTN: DRXMR-ATL Watertown, MA 02172
1	Commander US Army Natick Research and Development Command ATTN: DRXRE, Dr. D. Sieling Natick, MA 01762
1	Commander US Army Foreign Science and Technology Center ATTN: Rsch & Data Branch Federal Office Building 220 - 7th Street, NE Charlottesville, VA 22901
1	Director DARCOM Field Safety Activity ATTN: DRXOS-ES Charlestown, IN 47111
1	Director DARCOM, ITC ATTN: Dr. Chiang Red River Depot Texarkana, TX 75501
1	Commander US Army TRADOC Systems Analysis Activity ATTN: ATAA-SL (Tech Lib) White Sands Missile Range NM 88002
1	Commander US Army Nuclear Agency 7500 Backlick Road, Bldg. 2073 Springfield, VA 22150
1	Commandent US Army Engineer School Fort Belvoir, VA 22060
1	HQDA (DAMA-CSM-CA) Washington, DC 20310
2	HQDA (DAMA-AR; NCL Div) Washington, DC 20310
1	HQDA (DAMO-ODC, COL G.G. Watson) Washington, DC 20310
1	HQDA (DAEN-RDL) Washington, DC 20314
1	HQDA (DAEN-MCE-D/Mr. R. Wright) Washington, DC 20314
1	HQDA (DAEN-MCC-D/Mr. L. Foley) Washington, DC 20314

DISTRIBUTION LIST

No. of Copies	Organization
1	Office of The Inspector General Department of the Army ATTN: DAIG-SD Washington, DC 20310
1	Division Engineer US Army Engineer Division Fort Belvoir, VA 22060
1	US Army Eng Div ATTN: Mr. Char P.O. Box 1600 Huntsville, AL 35809
1	Director US Army Engineer Waterways Experiment Station ATTN: WESNP, Mr. L.F. Ingram P.O. Box 631 Vicksburg, MS 39180
1	Commander US Army Construction Engineering Research Laboratory P.O. Box 4005 Champaign, IL 61820
1	Commander US Army Research Office P.O. Box 12211 Research Triangle Park NC 27709
1	Director US Army Advanced BMD Technology Center ATTN: M. Whitfield Huntsville, AL 35807
1	Commander US Army Ballistic Missile Defense Systems Command ATTN: J. Veeneman P.O. Box 1500, West Station Huntsville, AL 35807
1	Assistant Secretary of the Navy (Research & Development) Navy Department Washington, DC 20350
4	Chief of Naval Operation ATTN: OP-41B, CPT S.N. Howard OP-411, Mr. J.W. Connelly OP-754 OP-985FZ Department of the Navy Washington, DC 20350
1	Commander Bureau of Naval Weapons ATTN: Code F121 Mr. H. Roylance Department of the Navy Washington, DC 20360
1	Commander Naval Air Systems Command ATTN: AIR-532 Washington, DC 20361
1	Commander Naval Sea Systems Command ATTN: SEA-04H, Mr. C.P. Jones Washington, DC 20362
1	Commander Naval Sea Systems Command ATTN: SEA-0333 Washington, DC 20362
2	Commander David W. Taylor Naval Ship Research & Development Center ATTN: Mr. A. Wilner, Code 1747 Dr. W.W. Murray, Code 17 Bethesda, MD 20084

DISTRIBUTION LIST

No. of Copies	Organization
3	Commander Naval Surface Weapons Center ATTN: E-23 Mr. J. C. Talley Dr. W. Soper Dahlgren, VA 22448
3	Commander Naval Surface Weapons Center ATTN: Dr. Leon Schindel Dr. Victor Dawson Dr. P. Huang Silver Spring, MD 20910
2	Commander Naval Surface Weapons Center ATTN: Code 241, Mr. Proctor R-15 Silver Spring, MD 20910
2	Commander Naval Weapons Center ATTN: Code 0632 China Lake, CA 93555
1	Commander Naval Weapons Support Center ATTN: NAPEC Crane, IN 47522
2	Commander Naval Explosive Ord Disposal Facility ATTN: Code 501, L. Wolfson Code D Indian Head, MD 20640
1	Command US Naval Ship Research and Development Center Facility ATTN: Mr. Lowell T. Butt Underwater Explosions Research Division Portsmouth, VA 23709
1	Commander US Naval Weapons Evaluation Facility ATTN: Document Control Kirtland AFB Albuquerque, NM 87117
1	Commander Naval Civil Engineering Laboratory ATTN: Code L51 Port Hueneme, CA 93041
1	Commander Naval Research Laboratory ATTN: Code 2027, Tech Lib Washington, DC 20375
2	Superintendent Naval Postgraduate School ATTN: Tech Reports Sec. Code 57, Prof R. Ball Monterey, CA 93940
1	HQ USAF (AFNIE-CA) Washington, DC 20330
3	HQ USAF (AFRIDQ; AFRDOSM; AFRDPM) Washington, DC 20330
1	AFSC (DSCPSL) Andrews AFB Washington, DC 20331
1	AFSC (IGFG) Andrews AFB Washington, DC 20334
1	AFRPL (M. Raleigh) Edwards AFB, CA 93523
1	ADTC (DLODL, Tech Lib) Eglin AFB, FL 32542

DISTRIBUTION LIST

No. of Copies	Organization
1	ADTC (DOM/S Reither) Eglin AFB, FL 32542
2	AFATL (ATRD, R. Brandt) Eglin AFB, FL 32542
1	AFATL (DLYV, Mr. R.L. McGuire) Eglin AFB, FL 32542
1	USAFTAWC (OA) Eglin AFB, FL 32542
1	Ogden ALC/MMWRE ATTN: (Mr. Ted E. Comins) Hill AFB, UT 84406
5	AFWL (DEO, Mr. F. H. Peterson; SYT, MAJ W. A. Whitaker; SRR; WSUL; SR) Kirtland AFB, NM 87117
2	Director of Aerospace Safety Headquarters, US Air Force ATTN: IGD/AFISC(SEV) & (SEW) COL G. J. Corak Norton AFB, CA 92409
1	AFCEC-DE/LTC Walkup Tyndall Air Force Base Panama City, FL 32401
1	AFFDL/(FBE, Mr. R. M. Bader) Wright-Patterson AFB, OH 45433
2	AFLC (MMWM/CPT D. Rideout; IGYE/K. Shopker) Wright-Patterson AFB, OH 45433
3	AFML (LLN, Dr. T. Nicholas; MAS; MBC, Mr. D. Schmidt) Wright-Patterson AFB, OH 45433
1	FTD (ETD) Wright-Patterson AFB, OH 45433

No. of Copies	Organization
1	Headquarters Energy Research and Development Administration Department of military Applications Washington, DC 20545
1	Director Division of Operational Safety Dept. of Energy ATTN: Carlo Ferrara, Jr. Washington, DC 20545
1	Albuquerque Operations Office Energy Research and Development Administration ATTN: ODI P.O. Box 5400 Albuquerque, NM 87115
1	Mason & Hangar-Sials Mason Co., Inc. Pantex Plant - ERDA ATTN: Director of Development P.O. Box 647 Amarillo, TX 79177
1	Research Director - Pittsburgh Mining & Safety Research Center ATTN: Mr. Richard W. Watson Bureau of Mines, dept. of the Interior 4800 Forbes Avenue Pittsburgh, PA 15213
1	Institute of Makers of Explosives ATTN: Mr. Harry Hampton Graybar Building, RM 2449 420 Lexington Avenue New York, NY 10017

DISTRIBUTION LIST

No. of Copies	Organization
1	Director Lawrence Livermore Laboratory Technical Information Division P.O. Box 808 Livermore, CA 94550
1	Director Los Alamos Scientific Laboratory ATTN: Dr. J. Taylor P.O. Box 1663 Los Alamos, NM 87544
2	National Aeronautics and Space Administration Aerospace Safety Research and Data Institute ATTN: Mr. S. Weiss Mail Stop 6-2 Mr. R. Kemp Mail Stop 6-2 Lewis Research Center Cleveland, OH 44135
1	Director National Aeronautics and Space Administration Marshall Space Flight Center Huntsville, AL 35812
1	Director National AEronautics and Space Administration Scientific and Technical Information Facility P.O. Box 8757 Baltimore/Washington International Airport, MD 21240
1	National Academy of Sciences ATTN: Mr. D. G. Groves 2101 Constitution Avenue, NW Washington, DC 20418
1	Aeronautical Research Associates of Princeton, Inc. ATTN: Dr. C. Donaldson 50 Washington Road Princeton, NJ 08540
1	Aerospace Corporation P.O. Box 95085 Los Angeles, CA 90045
1	Agbabian Associates ATTN: Dr. D. P. Reddy 250 N Nash Street El Segundo, CA 90245
2	AVCO Corporation Structures and Mechanics Dept ATTN: DR. William Broding Mr. J. Gilmore Wilmington, MA 01887
2	Battelle Columbus Laboratories ATTN: Dr. L.E. Hulbert Mr. J.E. Backofen, Jr. 505 King Avenue Columbus, OH 43201
1	Black & Veatch Consulting Engineers ATTN: Mr. H. L. Callahan 1500 Meadow Lake Parkway Kansas City, MO 64114
2	The Boeing Company Aerospace Group ATTN: Dr. Peter Grafton Dr. D. Strome Mail Stop 8C-68 Seattle, WA 98124

DISTRIBUTION LIST

No. of Copies	Organization
1	General American Research Div. General American Transportation Corp. ATTN: Dr. J. C. Shang 7449 N. Natchez Avenue Niles, IL 60648
1	Hercules, Inc. ATTN: Billings Brown Box 93 Magna, UT 84044
1	J. G. Engineering Research Associates 3831 Menlo Drive Baltimore, MD 21215
2	Kaman-AviDyne ATTN: Dr. N. P. Hobbs Mr. S. Criscione Northwest Industrial Park 83 Second Avenue Burlington, MA 01803
3	Kaman Sciences Corporation ATTN: Dr. F. H. Shelton Dr. D. Sachs Dr. R. Keefe 1500 Garden of the Gods Road Colorado Springs, CO 80907
1	Knolls Atomic Power Laboratory ATTN: Dr. R. A. Powell Schenectady, NY 12309
2	Martin Marietta Laboratories ATTN: Dr. P. F. Jordan Mr. R. Goldman 1450 S. Rolling Road Baltimore, MD 21227
1	McDonnell Douglas Astronautics Western Division ATTN: Dr. Lea Cohen 5301 Bosla Avenue Huntington Beach, CA 92647
1	Monsanto Research Corporation Mound Laboratory ATTN: Frank Neff Miamisburg, OH 45342
1	Physics International 2700 Merced Street San Leandro, CA 94577
1	R&D Associates ATTN: Mr. John Lewis P.O. Box 9695 Marina del Rey, CA 90291
2	Sandia Laboratories ATTN: Infor Distr Division Dr. W.A. von Riesemann Albuquerque, NM 87115
1	Science Applications, Inc. 8th Floor 2361 Jefferson Davis Highway Arlington, VA 22202
1	Brown University Division of Engineering ATTN: Prof R. Clifton Providence, RI 02912
1	Florida Atlantic University Dept of Ocean Engineering ATTN: Prof K. K. Stevens Boca Raton, FL 33432
1	Georgia Institute of Technology ATTN: Dr. S. Atluri 225 North Avenue, NW Atlanta, GA 30332

DISTRIBUTION LIST

No. of Copies	Organization
1	Lovelace Research Institute ATTN: Dr. E.R. Fletcher P.O. Box 5890 Albuquerque, NM 87115
1	Massachusetts Institute of Technology Aeroelastic and Structures Research Laboratory ATTN: Dr. E. A. Witmer Cambridge, MA 02139
3	Southwest Research Institute ATTN: Dr. H. N. Abramson Dr. W. E. Baker Dr. U. S. Lindholm 8500 Culebra Road San Antonio, TX 78228
1	Texas A&M University Department of Aerospace Engineering ATTN: Dr. James A. Stricklin College Station, TX 77843
1	University of Alabama ATTN: Dr. T. L. Cost P. O. Box 2908 University, AL 35486
1	University of Delaware Department of Mechanical and Aerospace Engineering ATTN: Prof J. R. Vinson Newark, DE 19711

No. of Copies	Organization
	Aberdeen Proving Ground
	Dir, USAMSAA ATTN: Dr. J. Sperrazza Mr. R. Norman, GWD DRXSY-MP, H. Cohen
	Cdr/Dir, CSL, EA ATTN: DRDAR-CLJ-L
	Cdr, USATECOM ATTN: DRSTE-SG-H
	US Army Toxic and Hazardous Materials Agency